

Hodler, Roland; Schaudt, Paul; Vesperoni, Alberto

Working Paper

Mining for Peace

CESifo Working Paper, No. 10207

Provided in Cooperation with:

Ifo Institute – Leibniz Institute for Economic Research at the University of Munich

Suggested Citation: Hodler, Roland; Schaudt, Paul; Vesperoni, Alberto (2023) : Mining for Peace, CESifo Working Paper, No. 10207, Center for Economic Studies and ifo Institute (CESifo), Munich

This Version is available at:

<https://hdl.handle.net/10419/271851>

Standard-Nutzungsbedingungen:

Die Dokumente auf EconStor dürfen zu eigenen wissenschaftlichen Zwecken und zum Privatgebrauch gespeichert und kopiert werden.

Sie dürfen die Dokumente nicht für öffentliche oder kommerzielle Zwecke vervielfältigen, öffentlich ausstellen, öffentlich zugänglich machen, vertreiben oder anderweitig nutzen.

Sofern die Verfasser die Dokumente unter Open-Content-Lizenzen (insbesondere CC-Lizenzen) zur Verfügung gestellt haben sollten, gelten abweichend von diesen Nutzungsbedingungen die in der dort genannten Lizenz gewährten Nutzungsrechte.

Terms of use:

Documents in EconStor may be saved and copied for your personal and scholarly purposes.

You are not to copy documents for public or commercial purposes, to exhibit the documents publicly, to make them publicly available on the internet, or to distribute or otherwise use the documents in public.

If the documents have been made available under an Open Content Licence (especially Creative Commons Licences), you may exercise further usage rights as specified in the indicated licence.

Mining for Peace

Roland Hodler, Paul Schaudt, Alberto Vesperoni

Impressum:

CESifo Working Papers

ISSN 2364-1428 (electronic version)

Publisher and distributor: Munich Society for the Promotion of Economic Research - CESifo GmbH

The international platform of Ludwigs-Maximilians University's Center for Economic Studies and the ifo Institute

Poschingerstr. 5, 81679 Munich, Germany

Telephone +49 (0)89 2180-2740, Telefax +49 (0)89 2180-17845, email office@cesifo.de

Editor: Clemens Fuest

<https://www.cesifo.org/en/wp>

An electronic version of the paper may be downloaded

- from the SSRN website: www.SSRN.com
- from the RePEc website: www.RePEc.org
- from the CESifo website: <https://www.cesifo.org/en/wp>

Mining for Peace

Abstract

The energy transition increases the demand for minerals from ethnically diverse, conflict-prone developing countries. We study whether and where mining is possible in such countries without raising the risk of civil conflict. We proceed in three steps: First, we propose a theoretical model to predict the occurrence and location of conflict events on the territory of a country based on the spatial distribution of ethnic groups and resource rents. Second, we verify the predictive power of this model using granular spatial data from Sierra Leone and confirm its broader applicability using less granular data from a sample of eight West African countries. Third, we employ our framework to simulate the potential impact of new (planned and unplanned) mining projects in Sierra Leone. A crucial insight is that new mining projects do not necessarily translate into more conflict but may pacify the country under the right conditions and the right policies.

JEL-Codes: D740, D820, L720, O130, Q340.

Keywords: civil conflict, ethnic conflict, natural resources, mining.

Roland Hodler
Department of Economics
University of St. Gallen / Switzerland
roland.hodler@unisg.ch

Paul Schaudt
Wyss Academy for Nature
University of Bern / Switzerland
paul.schaudt@unibe.ch

Alberto Vesperoni
Department of Political Economy
King's College London / United Kingdom
alberto.vesperoni@kcl.ac.uk

January 2023

We are thankful for helpful comments by conference participants at the Bari Conference on the Economics of Global Interactions, the Swiss Development Economics Conference; and seminar participants at King's College and the University of St.Gallen.

1 Introduction

The transition to less carbon emitting technologies significantly increases the global demand for minerals (Herrington, 2021; Hund et al., 2020). Increasingly, this demand is met by industrial mining activities in developing countries.¹ Many of these countries, especially those located in Sub-Saharan Africa, are ethnically diverse and politically unstable. There are widespread concerns that new mining projects may cause civil conflicts and misery in these countries. Civil conflicts have been fairly common over the last 50–60 years in Sub-Saharan Africa, and a large literature documents that natural resource rents and ethnic diversity have both contributed to these conflicts.² Even worse, these two factors may reinforce one another, as the rivalry among ethnic groups may trigger or exacerbate resource-fuelled conflict (Adhvaryu et al., 2021; Berman et al., 2017; Gehring et al., 2019; Hodler, 2006; Morelli and Rohner, 2015). These findings offer a bleak outlook regarding the social costs of new mining projects in developing countries. Minimizing these social costs is a key policy challenge to guarantee a just and equitable energy transition.

In this paper, we propose a framework that offers a more nuanced view than the previous literature and can be informative for policy-makers and other stakeholders. We think of a country as an interconnected system where the conflictuality of a location cannot be understood by local features in isolation but depends on the country’s entire ethnic geography and the location and revenues of all its active mines. At the core of our message lies the possibility that, by influencing the set of active mines and the prices for the corresponding licenses, carefully crafted governmental intervention can contribute to making the mining industry a facilitator of peace and prosperity rather than conflict and misery. We refer to this (theoretical, but as we will see, also empirical) possibility as “mining for peace.”

Our first contribution is a theoretical model to help understand how the interaction of the spatial distributions of ethnic groups and resource rents shapes the spatial distribution of the local conflict risks and the country’s overall tendency to conflict. In our model, ethnic groups constitute coalitions that can contend natural resource rents at the local level (in conflicts that involve their local populations fighting for the local resource rents) or at the national level (in a grand conflict that involves their whole ethnic group fighting for the entire pool of resource

¹The European and North American share of global minerals production has declined from 42 to 22 percent over the last 30 years (Reichl and Schatz, 2022).

²See, e.g., Corvalan and Vargas (2015); Eberle et al. (2020); Esteban et al. (2012, 2015); Esteban and Ray (2008); Matuszeski and Schneider (2006); Montalvo and Reynal-Querol (2005); Novta (2016) on the role of ethnic diversity; as well as Bazzi and Blattman (2014); Berman et al. (2017); Brückner and Ciccone (2010); Collier and Hoeffler (2004); Dube and Vargas (2013); Humphreys (2005); Lei and Michaels (2014) on the role of natural resource rents.

rents). We take a mechanism-design approach and assume that the central planner prioritizes the implementation of peace at the national level while simultaneously attempting to minimize local conflict risks.³ To do so, the planner redistributes the resource rents across ethnic groups and locations under uncertainty of the private conflict costs of the groups involved. We first show that the implementation of peace via the truthful revelation of such costs is generally impossible in the presence of ethnic segregation and spatial resource inequality. We introduce the notion of a peace deficit, which corresponds to the monetary amount that would be necessary to guarantee peace everywhere. We then characterize the probability of conflict at each location when the planner implements the second-best transfer scheme, which guarantees peace at the national level and minimizes local conflict risks based on prior information only. This scheme deprives ethnic groups that are generally over-represented in resource-rich locations (as compared to their national-level population shares) of some of the local resource rents because these rents are partly used to guarantee peace at the national level. These groups experience discord between high local resource rents and their comparatively low post-transfer well-being due to their weaker bargaining strength at the national level. Hence, we call them discordant groups. Importantly, it is only local coalitions of discordant groups that may initiate local conflicts. As a result, we predict that the local conflict risk increases in the local resource rents and a measure of local ethnic diversity among discordant groups. Thus our model can account for several prominent stylized facts: First, conflict events often occur in resource-rich locations (e.g., [Berman et al., 2017](#)). Second, conflict events often occur in ethnically diverse locations of segregated countries (e.g., [Corvalan and Vargas, 2015](#); [Eberle et al., 2020](#); [Matuszeski and Schneider, 2006](#); [McGuirk and Nunn, 2020](#)). Third, ethnic groups in resource-rich locations often feel economically deprived and politically excluded ([Berman et al., 2020](#)).

Our second contribution is to provide empirical support for our theoretical predictions. For this purpose, we use granular data from Sierra Leone.⁴ Sierra Leone is a suitable candidate for our empirical analysis for several reasons: First, there exists granular data on local ethnic diversity, the locations of mines, and the location of conflict events. Second, Sierra Leone has different sizeable ethnic groups. While many regions of Sierra Leone are ethnically diverse, most ethnic groups are still over-represented in their traditional homeland. Third, Sierra Leone produced and exported different minerals in large quantities during our sample period from 1997–2018: bauxite, diamonds, and iron (and, to a lesser extent, gold and rutile). Importantly, these

³National conflict is usually associated with higher costs for society and political leadership compared to local (limited) conflict. Thus avoiding national conflict could be the primary concern for benevolent politicians and for politicians prioritizing political survival.

⁴Sierra Leone suffered from a diamond-fuelled civil war that lasted from 1991–2002 and led to more than 50,000 casualties ([Bellows and Miguel, 2006](#); [Kaldor and Vincent, 2006](#)). Further details are provided below.

minerals are produced in different parts of the country, and their relative economic importance changed over the sample period. Within our sample period, diamonds were most important in the early years, bauxite in the intermediate years, and iron in the later years. This setting allows us to illustrate the intuition of our theoretical model and to test how these changes in Sierra Leone’s mining geography changed the set of discordant groups and, consequently, the spatial distribution of the local conflict risks and the country’s aggregate propensity to conflict.

The empirical analysis consists of three major parts. First, following the static nature of the model, we time-average the data over the entire sample period as well as different sub-periods (characterized by the economic importance of different minerals). We find a strong positive relationship between the theoretically predicted and the observed local conflict risks, which we confirm in an extension using less granular data for eight West African countries. These findings are reassuring. They suggest that changes in Sierra Leone’s mining geography coincide with changes in the observed local conflict in a manner consistent with our model’s predictions. Second, we leverage the panel dimension of our data and run standard OLS fixed effects regressions. We also adapt a shift-share instrumental variable approach that is commonly used in literature to deal with potentially endogenous mining operations (e.g., [Berman et al., 2017](#); [Dube and Vargas, 2013](#)). Again, we observe a pattern consistent with our model’s predictions. Third, we test to which degree aggregate conflict can be understood through the lens of our model. We leverage the notion of the peace deficit derived from the model, which is conceptualized as the transfer deficit that would guarantee peace in all locations. We find a strong correlation between this peace deficit and the actual conflict intensity in Sierra Leone across time. In summary, our empirical analysis suggests that our theoretical model is indeed helpful to predict how – conditional on a country’s ethnic geography – changes in its mining geography may shape the occurrence and location of conflict events.

Given the empirical support for our theoretical model, we turn to our third contribution: we apply the model to simulate the consequences of new industrial mining projects. We consider all known mineral deposits in Sierra Leone and run counterfactual analyses to predict how the hypothetical development of these deposits would affect the overall risk of conflict and the spatial distribution thereof. For example, we predict that the planned new gold mines on the Baomahun and Nimini deposits would increase the country’s aggregate propensity to conflict. Importantly, we also identify alternative (gold) deposits whose development would lower the aggregate propensity to conflict. Thereby we confirm that “mining for peace” is not only a theoretical but also an empirical possibility. Another important insight is that these hypothetical mining projects would have very different effects on the spatial distribution of

conflict risks. We document this heterogeneity by focusing on the effects on the local conflict risk around these deposits as well as around the currently active industrial mines.

The contributions of our paper are related to various strands of literature. Our theoretical contribution links directly to the theory of conflict.⁵ Our approach is inspired by Roth (2002), who argues that economists need to take an engineering approach when designing institutions and markets. In the same vein, we aim to take an engineering approach to the promotion of peace, adapting tools and ideas from contract theory and mechanism design with the distinctive purpose of assisting data analysis and permitting more sophisticated predictions and policy implications compared to purely data-driven approaches.⁶ A common theme in the literature on the theory of conflict is the reasons for why conflict can occur between rational actors (Fearon, 1995). A priori, one should expect that peaceful bargaining solutions should exist, given that conflict typically destroys resources. Jackson and Morelli (2011) discuss the different types of bargaining failures (see also Blattman, 2022). Within their taxonomy, the cause of conflict outbreak in our theoretical model can be interpreted as a bargaining failure caused by a commitment problem. This bargaining failure follows from the presence of multiple threat points, which may turn out incompatible with an efficient solution.⁷ Thereby, our model is related to previous models of first-strike advantage (reviewed in Jackson and Morelli, 2011) and, more importantly, the model by Morelli and Rohner (2015). They use a setup with two ethnic groups and two regions to study how the concentration of natural resources and ethnic groups shape the overall conflict risk. Despite the many technical differences, their model shares the feature that civil conflict can arise because it is hard to prevent conflict at the national and regional levels simultaneously. We extend this core insight to a more general framework with many locations and groups to predict the location of conflict events at the subnational level.

Our empirical contribution provides further nuance to studies focusing on the empirical relationship between natural resources, ethnic diversity, and conflict (see footnote 2 for references). Our framework allows us to capture aggregate and local effects of both factors while leveraging the identification advantages of recent micro designs. Thus, we build a bridge between cross-country (e.g., Collier and Hoeffler, 2004; Esteban et al., 2012, 2015; Hodler, 2006) and more

⁵For excellent reviews of the theoretical literature on conflict, see, e.g., Blattman and Miguel (2010) or Jackson and Morelli (2011).

⁶For earlier work on conflict outbreak relying on mechanism design, see, e.g., Bester and Wärneryd (2006), Fey and Ramsay (2009), and Hörner et al. (2015).

⁷Another way to think of this friction is through the lens of cooperative game theory, a point already made in Ray (2009) in the context of understanding conflict outbreak in presence of complete information. Specifically, as in the core and related solution concepts, a peaceful splitting of the surplus may be blocked by coalitions of participants threatening to boycott cooperation by leaving the enterprise.

granular spatial studies (e.g., [Adhvaryu et al., 2021](#); [Berman et al., 2017](#); [Eberle et al., 2020](#); [McGuirk and Nunn, 2020](#)) on conflict, ethnic diversity, and resources. In particular, we use granular spatial data and acknowledge the importance of local determinants for local conflict risks (by controlling for them in our main analysis and various robustness tests), but we build on a theoretical framework that allows us to focus on the systemic component of local conflict risks that results from a country’s entire ethnic and mining geography.⁸ At a broader level, we contribute to previous studies primarily interested in the circumstances under which resource extraction fosters social and human development ([Mehlum et al., 2006](#); [Van der Ploeg, 2011](#)) rather than in determining whether natural resources are a curse or a blessing on average.

Our model-based simulations illustrate the effects of new industrial mining projects on a country’s propensity to conflict both at the aggregate level and at the local level. In a sense, one can view the changes in conflict risks induced by new mining projects as externalities. We thus propose that governments and, to a lesser extent, international organizations and advocacy groups should make use of these insights when designing mining policies or conducting cost-benefit analyses. Ideally, the government could use information about these conflict externalities – monetized by the peace deficit – when setting the price of mining licenses or designing royalty and tax schemes. Alternatively, it could use this information to determine which deposits should be promoted and which ones should be discouraged (and, possibly, forcefully closed). Our analysis can also offer insights to international mining companies operating in conflict-prone countries. These may prefer developing new mines where they are least likely to fuel conflict in the same location, as local conflict may increase the costs of the actual mining activities as well as the “social licenses to operate,” which have become common in the mining industry (e.g., [Prno and Slocombe, 2012](#)). In addition, these companies may also prefer minimizing conflict outbreaks elsewhere in the country’s territory where they already have established interests.

The remainder of the paper is structured as follows. [Section 2](#) present our theoretical model. [Section 3](#) first introduces our empirical setting and data, after which we provide empirical support for our theoretical model in [Section 4](#). [Section 5](#) conducts the counterfactual analysis of how potential new mining projects would affect conflict. [Section 6](#) concludes the paper and provides some policy recommendations for making the mining industry a facilitator of peace and prosperity rather than conflict and misery.

⁸This interaction between local and systemic components at the center of our methodology is broadly in line with general principles in relational sociology and social networks (e.g., [Emirbayer, 1997](#)). Other contributions to the literature on the economics of conflict that adapt and concretize such principles include [König et al. \(2017\)](#) and [Amarasinghe et al. \(2020\)](#).

2 Model

Consider a country that is inhabited by a continuum of individuals. This population is partitioned into a finite set of ethnic groups $G \subset \mathbb{N}$ and a finite set of locations $L \subset \mathbb{N}$. These locations may represent subnational administrative or political units like wards in Sierra Leone. We denote the mass of individuals in ethnic group $g \in G$ and location $l \in L$ by $m_l^g \geq 0$, with $m_l := \sum_{g \in G} m_l^g$, $m^g := \sum_{l \in L} m_l^g$, and $m := \sum_{g \in G} m^g$.

Mining activities and the associated upstream and downstream services give rise to resource rents. The resource rent in location $l \in L$ is $r_l > 0$, where $r := \sum_{l \in L} r_l$ denotes the aggregate resource rent and \mathbf{r} their $|L|$ dimensional vector. Resource rents can be contended in conflicts at the local level or the national level. In case of local or national conflict, a fraction of the corresponding resources is destroyed while the rest is preserved. As such fractions are difficult to assess due to unpredictable conflict dynamics of winners and losers, their expectations remain impressionistic and heterogeneous across groups, and we can effectively think of them as subjective valuations. We thus denote by $v_l^g \in [0, 1]$ the fraction of the local resource rent r_l that the local representatives of group $g \in G$ believe to be preserved in case of a conflict they win in location $l \in L$ (their local valuation). Similarly, we denote by v^g the fraction of the national resource rent r that the national representative of group $g \in G$ believe to be preserved in case of a national conflict they win (their national valuation). These perceptions can be represented by a $|G| \times (|L| + 1)$ dimensional matrix \mathbf{v} with v_l^g and v^g as typical elements.

In line with the literature, we think of the expected shares of preserved local resource rents conquered by ethnic groups as their winning probabilities in winner-take-all conflicts. The expected share of ethnic group $g \in G$ in a local conflict at location $l \in L$ is denoted by $s_l^g \in [0, 1]$, where $\sum_{g \in G} s_l^g = 1$ for each $l \in L$. Similarly, the expected share of ethnic group $g \in G$ in a national conflict is $s^g \in [0, 1]$, where $\sum_{g \in G} s^g = 1$. The distribution of these expected shares can be represented by a $|G| \times (|L| + 1)$ dimensional matrix \mathbf{s} with s_l^g and s^g as typical elements. The expected aggregate payoff of members of ethnic group $g \in G$ in location $l \in L$ in case of conflict in location l is thus $r_l v_l^g s_l^g$. Similarly, the expected aggregate payoff of members of ethnic group $g \in G$ in the whole country in case of a national conflict is $r v^g s^g$.

In the theoretical literature on conflict, the expected shares \mathbf{s} are typically modeled as winning probabilities determined by the strategic interaction of the competing groups in conflict, where both group sizes and mobilization motives matter in determining the relative strength of a group. While the former can be directly determined by demography, i.e., the population shares of the ethnic groups (which may be considered exogenous in the short to medium run), the latter are complex and jointly determined by, among others, the salience of ethnic identity, the

incentives of leaders and followers, and the complementarity of labor and capital in collective action (see respectively [Atkin et al., 2021](#); [Jackson and Morelli, 2007](#); [Esteban and Ray, 2008](#)). In our model we abstract from such complex motives and simply assume that the expected shares are determined by the demographic representation of ethnic groups so that they are proportional to their population shares in the relevant context, i.e., $s_l^g = m_l^g/m_l$ and $s^g = m^g/m$.

The focus of our analysis is instead on the promotion of peace via transfers of resource rents across ethnic groups and locations. For this purpose, we consider a planner who can redistribute resource rents to implement peace both at the local and the national level. The focus on resource rents implies that the planner can transfer the income generated by the resource endowments but not the endowments themselves. In this setting, the transfer received by a group determines the group's payoff under peace: specifically, the aggregate payoff of members of ethnic group $g \in G$ in location $l \in L$ in case of peace at location l is their transfer $t_l^g \geq 0$, while the aggregate payoff of the whole ethnic population of group $g \in G$ in case of peace at the national level is their aggregate transfer $t^g := \sum_{l \in L} t_l^g$. A system of transfers is denoted by a $|G| \times |L|$ dimensional matrix \mathbf{t} with t_l^g as typical element.

The objective of the planner is to promote peace in the highest number of locations while guaranteeing peace at the national level. Hence, the planner first and foremost aims at avoiding the outbreak of a national conflict, e.g., because the consequences of such conflict are particularly uncertain and potentially detrimental for both the political leader and the entire country. Moreover, as locations may not be equally important to the planner, we assign a different priority weight $w_l \in (0, 1)$ to each location $l \in L$, with $\sum_{l \in L} w_l = 1$. For example, the planner may assign a higher weight to locations with active mining sites or locations where many co-ethnics live, as suggested by the literature on ethno-regional favoritism ([Burgess et al., 2015](#); [De Luca et al., 2018](#); [Hodler and Raschky, 2014](#)). We assume the planner maximizes the weighted sum of the peace probabilities $p_l \in [0, 1]$ across all locations,

$$\max_{\mathbf{t}} \sum_{l \in L} w_l p_l, \tag{1}$$

subject to guaranteeing peace at the national level, a budget constraint, and informational frictions. We call such objective *peace maximizing*. We will carry this objective across all stages of our theoretical inquiry in slightly different forms, adapted to the specific informational structure.

In our model, the crucial friction for peace is that transfers represent the status-quo income of

the groups (their peace payoff) and thus cannot be conditioned on the local or national nature of the conflict threat. Instead, the transfers should prevent conflict at both levels at the same time, as groups are not ex-ante committed to any, and either can work as a motive for conflict outbreak.⁹ On top of this commitment friction on the side of the groups, the planner has two fundamental constraints for promoting peace. The first is the limited budget for redistribution, which is determined by the aggregate value of the resource rents. The second is the limited information about the groups' perceptions of the wastefulness of conflict, as quantified by the v^g and v_l^g , which are privately known by the groups. In the course of our analysis, we will consider three alternative ways the planner may approach the latter (informational) constraint. The picture that emerges from these three steps motivates proxies of conflict and policy prescriptions that we consider in our empirical and counterfactual exercises. In a first step (Section 2.1), we study the conditions under which the planner can guarantee peace at the national level and all locations – thus achieving the *unconstrained maximum* of the planner's objective (1) – for any possible realization of \mathbf{v} and, therefore, in the absence of any reliable knowledge on \mathbf{v} . This exercise delivers a very restrictive condition for peace implementation (the *peace condition*), the set of groups that initiate conflict (the *discordant groups*), and the amount of extra funds necessary to pacify the country (the *peace deficit*). In a second step (Section 2.2), we inquire whether the constrained maximum of (1) can be reached via a system of transfers that incentivizes the groups to truthfully reveal their private information on v_l^g and v^g . We find that such a transfer system fails to exist whenever the peace condition is violated, thus suggesting a general impossibility. In a third step (Section 2.3), we study the constrained maximum of (1) based on prior information only (rather than revealed information). As a result of this analysis we obtain the probability of conflict at each location, which is the central prediction of our model.

2.1 Peace guaranteeing transfers

In this section, we inquire whether the planner can achieve the *unconstrained maximum* of the peace maximizing objective (1) in the absence of reliable knowledge and, therefore, for any \mathbf{v} .

As in all our model specifications, the planner will attempt to do so by appropriately redistrib-

⁹If groups were ex-ante committed to a type of conflict – with ethnic coalitions mobilizing either at the local or national level – conflict could always be prevented via an opportune transfer system which redistributes the peace surplus by rewarding coalitions proportionally to their strength. This, however, fails to occur as the timing is reversed: in our model transfers are determined before ethnic coalitions form so that groups choose to mobilize either at the local or national level only after their status-quo incomes are determined. For related approaches see Ray (2009) and Morelli and Rohner (2015).

uting resource rents. We therefore introduce some terminology that will carry on in subsequent sections. First, given \mathbf{r} , we say that a system of transfers \mathbf{t} is *budget feasible* if $\sum_{g \in G} t^g \leq r$. This condition requires the planner's intervention to be purely redistributive and does not allow for extra income.¹⁰ Second, given \mathbf{r} and \mathbf{s} , we say that a system of transfers \mathbf{t} *guarantees peace everywhere* if, for every possible \mathbf{v} , it does so simultaneously at the national level and in each location, i.e.,

$$t^g \geq s^g r v^g \text{ and } t_l^g \geq s_l^g r_l v_l^g \text{ for each } g \in G \text{ and } l \in L.$$

These conditions are very restrictive as they must hold even for the most demanding case of non-destructive conflict (i.e., $v_l^g = v^g = 1$). They can be seen as the ideal goal of a planner who is afraid of the chaotic consequences of conflict and wants to guarantee peace at every level and every location under any foreseeable contingency.

We are now ready to state our first result which characterizes the *peace condition*, i.e., the narrow set of configurations of \mathbf{r} and \mathbf{s} that can guarantee peace everywhere in a budget-feasible manner.

Proposition 1 *Given \mathbf{r} and \mathbf{s} , there exists a system of transfers \mathbf{t} that guarantees peace everywhere and is budget feasible if and only if*

$$1 = \sum_{l \in L} (r_l/r) (s_l^g/s^g) \text{ for each } g \in G. \quad (2)$$

Proof: Take any \mathbf{r} and \mathbf{s} . It is immediate that there exists such system of transfers if and only if peace can be feasibly implemented when $v_l^g = v^g = 1$ for each $l \in L$ and $g \in G$. Suppose this is the case. Guaranteed peace everywhere requires $t^g \geq r s^g$ and $t_l^g \geq r_l s_l^g$ for each $g \in G$ and $l \in L$. Budget feasibility requires $r \geq \sum_{g \in G} t^g$, which given the above implies $t^g = r s^g$ for all $g \in G$ and $t_l^g = r_l s_l^g$ for each $g \in G$ and $l \in L$. \mathbf{t} satisfies these two properties if and only if $t^g = r s^g$ and $t_l^g = r_l s_l^g$ for each $g \in G$ and $l \in L$. Given $t^g = \sum_{l \in L} t_l^g$, we can then conclude that such \mathbf{t} exists if and only if $r s^g = \sum_{l \in L} r_l s_l^g$ for each $g \in G$, which is equivalent to (2). \square

Given that the expected shares take the form $s_l^g = m_l^g/m_l$ and $s^g = m^g/m$ for all $l \in L$ and $g \in G$, it is straightforward that the peace condition (2) can be rewritten as

$$1 = \sum_{l \in L} (r_l/r) [(m_l^g/m_l)/(m^g/m)] \quad \text{or} \quad 1 = \sum_{l \in L} [(r_l/m_l)/(r/m)] (m_l^g/m^g).$$

¹⁰We will discuss the loosening of the budget constraint towards the end of this section, while introducing the peace deficit as a measure of a country's general tendency to conflict.

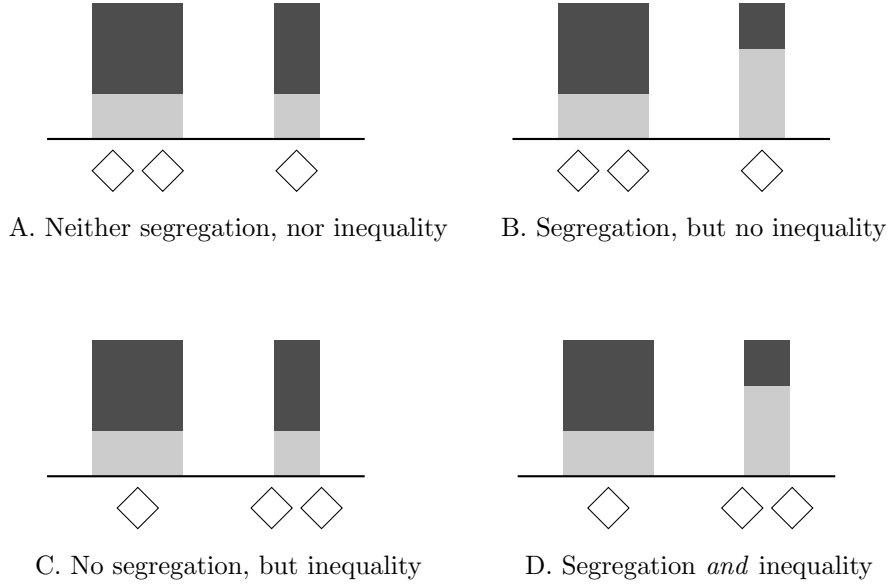


Figure 1: Each graph represents a different country where the horizontal axis represents different locations $l \in L\{1, 2\}$ and each tone of gray indicates a different ethnic group $g \in G\{1, 2\}$. The size of the gray rectangular areas above the horizontal axis indicate the population mass m_l^g of each group $g \in G$ in each location $l \in L$. The diamonds below the horizontal axis indicate the resource rent r_l at each location $l \in L$.

Hence, it holds in two special cases: First, it holds if there is no ethnic segregation, i.e., if $m_l^g/m_l = m^g/m$ for all $l \in L$ and $g \in G$, as understood from the first equality. Second, it holds if there is no inequality in per capita resource rents across locations, i.e., if $r_l/m_l = r/m$ for all $l \in L$, as understood from the second equality. However, in presence of ethnic segregation and spatial resource inequality the peace condition (2) does not generally hold. Hence, peace cannot typically be guaranteed.

Figure 1 illustrates these insights with a simple example. Panel A shows a country depicted with neither ethnic segregation, nor spatial resource inequality. Therefore, peace can be guaranteed in this country. Moreover, peace can also be guaranteed in the countries in Panels B and C which have either no ethnic segregation or no spatial resource inequality. In the former case, a peace guaranteeing, budget-feasible transfer scheme exists because per-capita resource rents are identical across locations. In the later case, such a transfer scheme exists because each group's population share is identical across locations. In contrast, peace cannot typically be guaranteed in all the countries like the one in Panel D where there is both, ethnic segregation and spatial resource inequality.¹¹

¹¹For the case with two locations and two ethnic groups the presence of spatial inequality *or* ethnic segregation is a necessary and sufficient condition for peace implementation. With more groups or more locations instead, it is only a sufficient condition.

We now take a closer look at why conflict emerges. Importantly, only some groups may initiate conflict, while others are always content with the status-quo. The set of groups that may initiate conflict is characterized by

$$G^* = \{g \in G : 1 < \sum_{l \in L} (r_l/r)(s_l^g/s^g)\}. \quad (3)$$

This definition can be easily understood in relation to the peace condition (2). Intuitively, if peace is guaranteed at the national level for every \mathbf{v} , the aggregate transfers to groups must equal their maximum claims at the national level, $t^g = s^g r$. Then, the groups that may initiate conflict are the ones that are over-represented in locations that are resource-rich. The reason is that they are short of transfers from the constraint at the national level:

$$r s^g = t^g = \sum_{l \in L} t_l^g < \sum_{l \in L} r_l s_l^g.$$

Therefore, these groups may feel deprived of the resource rents accruing in the locations where they predominately live, on which they have a stronger claim by means of the possibility of local conflict. Hence, they may experience a discord between these resource rents and their comparatively low post-transfer well-being. We subsequently refer to these groups as *discordant groups*. All other groups $g \notin G^*$ are over-represented in locations that are resource-poor, so that their total transfers $t^g = s^g r$ are more than sufficient to ensure they do not initiate conflict in any location, $t_l^g \geq s_l^g r_l$.

To see an example of the logic of discordant groups, consider again Figure 1. There, the set of discordant groups is empty in all panels but Panel D, which we already identified as the only case of conflict. In this panel, there is a single discordant group which is the one depicted in light gray, as it is over-represented in the resource-rich location on the right. The other group instead, depicted in dark gray, is non-discardant as it is under-represented in this location.

We conclude this section by defining a measure of the general tendency to conflict of a country. We call this measure the peace deficit, as it quantifies the amount of extra funds that would allow the planner to guarantee peace everywhere. By Proposition 1 and the related discussion of discordant groups, it is straightforward that the peace deficit can be written as

$$\Delta := \sum_{g \in G} \max \left\{ \sum_{l \in L} r_l s_l^g - r s^g, 0 \right\} = \sum_{g \in G^*} \left(\sum_{l \in L} r_l s_l^g - r s^g \right). \quad (4)$$

Intuitively, $\Delta = 0$ if the peace condition holds – which also implies that the set of discordant

groups is empty – while $\Delta > 0$ otherwise. In our empirical application to Sierra Leone, we will use the peace deficit Δ as a measure of the country’s average tendency for conflict across locations.

2.2 Peace implementing mechanism

In this section, we study whether the constrained maximum of the peace maximizing objective (1) can be reached via a system of transfers that incentivizes the groups to truthfully reveal their private information on v_l^g and v^g .

The desirability of such information revelation is straightforward. Having established that it is (generally impossible) to guarantee peace for every possible realization of \mathbf{v} , we now consider whether the planner can promote peace for at least some of these realizations. More specifically, conflict could always be prevented if known to be very wasteful (for an extreme, think of $v_l^g \approx 0$ so that nearly all resources are expected to be destroyed), as relatively low transfers are sufficient to guarantee that all groups opt for peace. Thus, if the planner was able to identify such realizations of \mathbf{v} , it could at least guarantee peace in contingencies where conflict is particularly wasteful. This however, is not immediate as the perceived wastefulness of conflict – as measured by v_l^g – is private information of the groups, and groups may not have an incentive to truthfully communicate this to the planner.

Taking a mechanism design approach, we focus on the scenario in which the members of group $g \in G$ inhabiting each location $l \in L$ are required to reveal their perceived preserved fraction $v_l^g \in [0, 1]$ to the planner via a corresponding message $\mu_l^g \in [0, 1]$, while the national representative of group g are required to reveal $v^g \in [0, 1]$ via $\mu^g \in [0, 1]$. In this context, a mechanism is a function $T : [0, 1]^{|G| \times (|L|+1)} \rightarrow \mathbb{R}_+^{|G| \times |L|}$ that maps each $|G| \times (|L| + 1)$ profile of messages $\mu := (\mu_l^g, \mu^g)$ into the corresponding transfer system $t_l^g = T_l^g(\mu)$ for each $l \in L$ and $g \in G$, where $t^g = \sum_{l \in L} T_l^g(\mu)$.¹² Given the transfer system is implemented, then all groups act upon their transfer and their perceived preserved fractions v_l^g and v^g so that there is conflict outbreak at location $l \in L$ if and only if $t_l^{g'} < s_l^{g'} r_l v_l^{g'}$ for some $g' \in G$, and there is conflict outbreak at the national level if and only if $t^{g'} < s^{g'} r v^{g'}$ for some $g' \in G$.

We now consider two desirable properties of a mechanism which are meant to hold for every given profile of preserved fractions $\mathbf{v} \in [0, 1]^{|G| \times (|L|+1)}$. In this context, we denote by \mathbf{v}_{-l}^{-g} the restriction of \mathbf{v} to all elements other than the representatives of group $g \in G$ in location $l \in L$,

¹²The extension to stochastic mechanisms – mapping message profiles into probability distributions over transfer systems – is omitted for ease of exposition but straightforward, leading to the same impossibility conclusions below.

and by \mathbf{v}^{-g} the restriction of \mathbf{v} to all elements other than the national representatives of group $g \in G$. Adapting (1) to the present setting, we say that a mechanism T is *peace maximizing* (PM) if it implements peace at the national level – requiring $\sum_{l \in L} T_l^g(\mathbf{v}) \geq s^g r v^g$ for each $g \in G$ – and, given that this is guaranteed, it implements peace at the local level – requiring $T_l^g(\mathbf{v}) \geq s_l^g r_l v_l^g$ for each $g \in G$ – for the highest (w_l -weighted) number of locations. Borrowing a conventional idea from the literature, we say that a mechanism T is *incentive compatible* (IC) if, for each $l \in L$ and $g \in G$, $T_l^g(\mathbf{v}) \geq T_l^g(\mu_l^g, \mathbf{v}^{-g})$ for any $\mu_l^g \in [0, 1]$ when $T_l^{g'}(\mathbf{v}) \geq s_l^{g'} r_l v_l^{g'}$ for all $g' \in G$, and $\sum_{l \in L} T_l^g(\mathbf{v}) \geq \sum_{l \in L} T_l^g(\mu^g, \mathbf{v}^{-g})$ for any $\mu^g \in [0, 1]$ when $\sum_{l \in L} T_l^{g'}(\mathbf{v}) \geq s^{g'} r v^{g'}$ for all $g' \in G$. Intuitively, IC requires the national and local representatives of each group to have the weak incentive to truthfully reveal their private information to the planner against all deviations in the form of untruthful messages whenever peace is implemented.

We are now ready to state our result which confirms that peace implementation is limited to the narrow set of cases satisfying the peace condition (2). Note that it is in exactly those cases that peace can be guaranteed also in the absence of information revelation. Therefore, this is effectively an *impossibility result* as the communication of private information fails to promote peace whenever relevant.

Proposition 2 *Given \mathbf{r} and \mathbf{s} , there exists a mechanism that is peace maximizing and incentive compatible if and only if the peace condition (2) holds.*

Proof: Suppose \mathbf{r} and \mathbf{s} take any value such that the peace condition (2) holds. Then, it is straightforward that the simple mechanism

$$T_l^g(\mathbf{v}) = s_l^g r_l \text{ for each } g \in G \text{ and } l \in L$$

satisfies PM and IC thus guaranteeing truthful revelation and the implementation of peace at every level. Now, suppose \mathbf{r} and \mathbf{s} take any value such that the peace condition (2) does not hold. We want to show that either PM or IC must be violated for some \mathbf{v} . We start by showing that, at the national level, it is impossible to extract truthful information about v^g from the groups' national representatives unless the budget is exhausted. To see this, consider any pair of valuation profiles \mathbf{v} and \mathbf{u} with $v^g < u^g \leq 1$ for some $g \in G$. As by PM peace is prioritized and thus always guaranteed at the national level, by IC we must have $\sum_{l \in L} T_l^g(\mathbf{v}) = \sum_{l \in L} T_l^g(\mathbf{u})$ or the national representative of group g would have an incentive to misreport either v^g or u^g . Then, PM and IC jointly require $\sum_{l \in L} T_l^g(\mu^g, \mathbf{v}^{-g}) = s^g r$ for all $\mu^g \in [0, 1]$ and $g \in G$. Having established this, we continue our analysis by considering the behavior of groups' local

representatives. Take any type profile \mathbf{v} and group $g' \in G$ such that

$$s^{g'} r = \sum_{l \in L} r_l s_l^{g'} v_l^{g'}$$

so that the budget is just enough to guarantee group g' is peaceful at each location. By PM we must have $T_l^{g'}(\mathbf{v}) = s_l^{g'} r_l v_l^{g'}$ for all $l \in L$, which combined with IC leads to

$$T_l^{g'}(\mathbf{v}) = s_l^{g'} r_l v_l^{g'} \geq T_l^{g'}(v_l^{g'} + \epsilon, \mathbf{v}_{-l}^{-g'}) \text{ for all } l \in L \text{ and } \epsilon > 0. \quad (5)$$

Consider the alternative profile \mathbf{u} such that $u_{l'}^{g'} = v_{l'}^{g'} + \epsilon$ for some $l' \in L$ and $\epsilon > 0$ while $u_l^{g'} = v_l^{g'}$ for all $l \neq l'$. Note that

$$s^{g'} r < \sum_{l \in L} r_l s_l^{g'} u_l^{g'},$$

so group g' is necessarily conflictual in some location under \mathbf{u} . Suppose ϵ is arbitrarily small so that by PM conflict is prevented in all locations but one, and without loss of generality let l' be among the peaceful locations. Then, by IC we must have

$$T_{l'}^{g'}(\mathbf{u}) = T_{l'}^{g'}(v_{l'}^{g'} + \epsilon, \mathbf{v}_{-l'}^{-g'}) \geq s_{l'}^{g'} r_{l'} (v_{l'}^{g'} + \epsilon),$$

which contradicts (5) as ϵ is assumed positive. \square

To see the intuition for this impossibility result, consider a profile \mathbf{v} such that the peace condition is violated. First, it is impossible to extract information from group representatives at the national level unless the budget is exhausted, so that $t^g = s^g r$. This is because peace is prioritized at the national level – meaning that the national representatives bear no consequence of tightening the budget – so that the only way to achieve their truthfulness is to give them the maximum they can claim. Second, we consider the local level and focus on situations where the budget for peace maximization is tight, so that there are just enough resources for implementing peace at every location. This means that there is a group $g \in G$ such that its representatives in each location $l \in L$ receive transfers $t_l^g = s_l^g r_l v_l^g$, where such transfers sum up to $\sum_{l \in L} t_l^g = t^g = s^g r$. Suppose that everyone truthfully reveals the perceived wastefulness of conflict, but one of these local representatives of group g , say the one in location l' , considers overstating $v_{l'}^g$. Now, such overstatement always increases the expected payoff of the representative of group g in location l' as (i) either conflict is triggered in location l' and the same expected payoff as under truthful revelation is achieved, $t_{l'}^g = s_{l'}^g r_{l'} v_{l'}^g$, or (ii) peace is maintained in l' and a higher transfer is obtained to cover for the overstatement of the preserved fraction, $t_{l'}^g > s_{l'}^g r_{l'} v_{l'}^g$, while conflict is triggered in some other location. If the gap $t_{l'}^g - s_{l'}^g r_{l'} v_{l'}^g$ is

sufficiently small, not all locations will be conflictual and – without loss of generality – we can suppose l' remains peaceful so that we fall into case (ii). Then, as for some local group there is (no loss and) always some benefit from overstating the preserved fraction, truthful revelation fails.

Proposition 2 proves that, due to the informational friction, conflict is unavoidable even when it is so wasteful that (in principle) there are enough transfers to convince all groups to sustain peace. This observation can be linked to the discussion of discordant groups defined in (3). Roughly speaking, our analysis shows that a local group may have an incentive to pretend being short of transfers when it is not so. This pretense is only to the advantage of the group's representatives in the location that claims the shortage of transfers, while against the interest of the remaining group members that face an increased exposure to conflict outbreak in other locations. At its core, the impossibility of conflict resolution via truthful revelation is thus a collective action problem within groups.

2.3 Constrained optimization and local conflict probabilities

In this section we study the planner's constrained optimization of the peace maximizing objective (1) based on prior information only (rather than no information or revealed information, as in the previous two sections). As a result of this analysis, we will obtain the probability of conflict at each location induced by the optimal transfer system.

Let us describe the framework in more detail. In line with our general assumptions on the planner's objective (1) and constraints, we assume that – for each resource distribution \mathbf{r} and group strength distribution \mathbf{s} that violate the peace condition (2) – the planner chooses the transfer scheme \mathbf{t} to maximize the expected (w_l -weighted) number of peaceful locations subject to ensuring peace at the national level:

$$\max_{\mathbf{t}} \sum_{l \in L} w_l p_l(\mathbf{t}_l, \mathbf{s}_l, r_l) \text{ s.t. } t^g = s^g r \text{ for each } g \in G.$$

Here, as previously defined $w_l \in (0, 1)$ denotes the priority weight of location $l \in L$, while $p_l(\mathbf{t}_l, \mathbf{s}_l, r_l)$ denotes the probability of peace at each location $l \in L$. This peace probability is determined by the commonly known distribution of perceived fractions of preserved resources at the local level, $v_l^1, \dots, v_l^{|G|}$, which for simplicity we assume to be independent across locations. For the sake of tractability we also assume that the perceived preserved fractions are independent and identically distributed within locations, according to the cumulative distribution function $\Phi : [0, 1] \rightarrow [0, 1]$. Then, the probability of peace at location $l \in L$ can be written

as¹³

$$p_l(\mathbf{t}_l, \mathbf{s}_l, r_l) = \prod_{g \in G} \Phi(\min\{t_l^g / (s_l^g r_l), 1\})$$

and the corresponding probability of conflict as

$$c_l(\mathbf{t}_l, \mathbf{s}_l, r_l) = 1 - p_l(\mathbf{t}_l, \mathbf{s}_l, r_l).$$

To capture the idea that preserved fractions are hard to predict but – perhaps due to the infamous reputation of ethnic conflict – generally expected to be low, we think of Φ as increasing, differentiable and concave, so that it corresponds to a decreasing density function rendering highly wasteful events comparatively more likely. The power form $\Phi(x) = x^\alpha$ with $\alpha \in (0, 1)$ satisfies these properties and, for α sufficiently small, turns out particularly convenient to obtain an explicit solution.¹⁴

We are now ready to state our result. As we are ultimately interested in an explicit formula for the risk of conflict $c_l(\mathbf{t}_l, \mathbf{s}_l, r_l)$ to be computed in the empirical application, we thereby focus on *interior solutions*, i.e., configurations of \mathbf{r} and \mathbf{s} such that, given the optimal transfer scheme is in place, each discordant group has a positive probability of initiating conflict in each location.¹⁵

Proposition 3 *Let $\Phi(x) = x^\alpha$ with $\alpha \in (0, 1/|G^*|)$. If the optimal system of transfers is implemented and the solution interior, the probability of conflict at each location $l \in L$ is*

$$c_l(\mathbf{t}_l, \mathbf{s}_l, r_l) = 1 - \frac{(w_l)^{|G^*|\alpha/(1-\alpha|G^*)} e_l(\mathbf{t}_l, \mathbf{s}_l, r_l)^{-|G^*|\alpha/[1-|G^*|\alpha]}}{\left[\sum_{l' \in L} (w_{l'})^{1/(1-\alpha|G^*)} e_{l'}(\mathbf{t}_{l'}, \mathbf{s}_{l'}, r_{l'})^{-|G^*|\alpha/[1-|G^*|\alpha]} \right]^{|G^*|\alpha}},$$

where

$$e_l(\mathbf{t}_l, \mathbf{s}_l, r_l) := (r_l/r) \left[\prod_{g \in G^*} (s_l^g / s^g) \right]^{1/|G^*|}. \quad (6)$$

¹³As in the rest of the analysis, we assume that group $g \in G$ at location $l \in L$ acts upon the perceived fraction v_l^g and thus refrains from starting local conflict if and only if $t_l^g < s_l^g r_l v_l^g$.

¹⁴This power form for the cumulative distribution function Φ corresponds to v_l^g following a Beta distribution with parameters $\beta_1 = 1 + \alpha$ and $\beta_2 = 1$.

¹⁵It is straightforward to show that the solution is interior if and only if $t_l^g / (s_l^g r_l) < 1$ for each $g \in G^*$ and $l \in L$, or equivalently

$$\frac{s_l^g r_l}{s^g r} > \frac{(w_l)^{1/(1-\alpha|G^*)} \left[(r_l/r)^{|G^*|} \prod_{g \in G^*} s_l^g \right]^{-\alpha/(1-|G^*|\alpha)}}{\sum_{l' \in L} (w_{l'})^{1/(1-\alpha|G^*)} \left[(r_{l'}/r)^{|G^*|} \prod_{g \in G^*} s_{l'}^g \right]^{-\alpha/(1-|G^*|\alpha)}},$$

which is always satisfied when the parameters are close to symmetric. The proof is available upon request.

Proof: The planner's problem is equivalent to the unconstrained maximization of the following Lagrangian with respect to \mathbf{t} and the vector of multipliers $\lambda := (\lambda_1, \dots, \lambda_{|G|})$,

$$\mathcal{L}(\mathbf{t}, \lambda) = \sum_{l \in L} \prod_{g \in G} w_l \Phi(\min\{t_l^g / (s_l^g r_l), 1\}) + \sum_{g \in G} \lambda^g (s^g r - \sum_{l \in L} t_l^g).$$

It is immediate that $\lambda_g = 0$ for each group $g \notin G^*$, as by (3) for any of them $t^g = r s^g \geq \sum_{l \in L} r_l s_l^g$ and we can thus guarantee they do not initiate conflict in any location $l \in L$ by setting $t_l^g \geq r_l s_l^g$. From now on we then focus on the groups within set G^* and assume an interior solution. By the definition of interior solution all groups in G^* have a chance to initiate conflict in each location, which implies $\lambda^g > 0$ and $\sum_{l \in L} t_l^g = s^g r$ for each $g \in G^*$. For each $l' \in L$ and $g' \in G^*$, the first-order condition for the optimality of $t_{l'}^{g'}$ is

$$\frac{\Phi'(t_{l'}^{g'} / (s_{l'}^{g'} r_{l'}))}{s_{l'}^{g'} r_{l'}} \prod_{g \in G^* \setminus \{g'\}} \Phi(t_{l'}^g / (s_{l'}^g r_{l'})) = \lambda_{g'} / w_{l'},$$

which leads to

$$\frac{\Phi(t_{l'}^{g'} / (s_{l'}^{g'} r_{l'}))}{\Phi'(t_{l'}^{g'} / (s_{l'}^{g'} r_{l'}))} s_{l'}^{g'} r_{l'} = \frac{w_{l'}}{\lambda_{g'}} p_{l'}(\mathbf{t}_{l'}, \mathbf{s}_{l'}, r_{l'}).$$

Given $\Phi(x) = x^\alpha$ with $\alpha \in (0, 1/|G^*|)$, we can write

$$\frac{t_{l'}^{g'}}{\alpha} = \frac{w_{l'}}{\lambda_{g'}} p_{l'}(\mathbf{t}_{l'}, \mathbf{s}_{l'}, r_{l'}).$$

By $s^g r = \sum_{l' \in L} t_{l'}^{g'}$ we then obtain $\lambda_{g'} = \frac{\alpha}{s^g r} \sum_{l \in L} w_l p_l(\mathbf{t}_l, \mathbf{s}_l, r_l)$, and thus

$$\frac{t_{l'}^{g'}}{s^g r} = \frac{w_{l'} p_{l'}(\mathbf{t}_{l'}, \mathbf{s}_{l'}, r_{l'})}{\sum_{l \in L} w_l p_l(\mathbf{t}_l, \mathbf{s}_l, r_l)} = \frac{w_{l'} \prod_{g \in G^*} (t_{l'}^g / (s_{l'}^g r_{l'}))^\alpha}{\sum_{l \in L} w_l \prod_{g \in G^*} (t_l^g / (s_l^g r_l))^\alpha}. \quad (7)$$

It follows that $t_l^g / t_{l'}^{g'} = (w_l / w_{l'}) [p_l(\mathbf{t}_l, \mathbf{s}_l, r_l) / p_{l'}(\mathbf{t}_{l'}, \mathbf{s}_{l'}, r_{l'})]$ for all $g \in G^*$ and $l, l' \in L$, which leads to

$$\frac{p_l(\mathbf{t}_l, \mathbf{s}_l, r_l)}{p_{l'}(\mathbf{t}_{l'}, \mathbf{s}_{l'}, r_{l'})} = \frac{\prod_{g \in G^*} (t_l^g / (s_l^g r_l))^\alpha}{\prod_{g \in G^*} (t_{l'}^{g'} / (s_{l'}^{g'} r_{l'}))^\alpha} = \left[\frac{p_l(\mathbf{t}_l, \mathbf{s}_l, r_l)}{p_{l'}(\mathbf{t}_{l'}, \mathbf{s}_{l'}, r_{l'})} \right]^{\alpha |G^*|} \left[\frac{w_l}{w_{l'}} \right]^{\alpha |G^*|} \left[\frac{r_l}{r_{l'}} \right]^{-\alpha |G^*|} \left[\frac{\prod_{g \in G^*} s_l^g}{\prod_{g \in G^*} s_{l'}^{g'}} \right]^{-\alpha}$$

and therefore to

$$\frac{w_{l'} p_{l'}(\mathbf{t}_{l'}, \mathbf{s}_{l'}, r_{l'})}{\sum_{l \in L} w_l p_l(\mathbf{t}_l, \mathbf{s}_l, r_l)} = \frac{(w_{l'})^{1/(1-\alpha|G^*|)} \left[(r_{l'}/r)^{|G^*|} \prod_{g \in G^*} (s_{l'}^g / s^g) \right]^{-\alpha/(1-|G^*|\alpha)}}{\sum_{l \in L} (w_l)^{1/(1-\alpha|G^*|)} \left[(r_l/r)^{|G^*|} \prod_{g \in G^*} (s_l^g / s^g) \right]^{-\alpha/(1-|G^*|\alpha)}}.$$

By (7), the transfer to each group $g \in G^*$ in location $l' \in L$ is then

$$t_{l'}^g = s^g r \frac{(w_{l'})^{1/(1-\alpha|G^*|)} \left[(r_{l'}/r)^{|G^*|} \prod_{g \in G^*} (s_{l'}^g/s^g) \right]^{-\alpha/(1-|G^*|\alpha)}}{\sum_{l \in L} (w_l)^{1/(1-\alpha|G^*|)} \left[(r_l/r)^{|G^*|} \prod_{g \in G^*} (s_l^g/s^g) \right]^{-\alpha/(1-|G^*|\alpha)}},$$

and given $p_{l'}(\mathbf{t}_{l'}, \mathbf{s}_{l'}, r_{l'}) = \prod_{g \in G^*} (t_{l'}^g/(s_{l'}^g r_{l'}))^{\alpha}$, the probability of peace in $l' \in L$ is

$$p_{l'}(\mathbf{t}_{l'}, \mathbf{s}_{l'}, r_{l'}) = \frac{(w_{l'})^{|G^*|\alpha/(1-\alpha|G^*|)} \left[(r_{l'}/r)^{|G^*|} \prod_{g \in G^*} (s_{l'}^g/s^g) \right]^{-\alpha/(1-|G^*|\alpha)}}{\left[\sum_{l \in L} (w_l)^{1/(1-\alpha|G^*|)} \left[(r_l/r)^{|G^*|} \prod_{g \in G^*} (s_l^g/s^g) \right]^{-\alpha/(1-|G^*|\alpha)} \right]^{|G^*|\alpha}}.$$

The corresponding probability of conflict is $c_{l'}(\mathbf{t}_{l'}, \mathbf{s}_{l'}, r_{l'}) = 1 - p_{l'}(\mathbf{t}_{l'}, \mathbf{s}_{l'}, r_{l'})$. \square

Proposition 3 delivers the principal testable prediction of our model. In particular, we expect a high correlation between the theoretical prediction of the local conflict risk c_l and the observed frequency of local conflict events. This conflict risk c_l is decreasing in the priority weight w_l that the planner assigns to location l but increasing in e_l , which we call the *conflict exposure index*. However, the priority weight is typically unknown but may well capture some known local determinants of local conflict, such as the presence of active mines or the share of the president's co-ethnics residing in a given ward. In contrast, the conflict exposure index captures the more systemic (and, arguably, more interesting) effects of the country's entire ethnic and mining geography on local conflict. In our empirical analysis, we will thus focus on the conflict exposure index while controlling for some known local determinants of local conflict.¹⁶

We now discuss the determinants and structure of the conflict exposure index. By its definition (6), this index – and, therefore, the corresponding conflict risk – depends on the interplay of two complementary forces. The first is the relative presence of contestable resources, r_l/r , which quantifies the greed motive for conflict initiation in the location. The second is the geometric mean of the discordant groups' relative population shares, $D_{l,G^*} := \left[\prod_{g \in G^*} (s_l^g/s^g) \right]^{1/|G^*|}$, which can be interpreted as a measure of the ethnic diversity among the discordant groups and quantifies the propensity to miscoordinate their grievance claims due to over-representation at

¹⁶The conflict exposure index, defined in (6), is not a probability, as it abstracts from average effects on a country's propensity to conflict across locations. Such average effects are instead captured by the denominator of c_l (which one can show is a measure of the dispersion of the distribution of the priority weights and the exposure indices) or perhaps more conveniently by the peace deficit Δ (which instead is independent of the unknown priority weights). Nevertheless, the conflict exposure index is perfectly valid and practically convenient to understand within-country variation in the relative propensity to conflict.

the local level.¹⁷ The complementarity of these two forces is captured by the multiplicative form of the conflict exposure index: $e_l = (r_l/r)D_{l,G^*}$. Intuitively, both greed and miscoordination must play a role for conflict to occur.

We now dig a bit deeper into why these two forces drive the propensity to conflict and, more generally, into the intuition behind Proposition 3. Recall that, as peace is always guaranteed at the national level, the total transfers t^g a group g gets are fixed by the national-level constraint determined by its overall demographic presence, $t^g = s^g r$. By the violation of the peace condition, there must be discordant groups that are over-represented in resource-rich locations. For the planner, it is impossible to provide local transfers t_l^g that are sufficiently high to prevent these groups from initiating conflict. Therefore, the planner will have to compromise trying to minimize the expected (w_l -weighted) number of conflictual locations taking into account that these groups might initiate conflict in each and every location (in the interior solution we focus on). However, the costs of “buying peace” differs across locations. First, it depends on the relative resource rents, r_l/r , as by the concavity of Φ the planner can buy peace with comparatively low local transfers by targeting the discordant groups in resource-poor locations. Therefore, the planner optimally allocates transfers such that the conflict probability is increasing in r_l/r . Second, by similar (concavity) arguments, the planner can buy peace with comparatively low transfers by targeting the representatives of a group in locations where this group is comparatively small. Therefore, the planner optimally allocates transfers such that the conflict probability increases in s_l^g/s^g for groups $g \in G^*$. Third, in locations where many discordant groups are over-represented – so that D_{l,G^*} is high – chances are high that at least one discordant group initiates local conflict.

3 Setting and data

In this section, we present the main tests of our theoretical model, which are based on granular data from Sierra Leone. In Appendix C, we document the external validity of our results in a sample of eight West African countries but relying on less granular data. After some background information about Sierra Leone, we introduce our data. We then test to which degree the theoretically predicted local conflict exposure explains the observed local conflict exposure. We do so both in the cross-section and a panel setting, presenting results from both OLS and 2SLS regressions. Finally, we show how the peace deficit correlates with the country-wide conflictuality in Sierra Leone over time.

¹⁷From a theoretical perspective, the interpretation of D_{l,G^*} as a measure of ethnic diversity follows from the application of the (inverse of) the principle of transfers in inequality measurement, as D_{l,G^*} increases whenever population is marginally transferred from an over-represented to an under-represented group.

3.1 Sierra Leone

Sierra Leone is a former British colony in West Africa with a current population of 8 million people and a landmass of $71,740 \text{ km}^2$ (similar to the Republic of Ireland or the State of Washington). Mineral mining has a long tradition in Sierra Leone. It started on a large scale in the 1930s with the founding of the Sierra Leone Development Company (DELCO), which obtained the rights to mine iron in Marampa, where there is still a large iron mine as of 2022. Sierra Leone became independent in 1961. The first few years after independence were characterized by peace and economic growth. However, soon politics was dominated by coups, a switch to a one-party constitution, the violent suppression of the opposition, and kleptocratic tendencies within the elite.

The Sierra Leonean civil war started in 1991 when the “Revolutionary United Front” (RUF) invaded from neighboring Liberia. The government of Sierra Leone was unable to react to this insurgency because of poor government finances, weak state capacity, a weak economy, and public unrest. The conflict spread over the entire country and was accompanied by two coups within the government of Sierra Leone and deteriorating discipline within the Sierra Leone Army (SLA) (Bellows and Miguel, 2009). Outright battles between the SLA and the RUF were the exception. Instead the primary targets of violence were civilians and, in case of RUF, local chiefs. The inability of the government to defend communities led to the formation of “Community Defence Forces” (CDF), mostly consisting of civilians and traditional hunter groups (Bellows and Miguel, 2006). The final phase of the civil war started with a RUF attack on the capital Freetown in 1999, which prompted a UN intervention led by the United Kingdom. This intervention ended the civil war in 2002. In total, more than 50,000 people were killed in this civil war (Bellows and Miguel, 2006).

Diamonds played a crucial role in the financing of all organized armed forces. All industrial mining operations came to a halt after the beginning of the civil war, but diamonds could easily be mined with forced labor and little capital. Moreover, given the prevailing disorder and chaos in the county, it was possible to export large quantities of illicitly mined diamonds. As a result, fighting was particularly fierce in diamond-rich areas (Bellows and Miguel, 2009), and all combatants had an incentive to keep the civil war and the war economy going (Bellows and Miguel, 2006).

Ethnicity, in turn, seems to have only played a minor role in the civil war, although initial recruitment within the CDF followed ethnic lines to some degree (Bellows and Miguel, 2006). There is no evidence that RUF rebels targeted specific ethnic groups or that ethnic-misalignment between armed groups and the local population explains abuse intensity (Bellows

and Miguel, 2009; Conibere et al., 2004; Humphreys, 2005). Moreover, although failing public services are associated with the unrest, there is no evidence that ethnic diversity itself is affecting the local provision of public goods within the country (Glennerster et al., 2013).

The importance of diamonds (especially artisanally mined ones) has constantly decreased since the end of the civil war. The resurgence of industrial mining operations in diamonds, bauxite, iron, and rutile has dramatically shifted the export portfolio of Sierra Leone over the last two decades. This portfolio is now dominated by bauxite and iron exports. Overall, the mining sector accounted for 65% of Sierra Leone’s exports in 2018 and for a large share of its government revenues (around 10% in recent years).¹⁸ Currently, most mineral production results from six industrial mining sites, with two gold mines being planned but not yet completed. In addition, there are known deposits of other precious metals, such as chromite, coltan, columbite, limonite, platinum, tantalite, and zircon.¹⁹

3.2 Data

The main reason for focusing on Sierra Leone is that we can obtain granular, i.e., spatially disaggregated, data on the distribution of ethnic groups, the location and size of mines, and conflict events. Another advantage, which we leverage below, is that different minerals are mined in different parts of Sierra Leone and that the relative importance of these minerals has changed multiple times over the last two decades.

We construct a panel dataset with 107 Sierra Leonean (electoral) wards as the cross-sectional dimension and 22 years as the temporal dimension. Most wards coincide with historical chiefdoms or encompass multiple smaller chiefdoms. They are the lowest level of aggregation for which we can obtain census information on the population shares of the different ethnic groups.²⁰ The average ward has an area of 670 km² (which is less than a quarter of the area of the 0.5 × 0.5 decimal degree grid cells commonly used in conflict studies). Our sample period starts in 1997 (as the conflict data is unavailable for earlier years) and ends in 2018 (as we have no access to some of the mining data for later years). In our cross-sectional analyses, we will use time-averaged values for each ward.

In what follows, we discuss the ethnicity and natural resource data necessary to compute our

¹⁸See <https://www.investingsierraleone.com/natural-resources/>. Prior to the civil war, minerals accounted for 90% of exports and 20% of government revenues (Kaldor and Vincent, 2006).

¹⁹See <https://www.trade.gov/country-commercial-guides/sierra-leone-mining-and-mineral-resources>.

²⁰To build a shape file representing the boundaries of these wards, we use the shape file of chiefdoms provided by Acemoglu et al. (2014) and aggregate the chiefdoms in their file to match the wards reported in the 2004 Population and Housing Census of Sierra Leone.

measure of predicted conflict exposure e_l . We then discuss our measure of observed conflict exposure. Summary statistics for all variables are provided in [Table B-1](#).

3.2.1 Ethnic geography and local over-representation

To compute the predicted conflict exposure, we need information on the population s_l^g of each ethnic group g in each ward l . We obtain this information from the 2004 Housing and Population Census of Sierra Leone ([IPUMS International, 2020](#)). The census provides information on the ethnic affiliation of each tenth household in Sierra Leone at the level of wards. The four most populous groups are the Mende (with a country-level population share of 32.9 percent), the Temne (32.2 percent), the Limba (8.3 percent), and the Kono (4.5 percent).²¹ Our sample includes for more groups with a population share of more than one percent. We have to assume that the spatial distribution of ethnic groups remains unchanged during our sample period; as such fine-grained data on the spatial distribution of ethnic groups is unavailable for other years. This assumption, however, is appealing given our interest in how conflict depends on the spatial distribution of resource rents (rather than on the country’s ethnic geography).

According to our theoretical model, what matters is the ethnic groups’ local over-representation s_l^g/s^g , i.e., the ratios of the population share of each group in each ward relative to the group’s national population share. [Figure 2](#) plots the local over-representation of the four most populous ethnic groups across wards. We see considerable spatial variation in their local over-representation. The Kono are concentrated in the east of the country, the Limba mainly in the north, the Mende in the south, and the Temne in the west and the center.²²

3.2.2 Mines and local resource rents

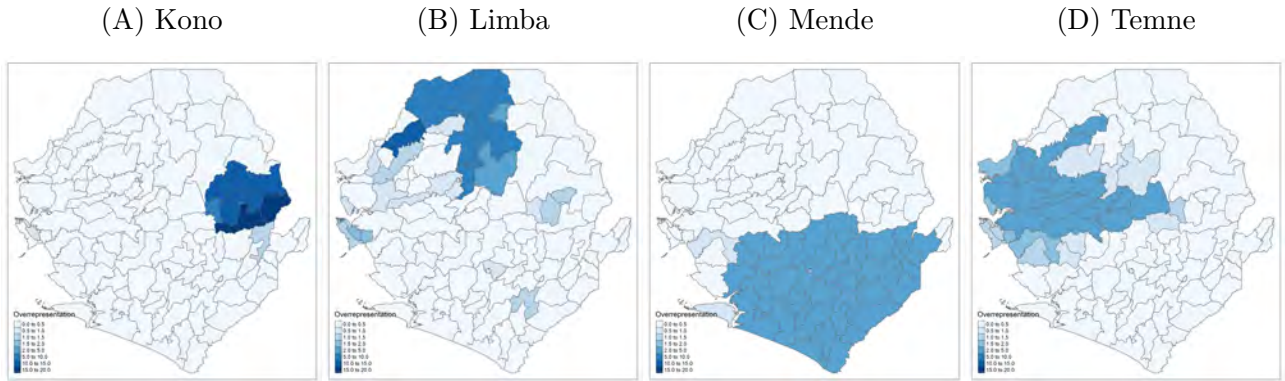
To build a time-varying measure of the resource rents r_l in each ward l , we use data on the location and size of industrial mines as well as data on the importance of the corresponding minerals over time. We first introduce these data and then discuss how we compute the resource rents r_l .

We use two geo-spatial datasets on industrial mines. The first is the Raw Material Data (RMD) of the S&P Global Market Intelligence Unit (accessed in June 2019). The RMD provides information on global mining activities since 1980, including the (approximate) location, name,

²¹These four largest ethnic groups are also the only groups that are politically important throughout the sample period according to the Ethnic Power Relations data by [Wucherpfennig et al. \(2011\)](#) and [Vogt et al. \(2015\)](#).

²²[Figure B-1](#) in [Appendix B](#) plots the local over-representation of the remaining eight groups with a national population share of more than one percent.

Figure 2: Local over-representation of the four largest ethnic groups



Notes: Panels A–D plot the local over-representation (s_i^g/s^g) across wards for the most populous ethnic groups.

owner, primary commodity, and the years in which a mine is active. It, however, lacks discovery dates, and its information on the amounts extracted is incomplete. The second dataset is the global dataset of mining areas produced by [Maus et al. \(2020\)](#). They leverage recent satellite images and machine learning techniques to identify the extent of actual mines within close proximity of the sometimes imprecise locations reported in the RMD. We match the two datasets so that we have information on the primary commodity of each industrial mine (from RMD) as well as the location and shapes (polygons) of the corresponding mining areas (from [Maus et al., 2020](#)).²³ Panel A of [Figure 3](#) shows the resulting spatial distribution of industrial mining areas, with different colors indicating different main minerals extracted. We can see that diamonds are exclusively mined in the east of the country, bauxite and rutile in the south-west, and iron primarily north of the center.

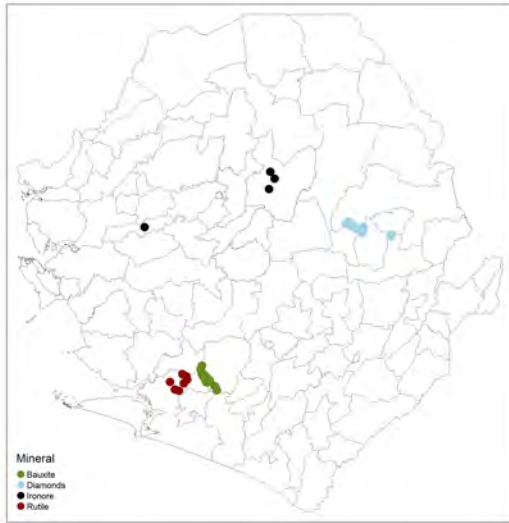
We measure the (time-varying) importance of the different minerals for Sierra Leone based on their net exports. For this purpose, we use the export and import data from [UN Comtrade \(2021\)](#) and compute the value of net exports in current prices for each mineral and year (thereby setting negative values to zero). Panel B of [Figure 3](#) shows each mineral’s net exports as a share of the total net exports from the five main minerals.²⁴ We see considerable intertemporal variation in the different minerals’ relative importance: Diamonds were the most important mineral up to 2004, bauxite from 2005–2011, and iron thereafter. Gold and rutile play only a minor role throughout the sample period.

²³Some mines consist of multiple mining areas in close proximity to one another. We check each individual industrial mine using Google Earth and verify the existence of the mine using auxiliary data (see [Section A-1](#)).

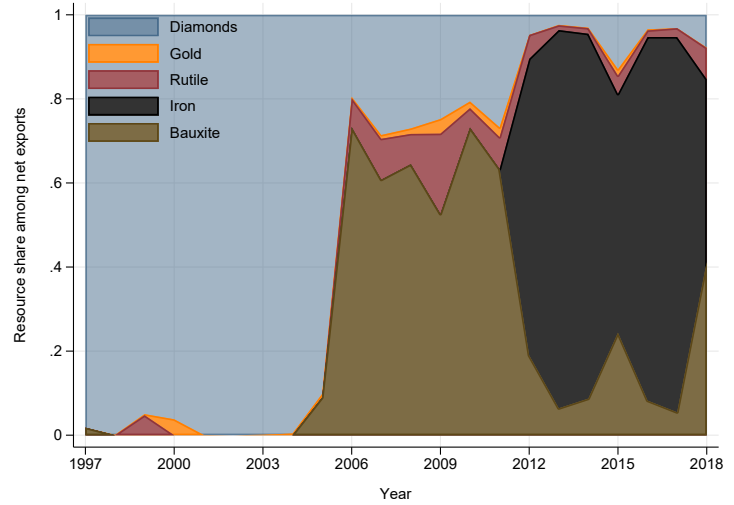
²⁴[Figure B-2](#) presents each mineral’s net exports relative to GDP in current prices. This figure highlights that the overall importance of the mining sector has been greatest during the civil war (given the imploding GDP) and in later years (thanks to the iron boom and in spite of robust growth).

Figure 3: Locations of mining areas and the relative importance of different mineral

(A) Locations of mining areas



(B) Share of net exports of different minerals



Notes: Panel A plots the locations of all industrial mining areas reported in [Maus et al. \(2020\)](#), with different colors indicating different minerals. Panel B plots the net exports from each mineral as a share of the total net exports from the five main minerals (bauxite, diamonds, gold, iron, rutile).

We use these data to build our measure of local resource rents r_l , which increases in the size and proximity of mining areas as well as the importance of the corresponding mineral in a given year. We proceed in two steps. First, we distribute the annual revenues (as measured by net exports) across mining areas. For each mineral, we distribute the mineral-specific annual revenues across all mining areas that primarily extract the respective mineral; and we do so in proportion to the size of these areas.²⁵ Second, we compute each ward's annual resource rents r_l based on the mining area-specific annual revenues. For each mining area, we assume that the rents that accrue in different wards are proportional to the inverse geodesic distance between the centroids of the mining area and the different wards. This assumption is consistent with the presence of spatial spillovers from resource extraction.²⁶ The use of the inverse distance represents a specific distance decay.²⁷ We test for the robustness of our results with respect to alternative distance decays in [Section 4.3](#).

²⁵That is, if Sierra Leone had two iron mining areas, labelled A and B, and if area A were twice as large as area B, then we would assign two-thirds of the annual iron revenues to area A and one-third to area B. We later present robustness tests using alternative approaches for distributing annual revenues in space.

²⁶[Aragón and Rud \(2013\)](#) document that spillovers from gold mining can extend up to 100 km. Another reason is that nearby localities may also host some crucial infrastructure or bear some negative externalities and may therefore lay claims on the royalties; see, e.g., [Bruederle and Hodler \(2019\)](#) for evidence of negative health externalities in nearby areas.

²⁷The resource literature and the conflict literature, unlike the trade literature, lack well established distance decay functions.

It is the relative local resource rents r_l/r that matter according to our theoretical model. Panel A of [Figure 4](#) below shows the distribution of r_l/r , averaged over the entire sample period, across wards. By construction, these shares are highest close to large mining areas and much smaller further away. The left-most columns of [Figure 5](#) show the corresponding distributions when averaging r_l/r over various shorter time periods. There are remarkable changes in the spatial patterns over time because different minerals are extracted in different parts of the country (seen in panel A of [Figure 3](#)) and important in different years (seen in panel B of [Figure 3](#)). For example, there is a large iron mine but no other mines north of the center. Therefore, this area had comparatively low relative local resource rents until the beginning of the iron boom in 2012.

3.2.3 Observed conflict exposure

We base our measure of observed conflict exposure on the Armed Conflict Location and Event Data (ACLED) ([Raleigh et al., 2020](#)). ACLED contains information on the date and type of conflict events, the involved actors (e.g., the government, rebel groups, or civilians), and the geo-location. It is widely used in the literature on civil conflict (e.g., [Berman and Couttenier, 2015](#); [Berman et al., 2017](#); [Eberle et al., 2020](#)). Following [Eberle et al. \(2020\)](#), we include events classified as battles, riots, or violence against civilians. However, our results are robust to including all events (including protests and strategic deployments as in [Berman et al. \(2017\)](#) and [McGuirk and Nunn \(2020\)](#)).

People typically feel exposed to conflict even if conflict events occur elsewhere in the country, e.g., because they know that there is some randomness in the exact location of every event. However, they tend to feel less exposed, the further away conflict events occur. We, therefore, construct our ward-level measure of observed conflict exposure in a similar manner as our ward-level measure of local resource rents. That is, we weigh each event by the inverse distance between the conflict location and the centroid of the ward and then calculate the sum of these inverse distance-weighted events for each ward. The resulting conflict exposure measure is strictly positive (albeit potentially very close to zero) whenever there is at least one conflict event (which holds true in any year of our sample period). This, in turn, will allow us to estimate elasticities using log-log specifications without adding an arbitrary constant ([Chen and Roth, 2022](#)).

4 Empirical validation

4.1 Cross-sectional evidence

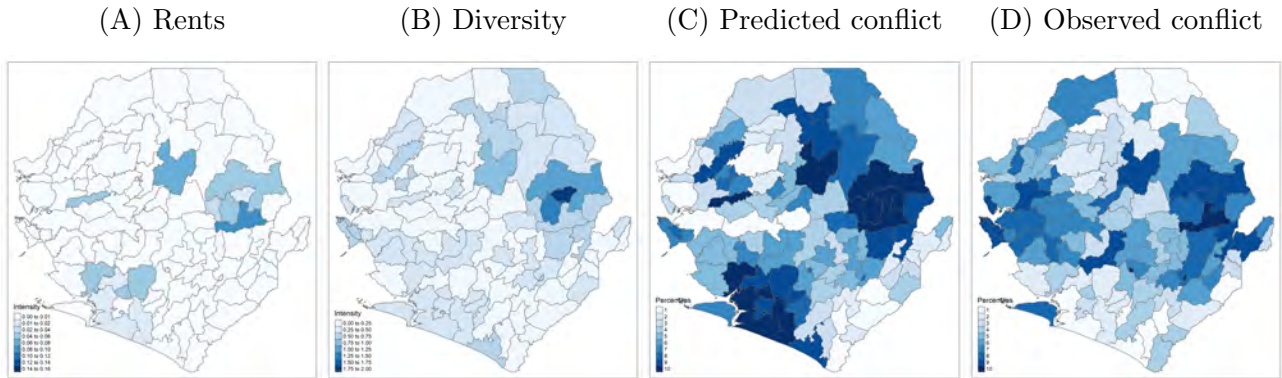
Given that our theoretical model is static, we first evaluate its predictive power by comparing the predicted and observed conflict exposure across the 107 wards in our sample. We do so with values averaged over the entire sample period as well as with values averaged only during the diamond-, bauxite- or iron-dominated periods.

Mechanism and graphical evidence: The predicted conflict exposure depends on the local over-representation of ethnic groups and the relative local resource rents. We now discuss how the interplay of this ethnic geography (seen in [Figure 2](#)) and this mining geography (e.g., seen in panel A of [Figure 4](#)) leads to the predicted local conflict exposures. In a first step, these geographies shape the set of discordant ethnic groups. To provide the intuition, let us focus on the four main ethnic groups and the three different time periods identified above. The Kono are over-represented in the diamond-mining area. According to our theoretical model, they were deprived from some local resource rents and part of the set of discordant groups in most years, except in some late years when diamonds played a very marginal role. The Mende, who are over-represented in the bauxite-mining area, were part of the discordant groups exclusively during the bauxite boom, and the Limba, who are over-represented in the iron-mining area were part of the discordant groups exclusively during the iron boom. The Temne too were part of the discordant groups in some years during the iron boom.²⁸ Knowing the set of discordant groups in any given year and their local over-representation allows computing the ethnic diversity among the discordant groups D_{l,G^*} for any ward and year. [Figure 4](#) maps these local diversity indices averaged over the entire sample period in panel B, while [Figure 5](#) depicts separate maps for the diamond-, bauxite- or iron-dominated periods in panels B, F and J. We see large changes in the ethnic diversity among discordant groups over time, resulting from the changes in the relative local resource rents and the associated changes in the set of discordant groups.

In a second step, the relative local resource rents and these diversity indices jointly determine the predicted conflict exposure across wards. Panel C of [Figure 4](#) maps the predicted conflict exposure (in percentiles) averaged over the entire sample period. It is particularly high in areas where both the relative local resource rents and the local diversity index are comparatively high (as seen in panels A and B of this figure). Finally, panel D shows the observed conflict exposure (in percentiles). Comparing panels C and D suggests a positive correlation between predicted and observed conflict exposures in most parts of the country. The raw correlation between the

²⁸[Figure B-4](#) shows how the set of discordant groups changes over time.

Figure 4: Resource rents, ethnic diversity among discordant groups, and predicted and observed conflict exposure averaged over the entire sample period



Notes: Panel A plots the relative local resource rents r_l/r ; panel B the ethnic diversity among discordant groups D_{l,G^*} ; panel C the predicted conflict exposure e_l (in percentiles); and panel D the time-averaged observed conflict exposure (in percentiles). All values are averaged over the entire sample period (1997–2008).

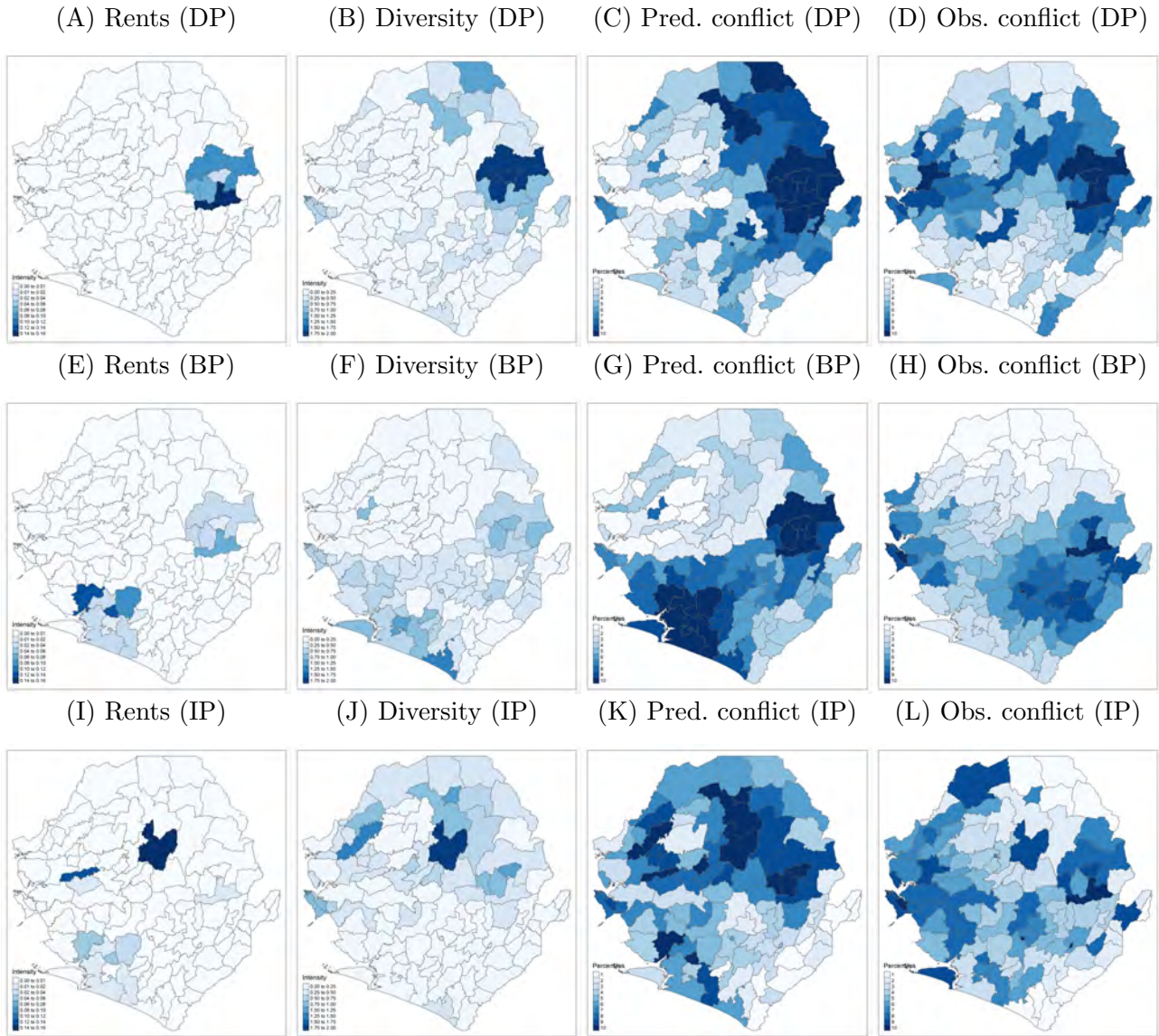
log-transformed predicted and observed conflict exposures is 0.23. The difference between these two measures is largest in the south west of the country. This area has been quite peaceful, but our predicted conflict exposure is fairly high. A possible reason is that these wards are not very populous and have relatively low population density (see [Figure B-3](#)), which may lower the number of actual conflict events and the probability of such events being reported ([Eck, 2012](#)). [Figure 5](#) maps the predicted and observed conflict exposure for the different sub-periods. We find that predicted and observed conflict exposure change in a somewhat synchronized manner over time, with the raw correlation ranging from 0.22 (in the diamond-dominated period, DP) to 0.29 (in the iron-dominated period, IP).

OLS estimates: We now evaluate the predictive power of our theoretical model using the following cross-sectional OLS regression in our sample of 107 wards:

$$\ln(\text{Observed conflict exposure}_l) = \beta \ln(\text{Predicted conflict exposure}_l) + \Gamma \mathbf{X}_l + \epsilon_l, \quad (8)$$

where \mathbf{X}_l is a vector of ward-level control variables that includes the log of population based on the 2004 census and the log of area, which jointly imply that we also control for the log of population density, as well as fixed effects for the four provinces. Coefficient β corresponds to the elasticity between predicted and observed conflict exposure across wards. When interpreting this elasticity, it is important to keep in mind that the theoretically predicted conflict exposure e_l only captures the systemic effect of a country’s ethnic and mining geographies on the probability of local conflict and, thereby, ignores mechanical determinants like population size and political

Figure 5: Resource rents, ethnic diversity among discordant groups, and predicted and observed conflict exposure across different time periods



Notes: Panels A–D are based on the period dominated by diamond exports (DP, 1997–2004); panels E–H on the period dominated by bauxite exports (BP, 2005–2011); and panels I–L on the period dominated by iron exports (IP, 2012–2018). Panels A, E and I plot time-averaged values of the relative local resource rents r_l/r ; panels B, F and J the time-averaged ethnic diversity among discordant groups $D_{l,C*}$; panels C, G and K the time-averaged predicted conflict exposure e_l (in percentiles); and panels D, H and L the time-averaged observed conflict exposure (in percentiles).

economy determinants related to, e.g., ethno-regional favoritism (see discussion at the end of [Section 2.3](#)). While our theoretical model is silent about the magnitude of this elasticity, we expect it to be positive and statistically significant.

Table 1: Cross-sectional elasticity between predicted and observed conflict exposure

	<i>Dependent variable: Log observed conflict exposure</i>			
	(1)	(2)	(3)	(4)
<i>Panel A: Full period</i>				
Log predicted conflict exposure	0.140*** (0.044)	0.120*** (0.041)	0.055** (0.024)	0.053* (0.028)
R2	0.0648	0.245	0.773	0.833
<i>Panel B: Diamond period</i>				
Log predicted conflict exposure	0.097*** (0.023)	0.085*** (0.016)	0.068** (0.030)	0.089** (0.035)
R2	0.0967	0.238	0.537	0.684
<i>Panel C: Bauxite period</i>				
Log predicted conflict exposure	0.105** (0.048)	0.117*** (0.044)	0.065** (0.027)	-0.021 (0.032)
R2	0.0649	0.245	0.736	0.794
<i>Panel D: Iron period</i>				
Log predicted conflict exposure	0.174* (0.096)	0.127* (0.074)	0.091*** (0.031)	0.071** (0.028)
R2	0.0695	0.218	0.762	0.832
Population control	–	✓	✓	✓
Area control	–	–	✓	✓
Province-fixed effects	–	–	–	✓
Observations	107	107	107	107

Notes: The table reports the result of regressing the log of observed conflict exposure on the log of predicted conflict exposure (see eq. 8), with different control variables and fixed effects across columns (1)–(4). Population control is the log of ward population based on the 2004 census. Area control is the log of ward area. Panel A provides cross-sectional evidence after time-averaging all the included variables across the entire sample period (1997–2018). Panel B averages all variables across the period dominated by diamond exports (1997–2004), panel C across the period dominated by bauxite exports (2005–2011), and panel D by the period dominated by iron ore exports (2012–2018). Standard error are spatially clustered with a distance cutoff of 100km. * $p < 0.1$, ** $p < 0.05$, *** $p < 0.01$

Table 1 presents our main cross-sectional estimates with spatially clustered Conley standard errors.²⁹ Panel A shows the results when all variables are time-averaged over the entire sample period (1997–2018). The different columns differ in the set of control variables and fixed effects. The estimated elasticity is positive in all columns and statistically significant at the 5 percent level unless we add province-fixed effects. The estimated elasticity is 14 percent in the absence

²⁹Standard errors are estimated using the `acreg` package by Colella et al. (2019). We enforce a linear decay in the spatial dependence of the error terms with a distance cutoff of 100km. We later show that the results do not depend on this specific distance cutoff.

of any control variables in column (1) and drops to around 5.5 percent in the more demanding specifications in columns (3) and (4). The R2 is 0.065 in column (1) and increases to 0.245 when controlling for the ward-level population in column (2).³⁰ Hence, the systemic component highlighted by our model can explain roughly one third of the variation explained by population, which is a well-established and rather mechanical predictor of conflict.

In panels B–D, we focus on different time periods dominated by different minerals. As discussed before, the spatial distribution of local resource rents and the theoretically predicted conflict exposure differ remarkably across these periods. Nevertheless, we find a positive and statistically significant elasticity between predicted and observed conflict exposure in all periods (except in column (4) of Panel C). In addition, the R2 is typically of similar size as in Panel A. We conclude that the main results reported in panel A are not driven by a single period.

4.2 Panel data and IV evidence

The cross-sectional evidence confirms the predictive power of our theoretical model but does not lend itself to a causal interpretation. To allow for causal interpretation, we use the entire panel of 107 wards over 22 years and run standard OLS fixed effects regressions and adapt a commonly used instrumental variables (IV) approach.

Empirical strategy: The OLS fixed effects specification is:

$$\ln(\text{Observed conflict exposure}_{lt}) = \delta \ln(\text{Predicted conflict exposure}_{lt}) + FE_l + FE_t + \varepsilon_{lt}, \quad (9)$$

where FE_l and FE_t are ward- and year-fixed effects, respectively. Our coefficient of interest is δ , which captures the intertemporal elasticity of observed conflict exposure with respect to predicted conflict exposure.

OLS estimates are potentially biased because conflict events may reduce mining activities and, thereby, local resource rents and the predicted conflict exposure. Such endogeneity concerns are common in studies on the effect of resource rents on conflict. Many researchers rely on plausibly exogenous variation in global mineral prices to mitigate these concerns (e.g., [Bazzi and Blattman, 2014](#); [Berman and Couttenier, 2015](#); [Berman et al., 2017](#); [Dube and Vargas, 2013](#)). We adopt this identification strategy and construct shift-share instruments that interact exogenous price shocks with cross-sectional exposure shares based on the wards' proximity to different mining areas. Following [Berman et al. \(2017\)](#), we measure these shocks by the log of

³⁰The R2 is 0.198 when regressing the log of observed conflict exposure on the log of ward population only (result not reported).

the global mineral prices. The exposure shares are based on the proximity of a ward to the different mining areas of a particular mineral, whereby we again weigh each mining area by its size relative to the size of the other mining areas extracting the same mineral. Hence, our shift-share instruments are proximity-price interactions.

The first stage of our main 2SLS specification is

$$\ln(\text{Predicted conflict exposure}_{it}) = \sum_{j=B,D,I} \gamma_j [\ln(\text{proximity}_i^j) \times \ln(\text{price}_t^j)] + FE_i + FE_t + \nu_{it}, \quad (10)$$

where B , D , and I stand for the three main minerals: bauxite, diamonds, and iron.³¹ The separate inclusion of the three proximity-price interaction terms implies that we are allowing their effects to be heterogeneous.³² These interaction terms allow for identification via exogenous shocks as in [Borusyak et al. \(2022\)](#) (rather than identification via exogenous exposure shares as in [Goldsmith-Pinkham et al., 2020](#)). Hence, our identification strategy relies on the assumption that conflict events in Sierra Leone do not impact global mineral prices. This assumption seems plausible given that Sierra Leone’s exports are rather unimportant in the global trade of these minerals, with global export shares below two percent for bauxite, diamonds, and iron ([UN Comtrade, 2021](#)). The second stage of our main 2SLS specification is identical to equation (9) except that we replace the explanatory variable with its predicted value.

Main results: [Table 2](#) presents our panel data estimates. Panel A reports the OLS fixed effects estimates. Column (1) presents the results of equation (9). We find an estimated intertemporal elasticity of observed conflict exposure with respect to predicted conflict exposure of around 6 percent. Columns (2)–(4) add linear time trends for ever smaller subnational administrative units. The coefficient estimates remain statistically significant but become somewhat smaller.

Panels B and C of [Table 2](#) present our 2SLS estimates, phasing in more local linear time trends throughout the columns. The second-stage results in Panel B show that the estimated intertemporal elasticity of observed conflict exposure with respect to predicted conflict exposure is around 16–19 percent, which is substantially higher than our OLS fixed effects estimates. This difference suggests that mining activities may indeed fall in response to conflict events. Panel

³¹Remember that net export revenues from gold and rutile are much smaller than those from the three main minerals (see [Figure 3](#)). We abstract from gold, as it is currently only mined in artisanal mines, and from rutile, as we only observe exports and prices for titanium metals (which include rutile), but not for rutile specifically. We later provide robustness tests using all industrially mined minerals in the first-stage.

³²[Figure B-5](#) shows the cross-sectional and temporal distributions of the different components of our shift-share instruments. The depicted variables entering the interaction terms are all absorbed by the ward and year-fixed effects.

Table 2: Within elasticity between predicted and observed conflict exposure

	<i>Dependent variable:</i> <i>Log observed conflict exposure</i>			
	(1)	(2)	(3)	(4)
<i>Panel A: OLS</i>				
Log predicted conflict exposure	0.064*** (0.020)	0.047*** (0.017)	0.041** (0.018)	0.041** (0.020)
R2	0.516	0.560	0.567	0.583
<i>Panel B: 2SLS (second stage)</i>				
Log predicted conflict exposure	0.189*** (0.066)	0.171** (0.069)	0.165** (0.069)	0.161*** (0.059)
R2	0.496	0.543	0.552	0.570
<i>Panel C: 2SLS (first stage) – Dependent variable: Log predicted conflict exposure</i>				
Bauxite proximity-price interaction	2.643*** (0.460)	2.882*** (0.434)	3.102*** (0.448)	3.286*** (0.407)
Diamond proximity-price interaction	-2.924*** (0.331)	-1.583*** (0.359)	-0.668* (0.362)	-0.650 (0.426)
Iron proximity-price interaction	0.311*** (0.112)	0.157 (0.113)	-0.014 (0.119)	-0.439*** (0.157)
First-stage F-stat	43.42	22.34	19.18	25.12
Ward-fixed effects	✓	✓	✓	✓
Year-fixed effects	✓	✓	✓	✓
Province trends	–	✓	–	–
District trends	–	–	✓	–
Ward trends	–	–	–	✓
Observations	2354	2354	2354	2354

Notes: The table reports the results of regressing the log of observed conflict exposure on the log of predicted conflict exposure as well as ward- and year-fixed effects (see eq. 9), with different time trends across columns (1)–(4). Panel A reports OLS fixed effects regressions. Panel B reports second-stage 2SLS regressions and panel C the corresponding first stage (see eq. 10 for the functional form of the interaction terms). The reported first-stage F-stat is the Kleibergen-Paap rk Wald F statistic. Standard errors are spatially clustered with a distance cutoff of 100km. * $p < 0.1$, ** $p < 0.05$, *** $p < 0.01$

C reports the first-stage results. The first-stage F-stats of the instruments exceed common thresholds for instruments' power. We observe that increases in bauxite prices have strong positive effects on the predicted conflict exposure of wards in close proximity to bauxite mines. We also see that increases in diamond prices reduce predicted conflict exposure in wards in close proximity to diamond mines. The main reason for this (maybe surprising) result is that the rise in diamond prices coincided with the decreasing importance of the diamond sector in Sierra Leone after the civil war. Taken together, these results lend further support to our

theoretical model’s predictive power.

4.3 Sensitivity analysis and external validity

We perform various tests to probe how sensitive our results are to various decisions in the operationalization of our variables of interest. First, we focus on the coding of our dependent variable: the observed conflict exposure. Specifically, we rerun our main specifications with various perturbations of our dependent variable. We start by including all ACLED events to construct our dependent variable (e.g., [Berman et al., 2017](#); [McGuirk and Nunn, 2020](#)), after which we drop single event categories in turn. [Figure B-6](#) documents that the coefficient estimates remain similar throughout the different perturbations of our observed conflict exposure measure.

Second, we probe how the construction of our independent variable affects our results. First, we distribute these revenues in proportion to the nighttime light emissions within the mining areas rather than in proportion to the size of these areas. Second, we include artisanal and small scale mining fields (see [Section A-2](#) on how we identify them) and distribute the mineral-specific export revenues across all industrial and artisanal mines (again based on their size). In all cases, results are not statistically or qualitatively different from our baseline specification. In a further exercise focusing on the construction of our independent variable, we recompute the ethnic diversity among discordant groups and, subsequently, the predicted conflict exposure only based on the population distribution among the four largest groups, which are the only groups that were politically relevant throughout the sample period (according to the ethnic power relations data by [Wucherpfennig et al., 2011](#)). [Table B-4](#) show that our results remain virtually unchanged.

Third, we test whether our results are driven by the distance decay ($distance^{-1}$) that we employ when computing our measures of the local resource rents and the observed conflict exposure. [Figure B-7](#) documents similar elasticities for a range of distance decays going from much less steep to much steeper decays ($distance^{-0.5}$ to $distance^{-2}$) in weighing nearby mining areas and conflict events for our measures of interest. Moreover, varying the decay only for the measurement of either local resource rents or observed conflict exposure provides similar results. Hence, we are confident that our estimated elasticities are not the byproduct of a common spatial decay function. Relatedly, we document in [Figure B-8](#) that the precision of our estimates is not dependent on the specific distance cutoff that we employ in the calculation of the Conley standard errors.

Fourth, we test whether the effect of predicted conflict exposure simply reflects the effect of

local resource rents. For this purpose, we control for the log of (absolute) local resource rents r_l in [Table B-5](#) and the relative local resource rents r_l/r in [Table B-6](#). We find that the effect of predicted conflict exposure remains statically significant and even tends to become stronger. In contrast, the effects of these local resource measures vary in sign and are typically not statistically significant. In [Table B-7](#), we follow [Berman et al. \(2017\)](#) and control for the interaction of an indicator variable for the presence of a mine and the log of the global price of the main mineral extracted in this ward. The estimated intertemporal elasticity of observed conflict exposure with respect to predicted conflict exposure remains virtually unchanged. These results underline the importance of the systemic conflict pressure that results from the interplay between the country’s ethnic- and resource geography.

Fifth, we control for the share of the population in a ward that identifies with the same ethnic group as the current political leader of Sierra Leone. This exercise is inspired by our theoretical model, in which the planner may have ward-specific priority weights (see equation (1), and the literature on ethno-regional favoritism. [Table B-8](#) reports virtually unchanged elasticity estimates, suggesting that ethno-regional favoritism does not substantially alter the systemic conflict pressure captured by our variable of interest.

Sixth, we show in [Table B-9](#) that including the proximity-price interaction for titanium metals, which include rutile, in the first stage leads to very similar 2SLS estimates.

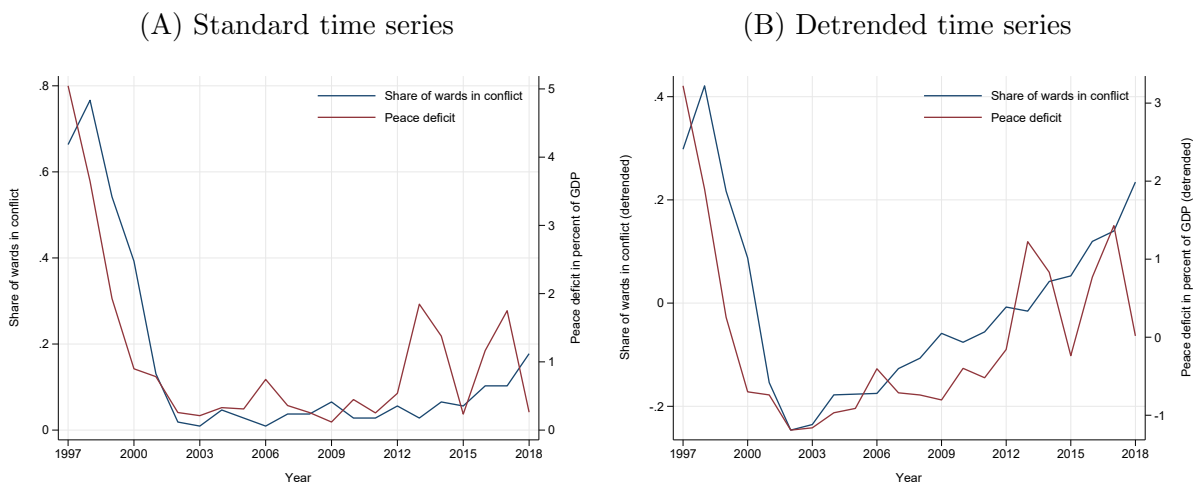
Finally, we assemble a second dataset to test the external validity of our main cross-sectional results. For that purpose, we prepare data at the level of 0.5×0.5 decimal degree grid cells across eight West African countries. To overcome the lack of high-quality data on the spatial distribution of ethnic groups, we combine the Spatially Interpolated Data on Ethnicity by [Müller-Crepon and Hunziker \(2018\)](#) with geospatial population estimates. We find that results are very similar when restricting our attention to the (only) 39 grid cells in Sierra Leone. The estimated elasticities become somewhat smaller but remain positive and statistically significant in the full sample of all these eight countries. We discuss this second dataset and our results in detail in [Appendix C](#).

4.4 Changes in country-wide conflict over time

The previous empirical results have shown that our theoretical model predicts the conflict exposure at the level of wards rather well – both in the cross-section and over time. We now want to see whether our theoretical model is also suited to predict changes in a country’s aggregate propensity to conflict.

As argued before, the peace deficit Δ is a good theoretical proxy for the country’s aggregate propensity to conflict. Within our model, this argument is based on the assumption of budget feasibility, which requires the mining sector to be fiscally self-sufficient. In practice, however, additional fiscal capacity for peacekeeping can be generated by taxing other sectors of the economy or by borrowing, and such fiscal capacity is arguably proportional to the size of the economy. We, therefore, predict the aggregate propensity to conflict by computing the peace deficit in percent of GDP for all years from 1997–2018. We measure the country’s actual aggregate conflictuality by the share of wards that experience at least one conflict event in a given year. Panel A of Figure 6 plots these two measures over time. We see that the two variables co-move quite strongly, with the raw correlation being 0.64. If anything, the share of wards with conflict events follows the peace deficit with a temporal lag.

Figure 6: Changes in country-wide conflict over time



Notes: Panel A plots the share of wards with at least on conflict event (blue line) and the peace deficit D in percent of GDP (red line) over time. Panel B replicates panel A, but with detrended time series.

Panel B plots the same time series after detrending them. The relation between the detrended time series tends to be even stronger, with the correlation being 0.80. We conclude that our theoretical model has also considerable predictive power when it comes to changes in a country’s aggregate conflictuality over time.

5 Counterfactual analyses

We now turn to predicting the effects of the development of known mineral deposits on conflict in Sierra Leone. For this purpose, we run counterfactual analyses that employ our (empirically

validated) theoretical model and our granular data. Before presenting these counterfactual analyses, we use our theoretical model to fix ideas about how changes in a country’s mining geography may impact upon its aggregate propensity to conflict and the spatial distribution of conflict exposure.

5.1 Theoretical considerations

Suppose a new mine opens in a particular location (or ward) $l' \in L$. In our model, this mine opening can be represented by an increase in the resource rent r_l in location $l = l'$. Assuming that resource rents r_l remain unchanged in locations $l \neq l'$, the relative local resource rents r_l/r increase in location $l = l'$ but decrease in locations $l \neq l'$.

To understand the complex effects of such a change in the spatial distribution of resource rents, we focus on the two complementary conflict measures used in the previous section: the peace deficit Δ and the conflict exposure index e_l , defined in equations (4) and (6), respectively. We again use the peace deficit Δ , which quantifies the extra transfers necessary to guarantee peace in every location, as our *absolute* measure of the aggregate propensity to conflict. In contrast, the conflict exposure index e_l captures the systemic component of local conflict pressure that results from the interaction of the country’s ethnic and mining geographies. It is monotonically related to the probability of conflict in location l but abstracts from average effects across locations. Hence, it is best seen as a *relative* measure of the local propensity to conflict determined by these systemic effects. By relying on these two measures, we can disentangle average effects from relative ones and thereby develop a thorough understanding of the complex effects of the opening of new mines on conflict.³³

We now discuss how the above-mentioned changes in r_l/r affect these two measures of conflict. Let us first assume that these changes do not alter the set of discordant groups G^* . In this case, the local conflict exposure e_l weakly increases in location $l = l'$, where the new mine opened, but weakly decreases in all other locations $l \neq l'$. The effect on the peace deficit Δ is ambiguous and depends on the extent to which discordant groups are over-represented in location $l = l'$. We refer to these effects as intensive-margin effects. In contrast, we refer to effects resulting from changes in the set of discordant groups G^* (in response to the mine opening) as extensive-margin effects. These effects can be complex, but there are typically two possible ways in which set G^* may change: groups severely over-represented in location l' ($s_{l'}^g/s^g \gg 1$) may enter set G^* ; or groups severely under-represented in location l' ($s_{l'}^g/s^g \ll 1$) may leave set

³³In addition, these two measures have the added advantage that they are independent of the priority weights in the planner’s objective, which is appealing for our application as such weights are typically arbitrary and unknown.

G^* . In both cases, the model typically predicts an increase in the local ethnic diversity among the discordant groups D_{l,G^*} in location $l = l'$ and, consequently, also an increase in the local conflict exposure $e_l = (r_l/r)D_{l,G^*}$. The effect on conflict exposure e_l in other locations $l \neq l'$ is ambiguous and depends on the spatial distributions of ethnic groups and resource rents. Note, however, that these are just tendencies. Comparative statics are too complex to characterize in full generality.

In principle, the effects of opening new mines on the peace deficit Δ and the conflict exposure e_l in different locations can be positive or negative, depending on the country-wide spatial distributions of ethnic groups and resource rents. Therefore, we now use our theoretical model in numerical simulations to predict how hypothetical mining projects in Sierra Leone would alter the aggregate propensity to conflict and local conflict exposure.

5.2 Predicted effects of new mines on conflict

We first study the effect of the hypothetical development of four different gold deposits on aggregate and local conflict. We later look at all other known deposits in Sierra Leone. The four gold deposits include two gold mines for which the government of Sierra Leone has already awarded mining licenses: The Baomahun project, whose license holder is FG Gold, and the Nimini–Komahun project, whose license holder is the Nimini Holdings Limited. We further look at the Bently deposit, which was prospected by Njahili Resources Limited, and the Pampana River deposit, which is owned by Sunergy. The Baomahun and the Pampana River deposits are in the center of the country, relatively far from any current mining site; the Bently deposit is located close to the capital Freetown in the country’s west and far away from any current mining site; and the Nimini–Komahun deposit is right next to the diamond mining area.³⁴

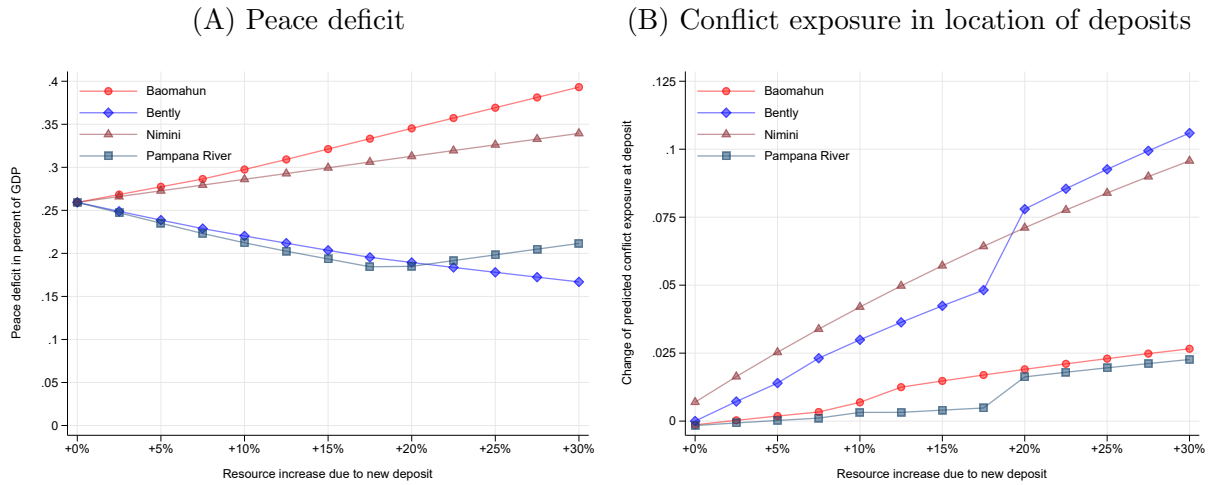
Our counterfactual exercises are based on two assumptions: First, the revenues generated by existing mines are the same as in the last year of our sample period.³⁵ Second, as the exact mining capacities of these new gold mines are unknown, we allow for different revenues generated by these mines. Specifically, we consider values corresponding to 0–30 percent of the aggregated revenues generated by the existing mines (in increments of 2.5 percent).

Figure 7 reports the effects of the development of these four gold deposits on our measures of conflict. Panel A shows that the peace deficit is increasing in the resource revenues generated by the Baomahun and the Nimini–Komahun projects. Hence, these two projects increase the

³⁴See the map in Figure B-9 for details on the location of these gold deposits.

³⁵It would be straightforward to run the counterfactual exercises with different assumptions about the revenues generated by existing mines.

Figure 7: Predicted effects of four new gold mines on aggregate and local conflict



Notes: Panel A plots the peace deficit Δ in percent of GDP for different simulated revenues (in relation to the revenues of all existing mines combined) generated at the Baomahun deposit (red dots), the Bentley deposit (blue diamonds), the Nimini deposit (brown triangles), and the Pampana River deposits (green squares). Panel B plots the local predicted conflict exposure e_l in the ward where the respective deposits are located for the same simulated revenues generated at the same four deposits.

aggregate propensity to conflict and thereby lead to relatively high social costs. In contrast, the development of the Bentley or the Pampana River deposits reduces the peace deficit (at least as long as their revenues are not very large) and, thus, the country’s aggregate propensity to conflict. Hence, these cases highlight that “mining for peace” is not just a theoretical construct but a concrete possibility for Sierra Leone. It follows that the Bentley and the Pampana River deposit would lead to much lower conflict-related social costs than the Baomahun and the Nimini–Komahun project.

Panel B looks at the conflict exposure e_l in the wards where these gold deposits are located. We see that the local conflict exposure is increasing in the revenues generated at any of these deposits, but that the magnitude of these increases differ remarkably across deposits. They are much less pronounced for the Baomahun and the Pampana River deposits than for the other two. Taken together, these two panels reveal that the aggregate and the local effects of the development of new gold deposits are both very heterogenous and, interestingly, that there is no strong (positive or negative) correlation between these two types of effects.

To illustrate this pattern, we focus on the Bentley deposit. Its development reduces the country’s aggregate propensity to conflict (measured by the peace deficit), but leads to a large increase in conflict exposure in the ward hosting this deposit. Our theoretical model can help us to understand these different effects. First, let us consider the effect on the peace deficit. New

mining activity in the resource-poor west of the country directly reduces the peace deficit by lowering the spatial resource inequality. In addition, this change in the mining geography leads to a change in the set of discordant groups: the Kono, who are over-represented in the diamond-mining area in the east, are no longer part of this sets.³⁶ This latter change results in a substantial decrease in the ethnic diversity among discordant groups in the diamond-mining area and, consequently, this area’s contribution to the country’s aggregate propensity to conflict. Let us now consider why the development of the Bently deposit increases local conflict exposure. Again, there is a direct effect due to the large increase in the relative local resource rents in the ward hosting this deposit. In addition, there are two ethnic groups, the Sherbro and Krio, that are over-represented in this ward and may join the set of discordant groups, thereby raising the local ethnic diversity among discordant groups and the local conflict exposure. The step-wise increase of the local conflict exposure (seen in Panel B) results from the fact that the Krio join the set of discordant groups only once the revenues generated by the Bentley deposit are equal to at least 20 percent of the revenues of all existing mines combined.

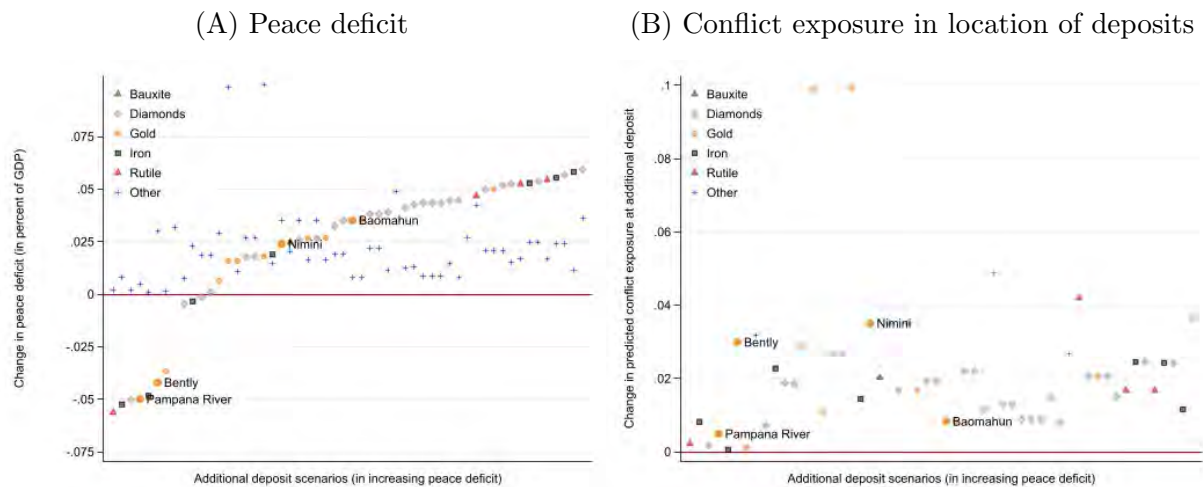
Figure 7 shows that there exists a deposit – the Pampana River deposit – whose development would reduce the country’s aggregate propensity to conflict (measured by the peace deficit) and would lead to a modest increase in the local conflict exposure only. The effect on the peace deficit is again negative because the spatial resource inequality tends to decrease and because the Kono are no longer part of the set of discordant groups. The effect on the local conflict exposure is modest because all initially discordant groups are under-represented in the corresponding ward. Hence, the local ethnic diversity among discordant groups is low, such that the increase in the local resource rents has only a small effect on the local conflict exposure.³⁷

To assess how general the insights gained from these four counterfactual analyses are, we run the same analyses for all discovered mineral deposits reported by the RMD as of 2019 (see Table A-1 in Appendix B). We assume that each of these deposits generates revenues equal to 10 percent of the revenues of all the existing mines combined. Figure 8 reports the effects of these hypothetical mining projects on our measures of conflict. Panel A shows the change in the peace deficit, and Panel B the change in the local conflict exposure in the wards hosting

³⁶Figure B-10 shows the effects of the development of the four gold deposits under consideration on the set of discordant groups.

³⁷Figure 7 also shows that the peace deficit starts increasing and that the local conflict exposure increases “discontinuously” once the revenues generated at the Pampana River deposit are equal to 20 percent. The reason is that the Temne, who are over-represented in the ward hosting the Pampana River deposit as well as the iron-mining area to its north, become part of the set of discordant groups. As a result, the local ethnic diversity among discordant groups increases in this ward and the iron-mining area to its north, causing increases in the local conflict exposure and the peace deficit.

Figure 8: Predicted effects of hypothetical mining projects on aggregate and local conflict



Notes: Panel A plots the change in the peace deficit Δ (measured in percent of GDP) for simulated revenues equal to 10 percent of all existing mines combined for all known deposits that are not directly located in the national or a provincial capital city. Panel B plots the change in the local conflict exposure e_l in the ward where these deposits are located. In both panels, the deposits are ordered by their effects on the peace deficit.

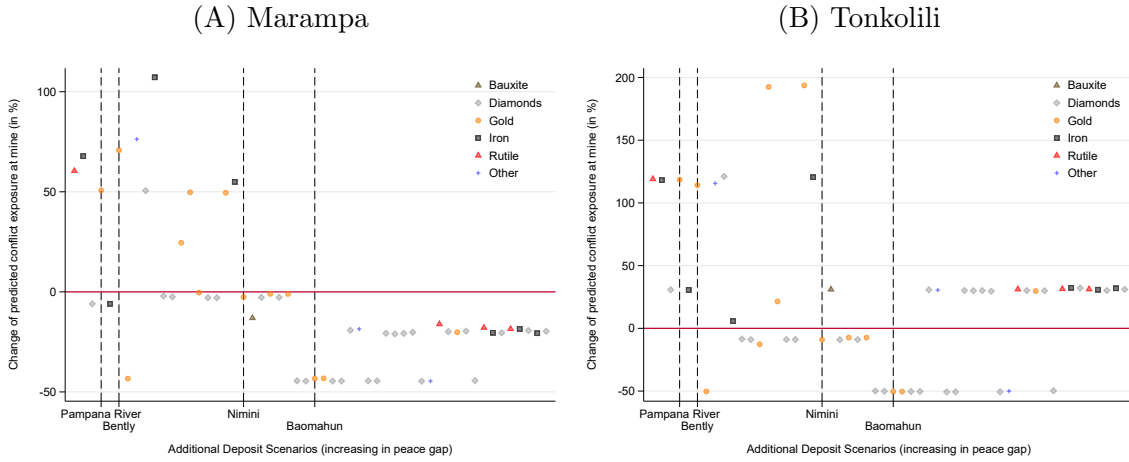
these deposits. In both panels, we order the deposits by their effects on the peace deficit. The results confirm the three observations made above. First, there is a large heterogeneity in the effects of these hypothetical mining projects on the peace deficit. While the effect is positive for the majority of these projects, it is – crucially – negative for around one fifth of them (11 out of 54 known deposits). Second, as expected, the effects on local conflict exposure is positive for all deposits. However, there is again substantial heterogeneity, ranging from effects close to zero for some deposits to very large effects for other deposits.³⁸ Lastly, the effects on the peace deficit and the conflict exposure in the wards hosting the deposits are basically uncorrelated.

The last observation suggests that the variation in how different mining projects affect the aggregate propensity to conflict must come from variation in their effects on local conflict exposure in wards other than those hosting these deposits. Figure 9 illustrates the differential effects of mining projects on conflict exposure across locations. It shows the effects of all hypothetical mining projects on the local conflict exposure in the two wards hosting active iron mines.³⁹ Many hypothetical new mining projects have very different effects across locations. For example, the development of the Nimini deposit increases local conflict exposure in the

³⁸The effect is highest for the Bunbana gold deposit, which is located right next to the large iron mine in the north of the center.

³⁹Figure B-11 shows the effects of these hypothetical mining projects on the local conflict exposure in the wards hosting the other industrial mines in Sierra Leone.

Figure 9: Predicted effects of hypothetical mining projects on conflict around two currently active iron mines



Notes: Panels A and B plot the change in the local conflict exposure e_l (in percent) in the wards hosting the currently operating industrial iron mines in Sierra Leone in response to the same simulated new mining activities as in Figure 8. The deposits are again ordered by their effects on the peace deficit (shown in Figure 8).

ward hosting the Tonkolili mine, but decreases local conflict exposure in the ward hosting the Marampa mine. This example nicely illustrates the complex web of conflict externalities across locations. This complex web also implies that even mining projects that are peace-promoting on the aggregate – like the development of the Bently and the Pampana River deposits – typically increase conflict in some locations.

6 Conclusion: Mining policies for peace

Previous research suggests that natural resource rents are typically a curse for resource-extracting countries and regions. Given the increasing global demand for minerals from ethnically diverse and historically conflict-prone countries, we have reassessed the effects of mining on conflict. We have gone beyond purely local average effects and focused on the systemic component of the local conflict risk that results from the country’s entire ethnic and mining geographies. We have seen that the development of different mineral deposits can have very different effects on both a country’s aggregate propensity to conflict as well as the spatial distribution of conflict risks. Governments, international mining companies, international organizations, and advocacy groups may benefit from taking these aggregate and local conflict externalities into account when deciding whether and under what terms certain deposits can be developed.

Governments, which may be primarily concerned with the country’s aggregate propensity for

conflict, should focus on the effect of potential mining projects on the peace deficit Δ . This variable measures the additional budget the planner would need in order to ensure peace everywhere. Therefore, the change in the peace deficit resulting from a new mining project corresponds to the (positive or negative) monetary transfer to the planner that would be necessary to ensure that this project leaves the country's aggregate propensity to conflict unchanged. Governments should make use of this information when designing policy. Ideally, they would include the change in the peace deficit in the price of the mining license. Alternatively, they could design the royalty and tax schemes in a manner that reflects the change in the peace deficit. Suppose a government is unwilling or unable to implement any of these relatively subtle policies. In that case, it should, at the very least, take the aggregate conflict externalities into account when deciding whether to allow a new mining project. In addition, governments may also want to act upon information about local conflict externalities, e.g., if they are particularly concerned by higher conflict exposure in economically or politically important locations.

Many international mining companies (IMCs) care about conflict risks as well, e.g., because conflict can increase their production and transportation costs or undermine their social license to operate, i.e., “the ongoing approval and broad acceptance of society to conduct [their] activities” (Prno and Slocombe, 2012, p. 346). Hence, these IMCs would benefit from knowing the aggregate and local conflict externalities of their potential new mining projects. For example, if an IMC knew how its new project shaped the spatial distribution of local conflict risks, it would be better positioned to estimate the production costs at the mining site, the transportation costs from this site to the port, and the difficulty of getting the social license to operate. Already today, many IMCs follow the UN Guiding Principles on Business and Human Rights, which are increasingly codified in national or supranational law. These principles require companies to conduct human rights due diligence, among others, in order to avoid harming local communities. We are not the first to argue that human rights due diligence should take the effects on conflict and violence into account.⁴⁰ However, we are the first to provide a useful theoretical framework which can readily be brought to the data and help assess both aggregate and local conflict externalities of new mining projects.

Our framework offers additional useful insights to IMCs that are already active in a country. It allows them to understand how the development of different deposits would affect conflict risks around already active and profitable mining projects. This understanding could inform their decisions which deposits to develop, how much to maximally pay for the corresponding

⁴⁰See, e.g., the [joint statement on conflict and due diligence legislation](#) in which many human rights experts criticize that the due diligence directive proposed by the European Commission lacks special provisions for (mining) companies active in conflict-prone areas.

mining license, or whether to lobby against new mining projects of other companies. But, of course, IMCs have typically no incentive to fully internalize all conflict externalities of their mining projects.

International organizations and advocacy groups could benefit from our framework as well, exactly because IMCs lack the incentive to fully internalize all conflict externalities and because governments may lack the willingness or capacity to implement well-designed policies. The information revealed by the change in the peace deficit may allow international organizations and advocacy groups to nudge the government and IMCs towards policies and actions that are in the country's best interest. Advocacy groups, which often represent local communities living close to mining sites, may also be interested in understanding the local conflict externalities around these sites.

In summary, we propose that governments, IMCs, international organizations, and advocacy groups should make use of frameworks like ours when assessing the likely aggregate and local conflict externalities of new mining projects. We argue that the quantification of such externalities should become a key part of any comprehensive cost-benefit analysis and human rights due diligence related to new mining projects. Of course, we are aware that our model offers just a first step towards a better understanding and comprehensive quantification of conflict externalities in complex settings. Therefore, and because the Global South should not bear the brunt of the costs from the energy transition (and the associated increase in the global demand for minerals), we consider future research on this topic to be of utmost importance.

References

- Acemoglu, D., T. Reed, and J. A. Robinson (2014). Chiefs: Economic development and elite control of civil society in Sierra Leone. *Journal of Political Economy* 122(2), 319–368.
- Adhvaryu, A., J. Fenske, G. Khanna, and A. Nyshadham (2021). Resources, conflict, and economic development in Africa. *Journal of Development Economics* 149, 102598.
- Amarasinghe, A., P. Raschky, Y. Zenou, and J. Zhou (2020). Conflicts in spatial networks. Technical report, CEPR.
- Aragón, F. M. and J. P. Rud (2013). Natural resources and local communities: evidence from a peruvian gold mine. *American Economic Journal: Economic Policy* 5(2), 1–25.
- Atkin, D., E. Colson-Sihra, and M. Shayo (2021). How do we choose our identity? A revealed preference approach using food consumption. *Journal of Political Economy* 129(4), 1193–1251.
- Bazzi, S. and C. Blattman (2014). Economic shocks and conflict: Evidence from commodity prices. *American Economic Journal: Macroeconomics* 6(4), 1–38.
- Bellows, J. and E. Miguel (2006). War and institutions: New evidence from Sierra Leone. *American Economic Review* 96(2), 394–399.
- Bellows, J. and E. Miguel (2009). War and local collective action in Sierra Leone. *Journal of Public Economics* 93(11-12), 1144–1157.
- Berman, N. and M. Couttenier (2015). External shocks, internal shots: the geography of civil conflicts. *Review of Economics and Statistics* 97(4), 758–776.
- Berman, N., M. Couttenier, and V. Girard (2020). Natural resources and the salience of ethnic identities. Technical report, Universidade Nova de Lisboa.
- Berman, N., M. Couttenier, D. Rohner, and M. Thoenig (2017). This mine is mine! How minerals fuel conflicts in Africa. *American Economic Review* 107(6), 1564–1610.
- Bester, H. and K. Wärneryd (2006). Conflict and the social contract. *Scandinavian Journal of Economics* 108(2), 231–249.
- Blattman, C. (2022). *Why We Fight: The Roots of War and the Paths to Peace*. Penguin.
- Blattman, C. and E. Miguel (2010). Civil war. *Journal of Economic Literature*, 3–57.
- Borusyak, K., P. Hull, and X. Jaravel (2022). Quasi-experimental shift-share research designs. *Review of Economic Studies* 89(1), 181–213.
- Brückner, M. and A. Ciccone (2010). International commodity prices, growth and the outbreak of civil war in Sub-Saharan Africa. *Economic Journal* 120(544), 519–534.
- Bruederle, A. and R. Hodler (2019). Effect of oil spills on infant mortality in Nigeria. *Proceedings of the National Academy of Sciences* 116(12), 5467–5471.

- Burgess, R., R. Jedwab, E. Miguel, A. Morjaria, and G. Padró i Miquel (2015). The value of democracy: Evidence from road building in Kenya. *American Economic Review* 105(6), 1817–51.
- Chen, J. and J. Roth (2022). Log-like? ATEs defined with zero outcomes are (arbitrarily) scale-dependent. Technical report, Havard University.
- Colella, F., R. Lalive, S. O. Sakalli, and M. Thoenig (2019). Inference with arbitrary clustering. Technical report, IZA.
- Collier, P. and A. Hoeffler (2004). Greed and grievance in civil war. *Oxford Economic Papers* 56(4), 563–595.
- Conibere, R., J. Asher, K. Cibelli, J. Dudukovich, R. Kaplan, and P. Ball (2004). Statistical appendix to the report of truth and reconciliation commission, report of Sierra Leone. *Human Rights Data Analysis Group, The Benetech Initiative* 134.
- Conteh, F. M. and R. Maconachie (2021). Artisanal mining, mechanization and human (in) security in Sierra Leone. *The Extractive Industries and Society* 8(4), 100983.
- Corvalan, A. and M. Vargas (2015). Segregation and conflict: An empirical analysis. *Journal of Development Economics* 116, 212–222.
- Couttenier, M., R. S.Di, L. Inguere, M. Mohand, and L. Schmidt (2022). Mapping artisanal and small-scale mines at large scale from space with deep learning. *Plos One* 17(9).
- De Luca, G., R. Hodler, P. A. Raschky, and M. Valsecchi (2018). Ethnic favoritism: An axiom of politics? *Journal of Development Economics* 132, 115–129.
- Dube, O. and J. F. Vargas (2013). Commodity price shocks and civil conflict: Evidence from Colombia. *Review of Economics and Studies* 80(4), 1384–1421.
- Eberle, U. J., D. Rohner, and M. Thoenig (2020). Heat and hate: Climate security and farmer-herder conflicts in Africa. Technical report, CEPR.
- Eck, K. (2012). In data we trust? A comparison of UCDP GED and ACLED conflict events datasets. *Cooperation and Conflict* 47(1), 124–141.
- Emirbayer, M. (1997). Manifesto for a relational sociology. *American Journal of Sociology* 103(2), 281–317.
- Esteban, J., L. Mayoral, and D. Ray (2012). Ethnicity and conflict: An empirical study. *American Economic Review* 102(4), 1310–42.
- Esteban, J., M. Morelli, and D. Rohner (2015). Strategic mass killings. *Journal of Political Economy* 123(5), 1087–1132.
- Esteban, J. and D. Ray (2008). On the salience of ethnic conflict. *American Economic Review* 98(5), 2185–2202.

- Fanthorpe, R. and C. Gabelle (2013). *Political Economy of Extractives Governance in Sierra Leone*. World Bank.
- Fearon, J. D. (1995). Rationalist explanations for war. *International Organization* 49(3), 379–414.
- Fey, M. and K. W. Ramsay (2009). Mechanism design goes to war: peaceful outcomes with interdependent and correlated types. *Review of Economic Design* 13(3), 233–250.
- Gehring, K., S. Langlotz, and K. Stefan (2019). Stimulant or depressant? Resource-related income shocks and conflict. Technical report, CESifo.
- Glennerster, R., E. Miguel, and A. D. Rothenberg (2013). Collective action in diverse Sierra Leone communities. *Economic Journal* 123(568), 285–316.
- Goldsmith-Pinkham, P., I. Sorkin, and H. Swift (2020). Bartik instruments: What, when, why, and how. *American Economic Review* 110(8), 2586–2624.
- Herrington, R. (2021). Mining our green future. *Nature Reviews Materials* 6(6), 456–458.
- Hodler, R. (2006). The curse of natural resources in fractionalized countries. *European Economic Review* 50(6), 1367–1386.
- Hodler, R. and P. A. Raschky (2014). Regional favoritism. *Quarterly Journal of Economics* 129(2), 995–1033.
- Hörner, J., M. Morelli, and F. Squintani (2015). Mediation and peace. *Review of Economic Studies* 82(4), 1483–1501.
- Humphreys, M. (2005). Natural resources, conflict, and conflict resolution: Uncovering the mechanisms. *Journal of Conflict Resolution* 49(4), 508–537.
- Hund, K., D. La Porta, T. P. Fabregas, T. Laing, and J. Drexhage (2020). Minerals for climate action: The mineral intensity of the clean energy transition. *World Bank*.
- IPUMS International (2020). Minnesota population center. integrated public use microdata series, international: Version 7.3 2004 population and housing census. <https://doi.org/10.18128/D020.V7.2>.
- Jackson, M. O. and M. Morelli (2007). Political bias and war. *American Economic Review* 97(4), 1353–1373.
- Jackson, M. O. and M. Morelli (2011). The reasons for wars: an updated survey. In *The Handbook on the Political Economy of War*. Edward Elgar Publishing.
- Kaldor, M. and J. Vincent (2006). Evaluation UNDP assistance to conflict-affected countries: Case study Sierra Leone. Technical report, United Nations Development Programme Evaluation Office.

- König, M. D., D. Rohner, M. Thoenig, and F. Zilibotti (2017). Networks in conflict: Theory and evidence from the great war of Africa. *Econometrica* 85(4), 1093–1132.
- Lei, Y.-H. and G. Michaels (2014). Do giant oilfield discoveries fuel internal armed conflicts? *Journal of Development Economics* 110, 139–157.
- Matuszeski, J. and F. Schneider (2006). Patterns of ethnic group segregation and civil conflict. Technical report, Harvard University.
- Maus, V., S. Giljum, J. Gutschlhofer, D. M. da Silva, M. Probst, S. L. Gass, S. Luckeneder, M. Lieber, and I. McCallum (2020). A global-scale data set of mining areas. *Scientific Data* 7(1), 1–13.
- McGuirk, E. F. and N. Nunn (2020). Transhumant pastoralism, climate change, and conflict in Africa. Technical report, National Bureau of Economic Research.
- Mehlum, H., K. Moene, and R. Torvik (2006). Institutions and the resource curse. *Economic Journal* 116(508), 1–20.
- Montalvo, J. G. and M. Reynal-Querol (2005). Ethnic polarization, potential conflict, and civil wars. *American Economic Review* 95(3), 796–816.
- Morelli, M. and D. Rohner (2015). Resource concentration and civil wars. *Journal of Development Economics* 117, 32–47.
- Müller-Crepon, C. and P. Hunziker (2018). New spatial data on ethnicity: Introducing SIDE. *Journal of Peace Research* 55(5), 687–698.
- Novta, N. (2016). Ethnic diversity and the spread of civil war. *Journal of the European Economic Association* 14(5), 1074–1100.
- Prno, J. and D. S. Slocombe (2012). Exploring the origins of ‘social license to operate’ in the mining sector: Perspectives from governance and sustainability theories. *Resources Policy* 37(3), 346–357.
- Raleigh, C., A. Linke, and C. Dowd (2020). Armed Conflict Location and Event Dataset (ACLED), Codebook Version 2. Technical report.
- Ray, D. (2009). Costly conflict under complete information. Technical report, New York University.
- Reichl, C. and M. Schatz (2022). World mining data. Technical report, Federal Ministry of Agriculture, Regions and Tourism, Austria, and International Organizing Committee for the World Mining Congresses.
- Ronkainen, J., J. De Haan, K. Anderson, and A. M. Kamara (2019). The ASGM overview of Sierra Leone. Technical report, Environment Protection Agency Sierra Leone.
- Roth, A. E. (2002). The economist as engineer: Game theory, experimentation, and computation as tools for design economics. *Econometrica* 70(4), 1341–1378.

- Tollefsen, A. F., H. Strand, and H. Buhaug (2012). Prio-grid: A unified spatial data structure. *Journal of Peace Research* 49(2), 363–374.
- UN Comtrade (2021). International Trade Statistics Database.
- Van der Ploeg, F. (2011). Natural resources: curse or blessing? *Journal of Economic Literature* 49(2), 366–420.
- Vogt, M., N.-C. Bormann, S. Rügger, L.-E. Cederman, P. Hunziker, and L. Girardin (2015). Integrating data on ethnicity, geography, and conflict: The ethnic power relations data set family. *Journal of Conflict Resolution* 59(7), 1327–1342.
- Wilson, S. A. (2013). Diamond exploitation in Sierra Leone 1930 to 2010: a resource curse? *GeoJournal* 78(6), 997–1012.
- Wucherpfennig, J., N. B. Weidmann, L. Girardin, L.-E. Cederman, and A. Wimmer (2011). Politically relevant ethnic groups across space and time: Introducing the GeoEPR dataset. *Conflict Management and Peace Science* 28(5), 423–437.
- Zulu, L. C. and S. A. Wilson (2009). Sociospatial geographies of civil war in Sierra Leone and the new global diamond order: Is the Kimberley process the panacea? *Environment and Planning C: Government and Policy* 27(6), 1107–1130.

A Industrial and artisanal mining in Sierra Leone

A-1 Verifying the industrial mines of Sierra Leone


Our baseline set of industrial mines is identified via two main sources (see [Section 3.2](#)). First, the RMD database provides operational information at the deposit level for different minerals. [Table A-1](#) lists all these deposits. The six deposits with an active industrial mine in 2019 are highlighted in bold font. Second, for these six mines, we leverage the mining areas identified by [Maus et al. \(2020\)](#).


Table A-1: Mineral deposits (RMD)


Allotropes	Bagla Hills	Baomahun	Bently
Bunbana	Casierra	Chetham	Coastal Block
Ferensola	Freetown Complex	Gbangbaia	Gendema
Gori Hills	Jabwema	Kangari Hills	Kariba Kono
Koidu	Koidu Pipe 3	Konama-Bafi River	Kono
Kono Operations	Kukuna	Little Scarcies	Madina
Magna Egoli	Marampa	Matemu	Millennium
Mokanji	Nimini	Nimini Hills	No 12
Northwest Block	Pampana	Pampana North	Pampana River
Panguma	Plant 11	Plant 6	Rokel
Semabu	Sewa	Sewa-Bafi River	Sewa River
Sierra Rutile	SML	Sierra Leone	Sierra Leone Kimberlite
Sierra Leone SE Reg.	Sonfon	STHG Sewa River	Sula Mountains
Tongo	Tongo Fields	Tonkolili	Upper/Lower Sewa
Wara Wara	Zimmi		


Notes: The table lists the mineral deposits reported in the RMD. Deposits which are exploited as of 2019 with an industrial mine are highlighted in bold.


We conduct a background search for each of these six active industrial mines in order to confirm the location identified by [Maus et al. \(2020\)](#) (using Google Earth images), the primary commodity mined, and whether it has been operational for at least one year within our 1997-2018 sample period. These background searches are listed in alphabetical order of the individual mines:


Mine Name	Koidu Diamond Mine
Primary commodity	Diamonds (source: RMD)
Image	
Operation History	2003-2022 (source: RMD, and https://www.koidulimited.com/company/)
Operator History	Koidu limited (source: RMD, https://www.koidulimited.com/company/)
Notes	Koidu Diamond Mine is an industrial-sized diamond mine. The image depicts the spatial extent of the Koidu mine as detected by Maus et al. (2020).

Mine Name	Konoma Operations
Primary commodity	Diamonds (source: RMD)
Image	
Operation History	2005 - 2022 (source RMD, https://www.rough-polished.com/en/news/36300.html)
Operator History	African minerals, since 2010 Obtala Resources (source: proactiveinvestors.co.uk ⁴¹)
Notes	Kono Operations is an industrial-sized alluvial diamond mining operation. The image depicts the spatial extent of Kono Operations as detected by Maus et al. (2020).

Mine Name	Marampa Mine
Primary commodity	Iron (source: RMD, https://www.mining-technology.com/projects/marampamine/)
Image	
Operation History	2011 - 2022 (source: RMD, https://marampamines.com/)
Operator History	London Mining, Marampamines (subsidiary of Gerald Group) (source: https://marampamines.com/about-us/)
Notes	Marampa mine is an industrial-sized iron mine. The image depicts the spatial extent of the Marampa mine as detected by Maus et al. (2020).

Mine Name	Sierra Rutile Mine
Primary commodity	Rutile (source: RMD)
Image	
Operation History	1979-1995, 2006-2022 (source: Minex, https://en.wikipedia.org/wiki/Sierra_Rutile_Limited)
Operator History	Sierra Rutile Limited (source: RMD, https://sierra-rutile.com/)
Notes	Sierra Rutile is an industrial-sized rutile mine, also producing ilmenite and zircon. The image depicts the spatial extent of the Sierra Rutile mine as detected by Maus et al. (2020).

Mine Name	SML Mine
Primary commodity	Bauxite (source: RMD)
Image	
Operation History	1963-1995, 2006-2022 (source: https://vimetcobauxite.com/history/)
Operator History	SML (Alusuisse) Sieromco (source: RMD, bloomberg.com ⁴²)
Notes	Sierra Rutile is an industrial-sized rutile mine, also producing ilmenite and zircon. The image depicts the spatial extent of Sierra Rutile mine as detected by Maus et al. (2020).

Mine Name	Tonkolili Min
Primary commodity	Iron (source: RMD)
Image	
Operation History	2011-2022 (source: https://www.mining-technology.com/projects/tonkolili-iron-ore-mine/)
Operator History	African Minerals (AML), Shandong Iron & Steel Group (owner since 2015) (source: https://www.mining-technology.com/projects/tonkolili-iron-ore-mine/)
Notes	Tonkolili Mine is an industrial-sized iron mine. The image depicts the spatial extent of the Tonkolili mine as detected by Maus et al. (2020).

A-2 Artisanal and small-scale mining (ASM)

Artisanal and small scale mining (ASM) activities are hard to track for two reasons. First, many operations are not official (i.e., they are illegal), second operations are relatively easy to move and can be tiny (thus easily covered by trees and other vegetation). Nonetheless some recent progress has been made. [Couttenier et al. \(2022\)](#), for example, use machine learning and high resolution images to track artisanal mining operations across West Africa. However, this approach can only be used in recent years (from around 2017 onwards) for which images with a resolution of 10 square meter or smaller are available. In the absence of any publicly available data, and with the potential for measurement error in mind, we proceed by generating proxies for artisanal and small-scale gold mining (ASGM) and artisanal and small-scale diamond mining (ASDM) ourselves. There is no ASM of bauxite, iron and rutile in Sierra Leone.

A-2.1 Artisanal and small-scale gold mining (ASGM)

To proxy for ASGM-based local resource rents, we rely on “The ASGM Overview of Sierra Leone” ([Ronkainen et al., 2019](#)). The report lists in its supplementary material the number of ASGM sites per chiefdom in 2018. [List A-1](#) lists the wards with a positive number of ASGM sites.

List A-1: Wards with ASGM

Jawie (6); Kissi Kama, Kissi Teng (1); Kpeje Bongre, Penguia, Yawei (17); Kpeje West, Njaluahun (20); Malema (5); Dodo, Wandor (3); Gorama Mende (13); Kandu Lekpeama, Simbaru (25); Kenema Town (1); Koya (Kenema); Langrama, Niawa (8); Lower Bambara, Malegohun (16); Nomo, Tunkia (7); Nongowa (11); Small Bo (1); Fiama, Lei, Sandor, Toli (13); Dbane Kandor, Mafindor, Soa (3); Gbane, Gorama Kono, Tankoro (33); Gbense, Kamara (3); Nimikoro (87); Nimiyama (8); Biriwa, Magbaimba Ndorhahun (4); Bombali Sebor (3); Gbendembu Ngowahun, Libeisaygahun, Sanda Tenraran (11); Makari Gbanti (1); Sanda Loko (50); Sella Limba, Tambakka (62); Magbema (2); Masungbala (6); Dembelia Sinkunia, Sulima (1); Diang, Kasunko (98); Follasaba Dembelia, Wara Wara Bafodia (1); Nieni (8); Sengbe (1); Maforki (1); Masimera (4); Gbonkolenken (5); Kafe Simira, Kalansogoia, Sambaya (172); Kholifa Mabang, Malal Mara (3); Kholifa Rowalla (61); Kunike Barina, Kunike Sanda (79); Tane (154); Yoni (18); Badjia, Komboya (8); Bagbwe, Niawa Lenga (3); Baoma (16); Bo Town (2); Bumpe Ngawo (5); Gbo, Selenga, Valunia (32); Kakua (2); Lugbu (2); Tikonko (11); Bum, Kpanda Kemo, Kwamebai Krim, Sogbini (1); Gasse, Kamajei, Kowa (1); Barri (5); Gallinasperi (2); Kpanga-Kabonde, Panga Krim, Pejeh, Sowa (6); Makpele (5); Soro Gbema (2).

To compute ASGM-based local resource rents, we use this number as an imperfect proxy for the scale of gold mining activity per ward (as it is the only publicly available information on ASGM covering the entire country) and assign the centroid of the ward as the location of the mines. Given the lack of further information, we assume that the distribution of ASGM activities remains proportional over time (i.e., if a ward has twice as many ASGM sites as another ward

in 2018, then we assume that this former ward generates twice as much gold export revenues in all years), which is unlikely to hold. Moreover, using the ward centroids as point coordinates to distribute gold export revenues in proportion to the number of mines further introduces some error. In summary, there is some measurement in our measure of ASGM-based local resource rents, but we do not have any evidence that this occurs in a systematic way.

A-2.2 Artisanal and small-scale diamond mining (ASDM)

To incorporate ASDM in the computation of the local resource rents, we rely on [Zulu and Wilson \(2009\)](#), who analyze the effect of the Kimberley Process (which aims to classify conflict diamonds and reduce trade therein) on civil conflict in Sierra Leone. They highlight that most traditional ASDM areas are in the kimberlite belts in Sierra Leone, where ASDM takes place mostly in the river deltas. [Figure A-1](#) shows these alluvial diamond mining areas along the kimberlite belts as depicted in [Zulu and Wilson \(2009\)](#).

Figure A-1: Kimberlite belts

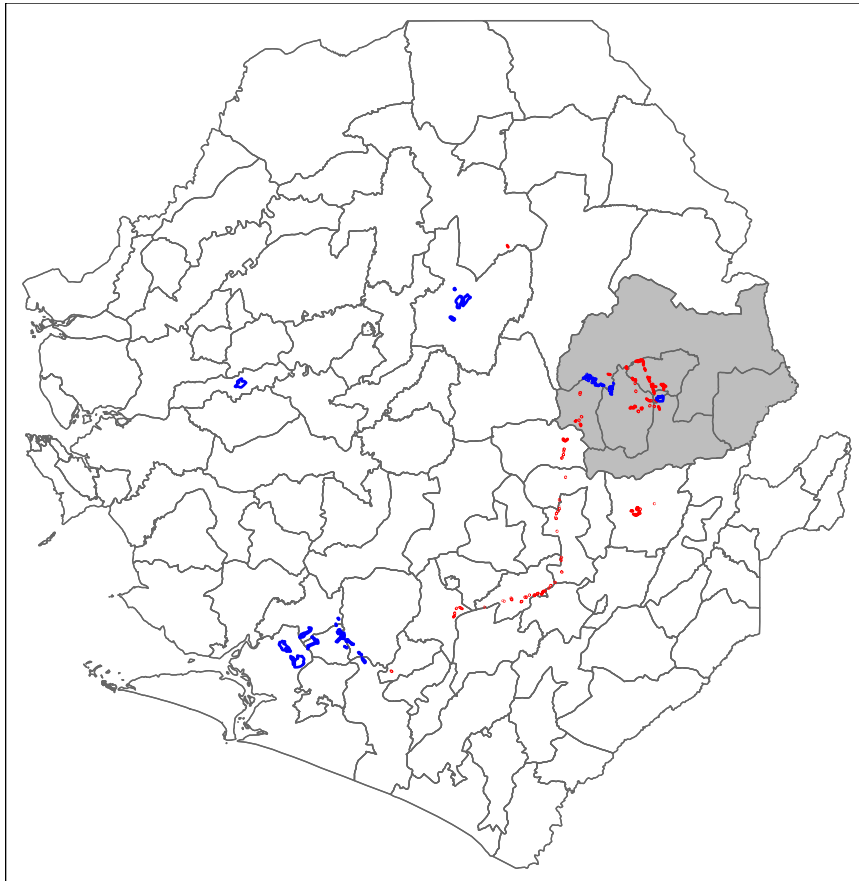


Figure 1. Map of Sierra Leone and locations of known diamond deposits (source: adapted from PAC, 2005, page 3).

Notes: This is Figure 1 from [Zulu and Wilson \(2009\)](#).

Based on this classification, we manually delineate ASDM areas in those belts based on current (spring 2022) Google Earth images. [Figure A-2](#) plots the distribution of the industrial diamond mines (in blue) and the additional ASDM areas (in red). As discussed in [Zulu and Wilson \(2009\)](#), most ASDM areas are located in the Kono district (highlighted in grey), which also hosts large industrial mines.

Figure A-2: Industrial and ASDM distribution



Notes: Figure depicts the industrial mines as identified by [Maus et al. \(2020\)](#) in blue and the manually coded ASDM area in red. The Kono district is highlighted in grey.

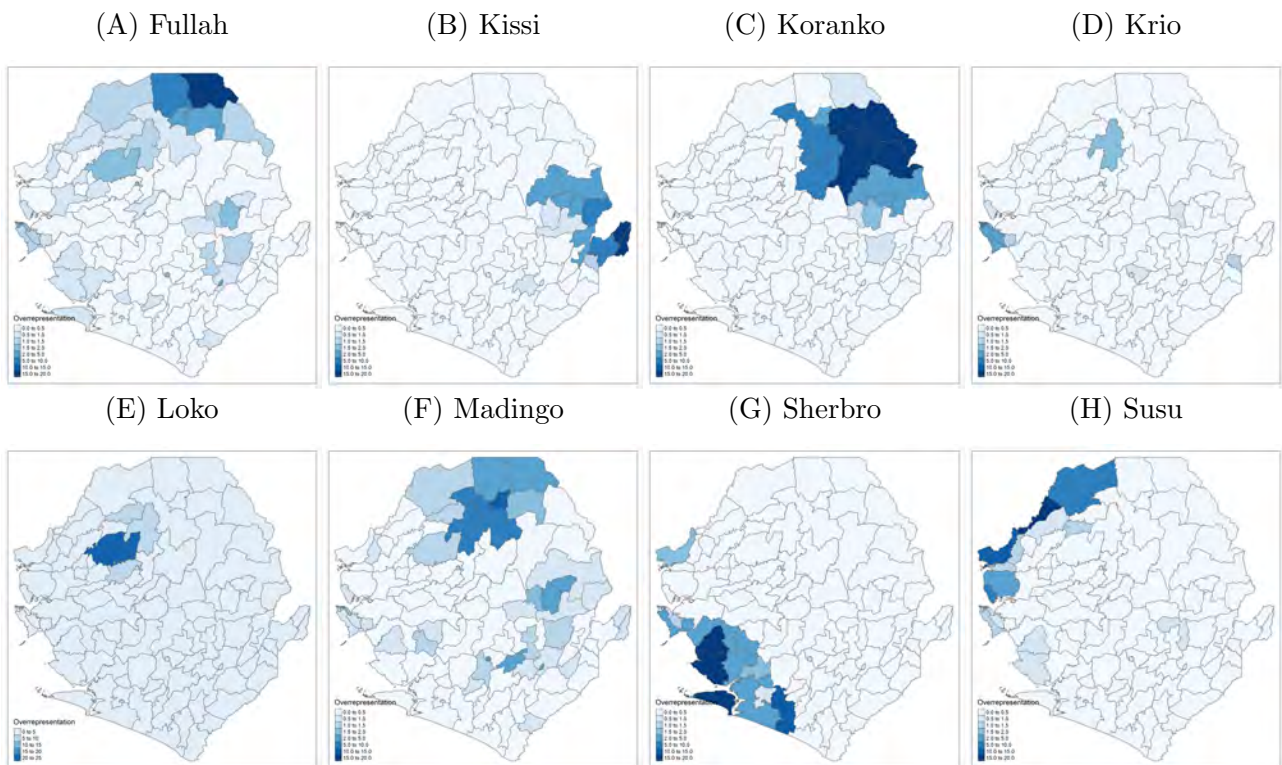
Similar to the ASGM case, we only have a cross-sectional snapshot of ASDM areas and again assume that the general distribution of ASDM revenues does not change over time. It is, however, a bit more complicated to distribute the net export values than in the ASGM case, because of the existence of industrial diamond mines. Different source suggest different production shares of the mine types, with the shares from ASDM ranging from 39 to 75 percent ([Conteh and Maconachie, 2021](#); [Fanthorpe and Gabelle, 2013](#); [Wilson, 2013](#); [Zulu and Wilson, 2009](#)). The inclusion of ADSM in the computation of the (diamond-based) resource rents will

again introduce noise. However, given that most ASDM are located close to the industrial diamond mines, the distortion should not matter too much because the relative proximity of the different wards to the diamond mines remains relatively stable. Hence, it is no big surprise that the results remain similar if we include ASDM in the computation of the local resource rents (see [Table B-3](#)), and that they do not depend on whether the share of annual net diamonds exports resulting from ASDM is assumed to be 39 or 75 percent.

B Additional figures and tables for Sierra Leone-based data and analyses

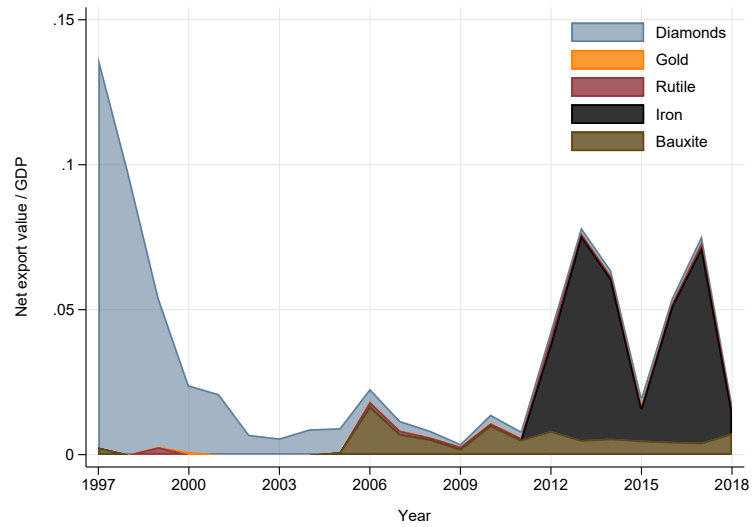
B-1 Additional figures

Figure B-1: Local over-representation of eight small ethnic groups



Notes: This figure complements [Figure 2](#) by plotting the local over-representation (s_i^g/g^g) across wards for the eight smaller ethnic groups in our sample, with national-level population shares from 1.4–4.2 percent.

Figure B-2: Net exports of different minerals as a share of GDP

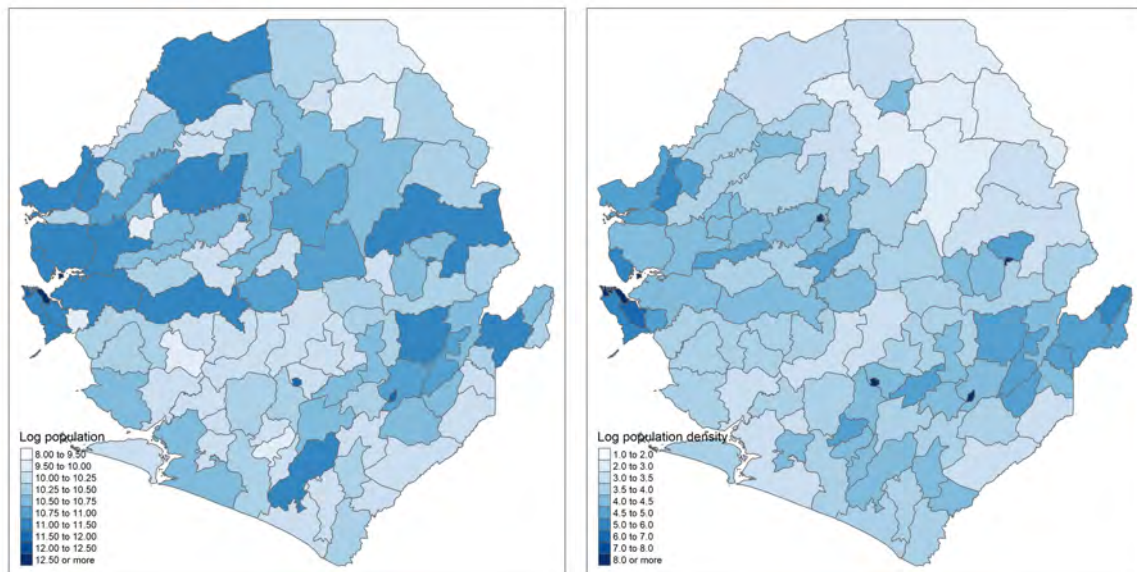


Notes: This figure plots the value of the next exports relative to GDP in current prices for each of the five main minerals mined in Sierra Leone over time. GDP data are from the World Bank.

Figure B-3: Population across wards

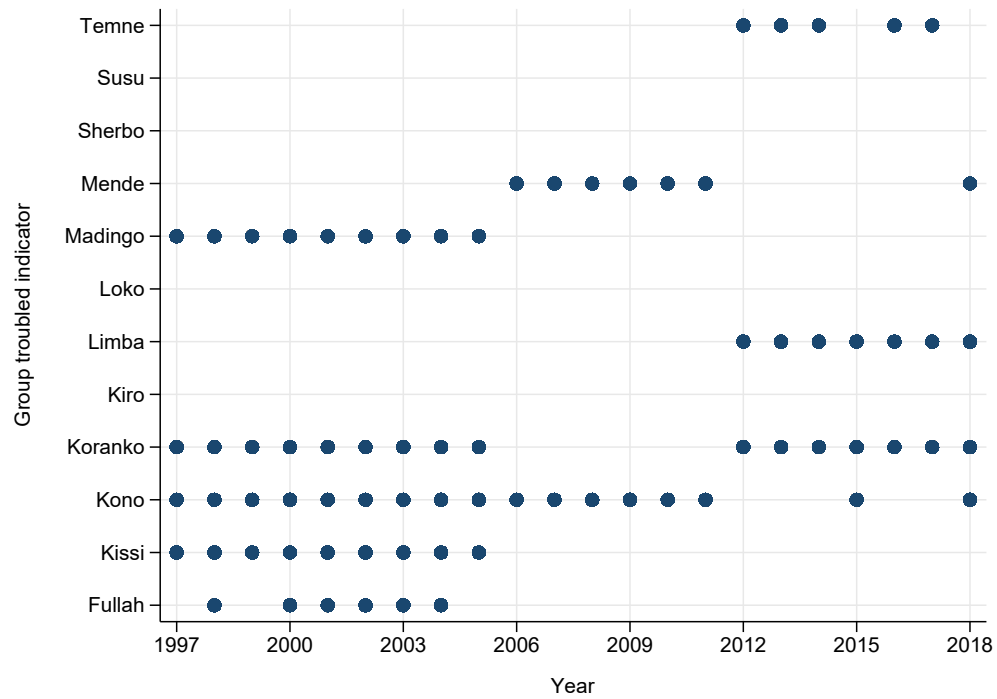
(A) Log population

(B) Log population density



Notes: Panel A plots the log of population (based on the 2004 census) across wards. Panel B plots the log of population density (again based on the 2004 census).

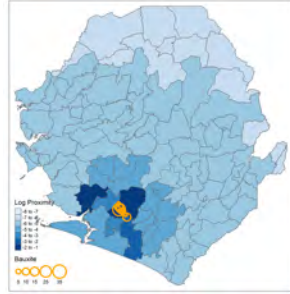
Figure B-4: The set of discordant groups over time



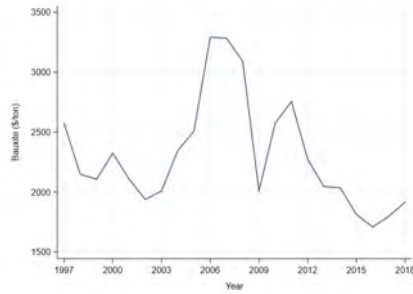
Notes: This figure plots the set of discordant groups, indicated by blue dots, for each year of our sample period.

Figure B-5: Components of the instrumental variables

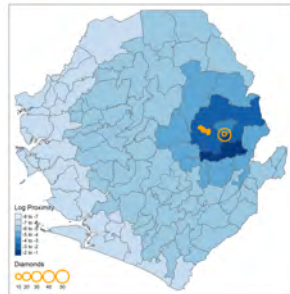
(A) Proximity to bauxite mines



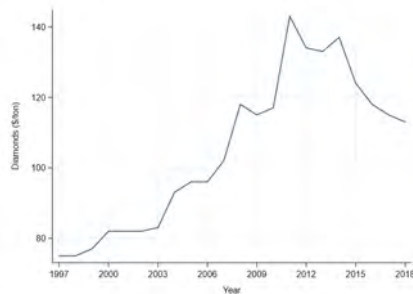
(B) Global bauxite price



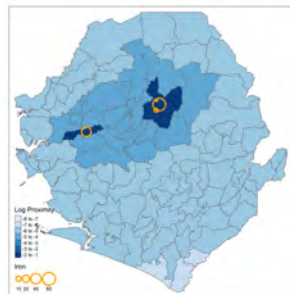
(C) Proximity to diamond mines



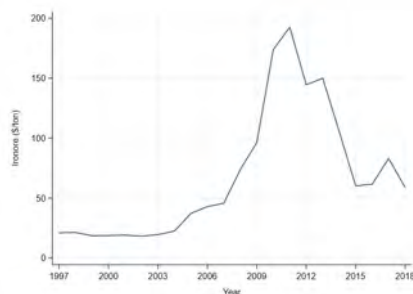
(D) Global diamond price



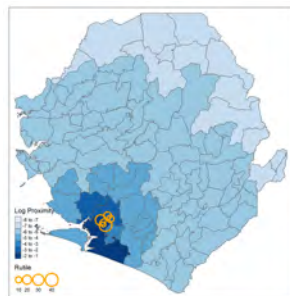
(E) Proximity to iron mines



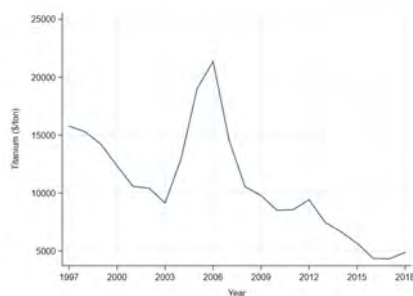
(F) Global iron price



(G) Proximity to rutile mines



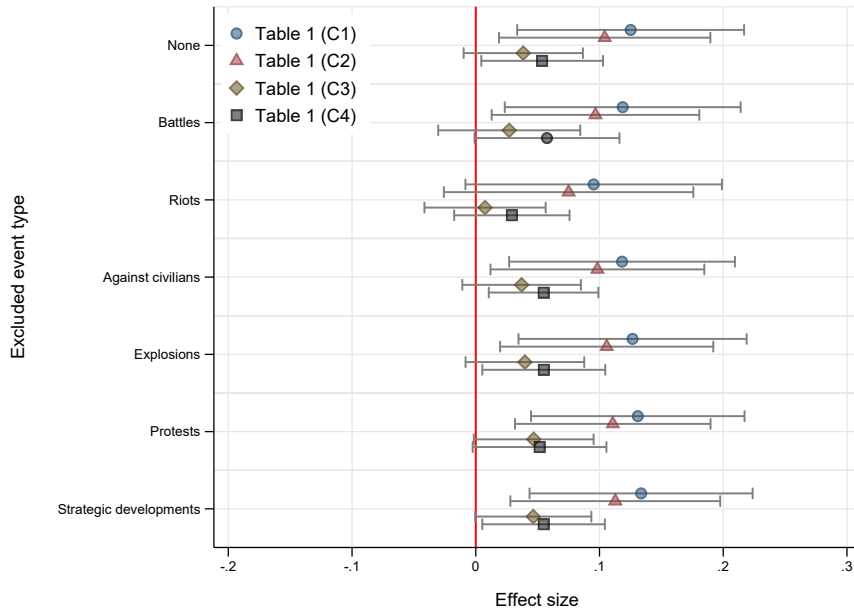
(H) Global price titanium metals



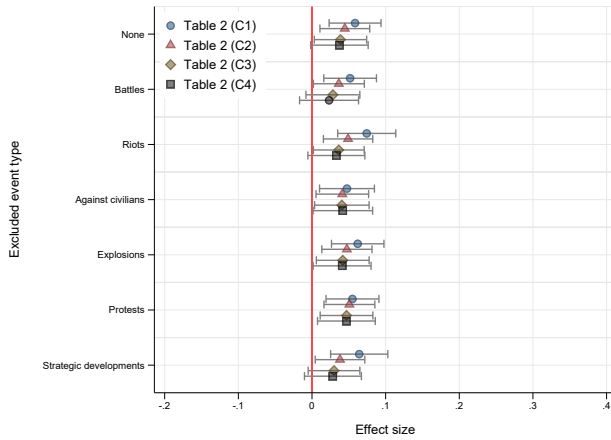
Notes: Panels A, C, E and G plot the log of the proximity of each ward to the (area-weighted) mines for bauxite, diamonds, iron, and rutile, respectively. Panels B, D, F and H plot the global prices of these minerals over time.

Figure B-6: Robustness: Alternative outcome variables

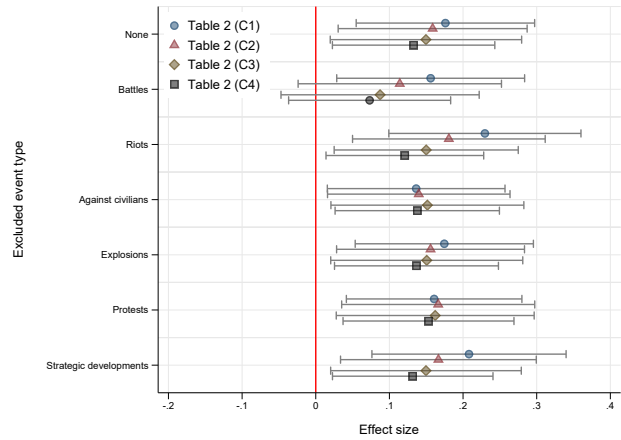
(A) OLS cross-section



(B) OLS panel

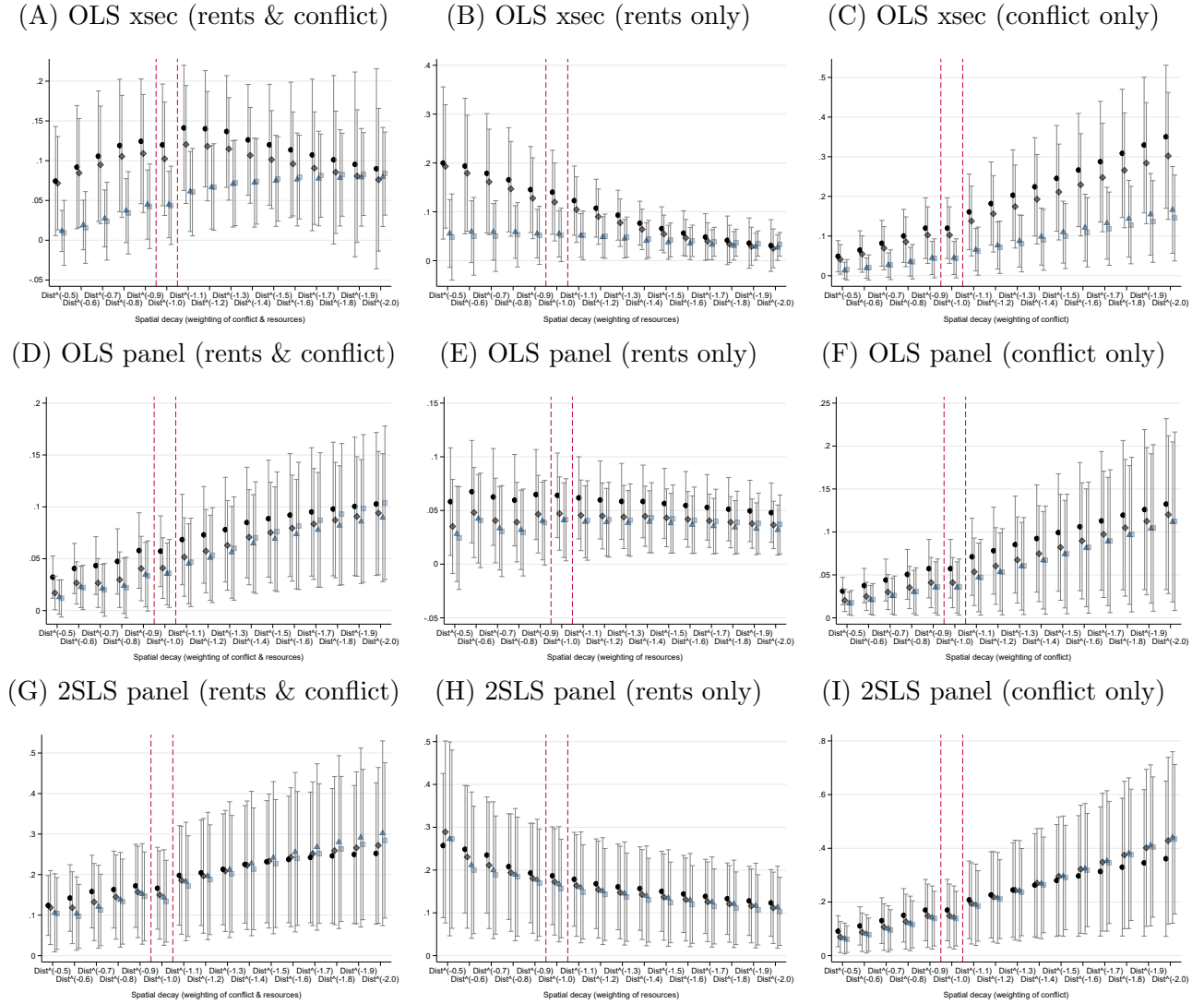


(C) 2SLS panel (second stage)



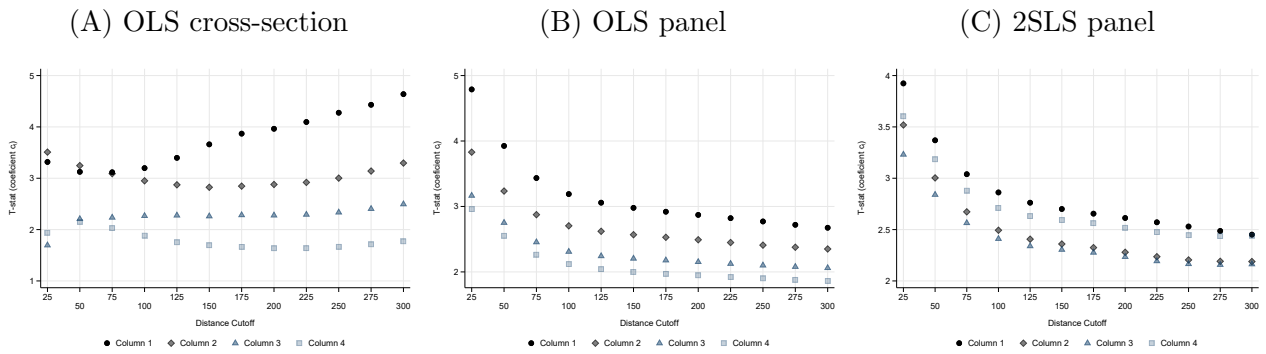
Notes: This figure replicates the main results reported in [Table 1](#) and [Table 1](#) using alternative measures of observed conflict exposure based on the inclusion of all ACELD event types (top row) or the exclusion of one single event type (battles in second row, riots in third row, violence against civilians in fifth row, explosions in sixth row, protests in seventh, and strategic developments in last row). Panel A follows panel A of [Table 1](#), and panels B and C follow panels A and B of [Table 2](#). The different colors and shapes of the point coefficients refer to the different specifications used in columns (1)–(4) of these tables. The confidence intervals are depicted as grey bars and based on spatially clustered Conley standard errors with a 100km distance cutoff.

Figure B-7: Robustness: Alternative distance decays



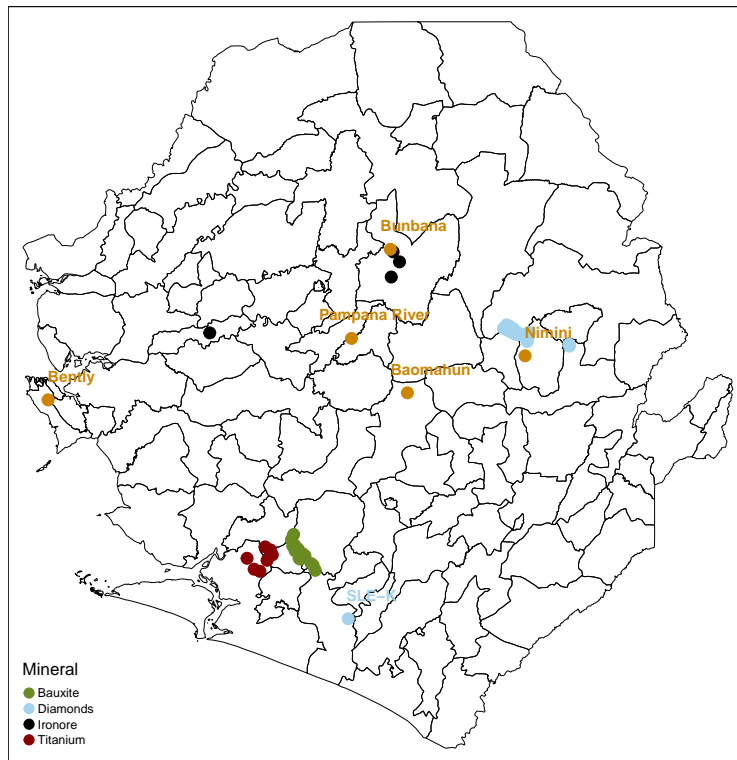
Notes: This figure replicates the main results reported in [Table 1](#) and [Table 2](#) using different distance decays, ranging from $distance^{0.5}$ to $distance^2$, in the computation of both the local resource rents and the observed conflict exposure. Panel A reports the cross-sectional results from replicating panel A of [Table 1](#) for these different distance decays. Black dots report the point coefficient corresponding to column (1), grey diamonds to column (2), blue triangles to column (3), and bright blue squares to column (4). Panels B and C report results from similar replication exercises when changing the distance decay only for either the local resource rents or the observed conflict exposure. Panels D–F are analogous to panels A–C but report OLS panel results from replicating panel A of [Table 2](#). Panels G–I too are analogous to panels A–C but report second-stage 2SLS panel results from replicating panel B of [Table 2](#). The confidence intervals are depicted as grey bars and based on spatially clustered Conley standard errors with a 100km distance cutoff.

Figure B-8: Robustness: Alternative distance cutoffs for the spatially clustered standard errors



Notes: This figure replicates the main results reported in [Table 1](#) and [Table 2](#) using different distance cutoffs, ranging from 25–300 km, in the computation of the spatially clustered Conley standard errors. Panel A plots the t-statistics for our main coefficient for all four columns of panel A [Table 1](#) for different distance cutoffs. Panel B does the same for the panel OLS results reported in panel A of [Table 2](#). Panel C does the same for the second-stage 2SLS results reported in panel B of [Table 2](#). In all panels, we impose a linear decline in the spatial dependence structure (using the Bartlett option in the `acreg` package by [Colella et al. \(2019\)](#)).

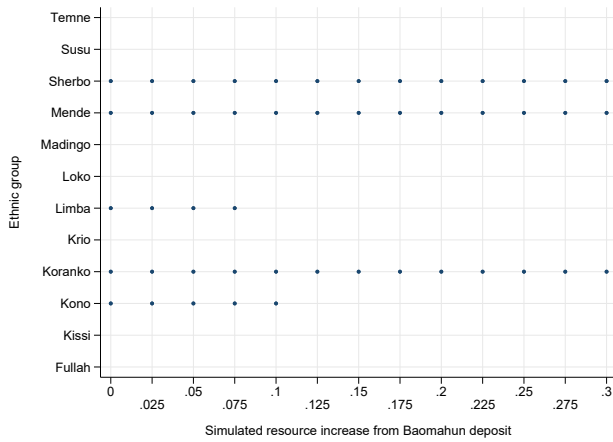
Figure B-9: Selected (potential) future mining locations



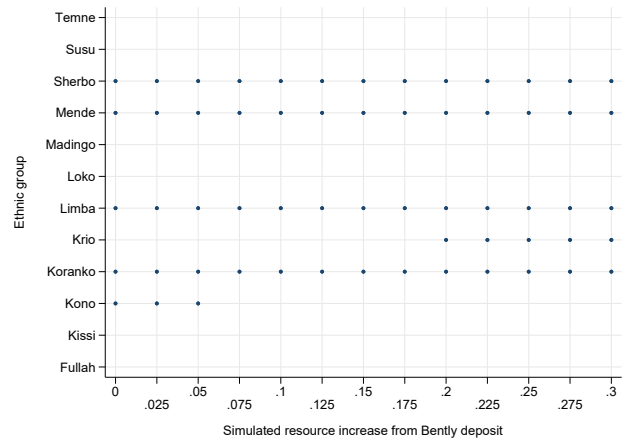
Notes: This map depicts the locations of the current industrial mines, with different colors indicating different minerals, and the locations and names of the four potential new gold mines explicitly mentioned in [Section 5](#).

Figure B-10: The set of discordant groups for simulated mine openings

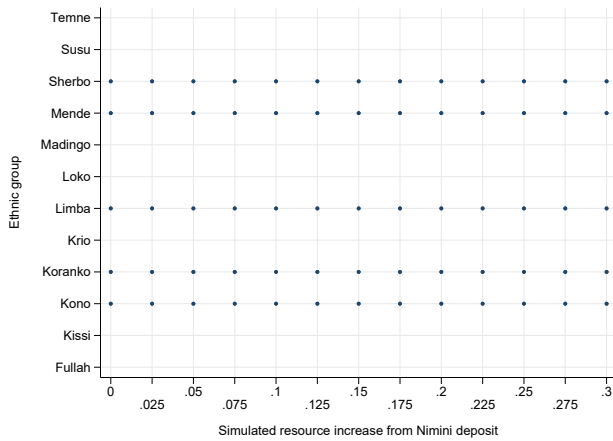
(A) Baomahun deposit



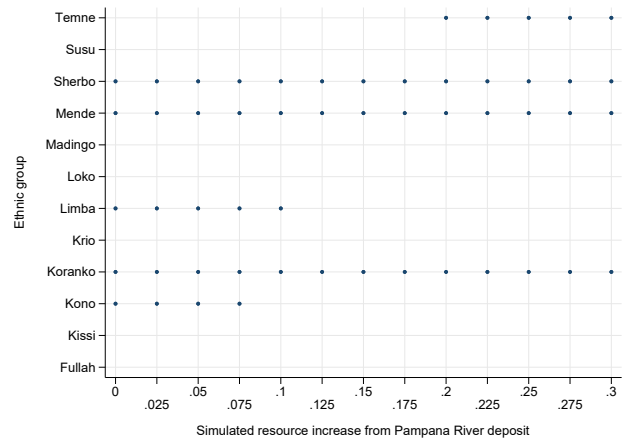
(B) Bently deposit



(C) Nimini deposit

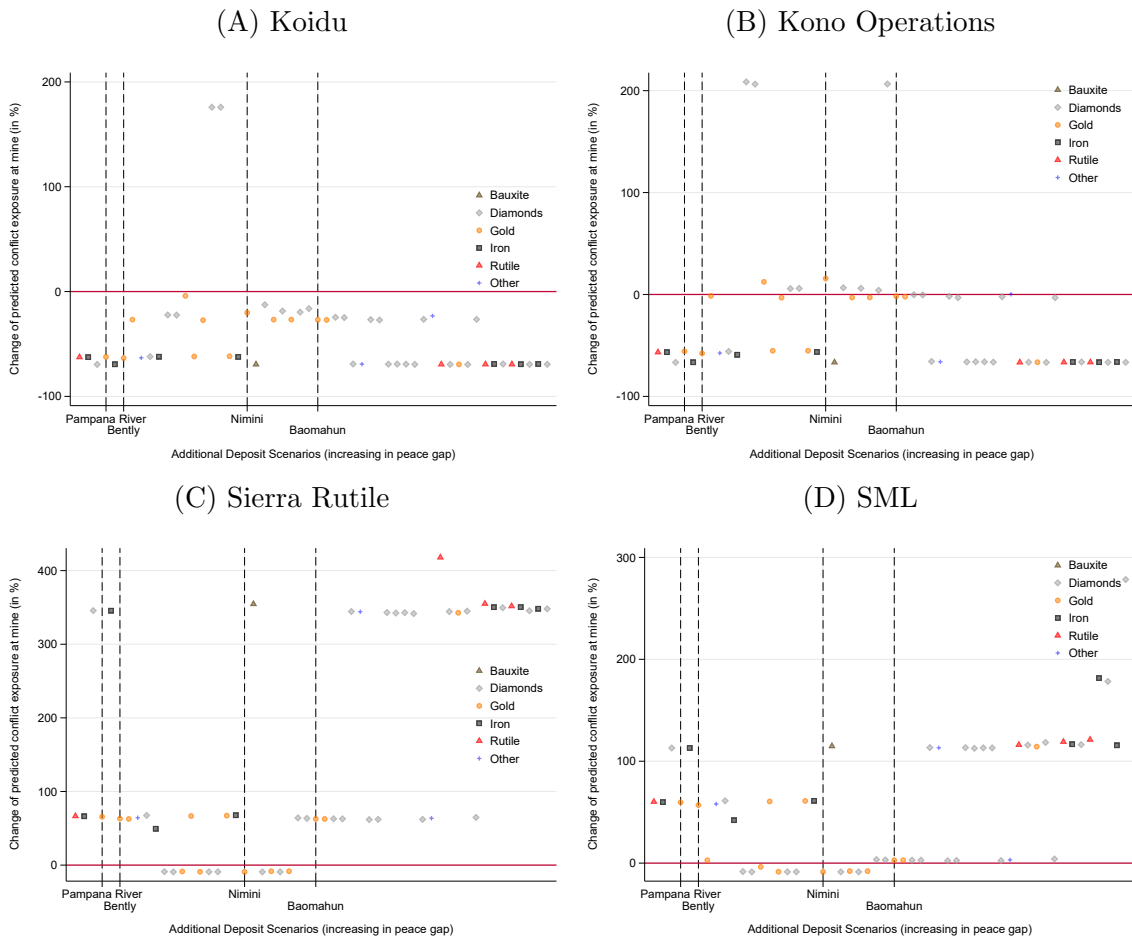


(D) Pampana River deposit



Notes: This figure accompanies Figure 7. Panels A–D report the set of discordant ethnic groups for different simulated revenues (in relation to the revenues of all existing mines combined) generated at the Baomahun deposit, the Bently deposit, the Nimini deposit, and Pampana River deposit, respectively. The revenues of all other mines are fixed to their 2018 values.

Figure B-11: Predicted effects of hypothetical mining project around four currently active mines



Notes: This figure accompanies Figure 9. Panels A–D plot the change in the local conflict exposure e_l (in percent) in the wards hosting the four additional industrial mines in Sierra Leone in response to the same simulated new mining activities as in Figure 8. The deposits are again ordered by their effects on the peace deficit (shown in Figure 8).

B-2 Additional tables

Table B-1: Summary statistics

Variable	Mean	SD	Min	Max	N
<i>Panel A: Cross-sectional sample</i>					
Relative resource rents	0.01	0.02	0.00	0.10	107
Diversity among discordant groups	0.34	0.30	0.04	1.76	107
Log observed conflict exposure	-5.51	0.65	-6.33	-3.00	107
Log predicted conflict exposure	-7.04	1.18	-9.13	-2.63	107
Log population (2004)	10.57	0.50	9.53	12.67	107
Log area	5.93	1.61	-0.23	7.97	107
<i>Panel B: Panel sample</i>					
Log observed conflict exposure	-5.51	1.04	-7.43	-0.81	2,354
Log predicted conflict exposure	-7.04	1.68	-11.24	-0.16	2,354
Log bauxite proximity \times log bauxite price	-41.58	6.24	-50.90	-10.82	2,354
Log diamond proximity \times log diamond price	-24.96	4.25	-30.48	-7.91	2,354
Log iron proximity \times log iron price	-20.74	5.07	-32.06	-3.34	2,354

Notes: This table reports the summary statistics for the ward-level variables used in [Figure 4](#), [Table 1](#) (panel A), and [Table 2](#).

Table B-2: Summary statistics for variables in appendix figures and tables

Variable	Mean	SD	Min	Max	N
<i>Panel A: Cross-sectional sample</i>					
Log observed conflict exp. (all events)	-5.48	0.65	-6.20	-2.97	107
Log observed conflict exp. (excl. battles)	-5.51	0.70	-6.23	-2.82	107
Log observed conflict exp. (excl. riots)	-5.51	0.65	-6.22	-2.96	107
Log observed conflict exp. (excl. civilians)	-5.48	0.61	-6.17	-3.16	107
Log observed conflict exp. (excl. explosions)	-5.48	0.65	-6.21	-2.97	107
Log observed conflict exp. (excl. protests)	-5.46	0.64	-6.20	-2.99	107
Log observed conflict exp. (excl. deployment)	-5.51	0.65	-6.33	-2.99	107
Log predicted conflict exp. (large groups)	-7.19	1.68	-10.31	-1.80	107
Log predicted conflict exp. (incl. ASM)	-7.00	1.20	-9.22	-3.16	107
Log predicted conflict exp. (light-weighted)	-7.07	1.17	-9.40	-2.71	107
Log relative resource rents	-5.38	0.63	-6.04	-2.81	107
Log resource rents	8.10	0.75	7.40	11.25	107
Share ethnic group of leader	0.01	0.01	0.00	0.03	107
<i>Panel B: Panel sample</i>					
Log observed conflict exp. (all events)	-5.48	1.02	-7.29	-0.81	2,354
Log observed conflict exp. (excl. battles)	-5.51	1.05	-7.27	-1.56	2,247
Log observed conflict exp. (excl. riots)	-5.51	1.04	-7.31	-0.81	2,354
Log observed conflict exp. (excl. civilians)	-5.48	1.02	-7.29	-0.81	2,354
Log observed conflict exp. (excl. explosions)	-5.48	1.03	-7.29	-0.81	2,354
Log observed conflict exp. (excl. protests)	-5.46	1.02	-7.17	-0.81	2,354
Log observed conflict exp. (excl. deployment)	-5.51	1.04	-7.43	-0.81	2,354
Log predicted conflict exp. (large groups)	-7.19	2.32	-12.20	1.06	2,354
Log predicted conflict exp. (light-weighted)	-7.07	1.67	-11.27	0.89	2,354
Log predicted conflict exp. (incl. ASM)	-7.00	1.72	-11.25	-0.17	2,354
Log relative resource rents	-5.38	0.83	-6.40	-1.25	2,354
Log resource rents	8.10	0.87	6.82	12.60	2,354
Mine ward \times log mineral price	0.17	0.52	0.00	2.09	2,354
Share ethnic group of leader	0.01	0.02	0.00	0.08	2,354
Log rutile proximity \times log titanium price	-49.85	7.39	-62.74	-8.77	2,354

Notes: This table reports the summary statistics for variables only used in figures and tables presented in the Online Appendix.

Table B-3: Robustness: Alternative computation of resource rents

		<i>Dependent variables: Log conflict exposure</i>							
		<i>Difference in computation of resource rents:</i>							
		<i>Light-weighted industrial mines</i>				<i>Inclusion of artisanal mines</i>			
		(1)	(2)	(3)	(4)	(5)	(6)	(7)	(8)
<i>Panel A: OLS cross-section</i>									
Log predicted conflict exp.		0.133*** (0.039)	0.117*** (0.036)	0.049* (0.026)	0.047 (0.031)	0.125*** (0.034)	0.105*** (0.033)	0.044* (0.025)	0.046 (0.028)
Population control		✓	✓	✓	✓	✓	✓	✓	✓
Area control		–	✓	✓	✓	–	✓	✓	✓
Province-fixed effects		–	–	–	✓	–	–	–	✓
Obs.		107	107	107	107	107	107	107	107
<i>Panel B: OLS panel</i>									
Log predicted conflict exp.		0.066*** (0.021)	0.051*** (0.019)	0.048** (0.019)	0.048** (0.021)	0.066*** (0.021)	0.051*** (0.019)	0.048** (0.019)	0.048** (0.021)
<i>Panel C: 2SLS panel (second stage)</i>									
Log predicted conflict exp.		0.184*** (0.058)	0.167*** (0.064)	0.154** (0.068)	0.134** (0.058)	0.184*** (0.058)	0.167*** (0.064)	0.154** (0.068)	0.134** (0.058)
First-stage F-stat		22.61	12.57	11.08	14.82	22.61	12.57	11.08	14.82
Ward-fixed effects		✓	✓	✓	✓	✓	✓	✓	✓
Year-fixed effects		✓	✓	✓	✓	✓	✓	✓	✓
Province trends		–	✓	–	–	–	✓	–	–
District trends		–	–	✓	–	–	–	✓	–
Ward trends		–	–	–	✓	–	–	–	✓
Obs.		2354	2354	2354	2354	2354	2354	2354	2354

Notes: This table replicates the main results reported in [Table 1](#) and [Table 2](#) using log predicted conflict exposure based on alternatively computed local resource rents r_l . In columns (1)–(4), we distribute the mineral-specific annual revenues across all industrial mining areas extracting the respective mineral in proportion to the average nighttime light emissions within these mining areas (rather than in proportion to their size). In columns (5)–(8), we distribute the mineral-specific annual revenues across all industrial and artisanal mining areas extracting the respective mineral. For industrial mining areas, we do so again in proportion to their size. [Section A-2](#) explains how we identify artisanal diamond and gold mining areas. Here we assume that 39 percent of the annual diamond revenues come from artisanal mining. Results are close to identical when assuming that this share is 75 percent. Panel A follows panel A of [Table 1](#), and panels B and C follow panels A and B of [Table 2](#). Standard error are spatially clustered with a distance cutoff of 100km. * $p < 0.1$, ** $p < 0.05$, *** $p < 0.01$

Table B-4: Robustness: Large ethnic groups only

	<i>Dependent variable:</i> <i>Log observed conflict exposure</i>			
	(1)	(2)	(3)	(4)
<i>Panel A: OLS cross-section</i>				
Log predicted conflict exposure	0.089** (0.038)	0.076** (0.034)	0.031* (0.018)	0.023 (0.022)
Population control	–	✓	✓	✓
Area control	–	–	✓	✓
Province-fixed effects	–	–	–	✓
Obs.	107	107	107	107
<i>Panel B: OLS panel</i>				
Log predicted conflict exposure	0.055*** (0.017)	0.047*** (0.016)	0.046*** (0.015)	0.050*** (0.019)
<i>Panel C: 2SLS panel (second stage)</i>				
Log predicted conflict exposure	0.156*** (0.055)	0.161*** (0.059)	0.152** (0.064)	0.149*** (0.056)
First-stage F-stat	34.25	23.59	17.56	23.72
Ward-fixed effects	✓	✓	✓	✓
Year-fixed effects	✓	✓	✓	✓
Province trends	–	✓	–	–
District trends	–	–	✓	–
Ward trends	–	–	–	✓
Obs.	2354	2354	2354	2354

Notes: This table replicates the main results reported in [Table 1](#) and [Table 2](#) using log predicted conflict exposure computed based on the four largest and politically most relevant ethnic groups only. These are the Kono, the Limba, the Mende, and the Temne. Panel A follows panel A of [Table 1](#), and panels B and C follow panels A and B of [Table 2](#). Standard error are spatially clustered with a distance cutoff of 100km. * $p < 0.1$, ** $p < 0.05$, *** $p < 0.01$

Table B-5: Robustness: Controlling for (absolute) local resource rents r_l

	<i>Dependent variable:</i>			
	<i>Log observed conflict exposure</i>			
	(1)	(2)	(3)	(4)
<i>Panel A: OLS cross-section</i>				
Log predicted conflict exposure	0.331** (0.139)	0.075** (0.030)	0.075** (0.030)	-0.006 (0.032)
Log resource rents	-0.549* (0.332)	-0.048 (0.059)	-0.048 (0.059)	0.143*** (0.053)
Population control	–	✓	✓	✓
Area control	–	–	✓	✓
Province-fixed effects	–	–	–	✓
Obs.	107	107	107	107
<i>Panel B: OLS panel</i>				
Log predicted conflict exposure	0.065*** (0.019)	0.047*** (0.017)	0.041** (0.018)	0.042** (0.020)
Log resource rents	-0.082 (0.171)	0.053 (0.180)	0.064 (0.190)	0.218 (0.283)
<i>Panel C: 2SLS panel (second stage)</i>				
Log predicted conflict exposure	0.183*** (0.055)	0.151*** (0.058)	0.156** (0.065)	0.166*** (0.062)
Log resource rents	-0.167 (0.189)	0.077 (0.189)	0.088 (0.196)	0.282 (0.291)
First-stage F-stat	66.76	38.83	27.94	25.17
Ward-fixed effects	✓	✓	✓	✓
Year-fixed effects	✓	✓	✓	✓
Province trends	–	✓	–	–
District trends	–	–	✓	–
Ward trends	–	–	–	✓
Obs.	2354	2354	2354	2354

Notes: This table replicates the main results reported in [Table 1](#) and [Table 2](#), controlling for the log of (absolute) local resource rents r_l . Panel A follows panel A of [Table 1](#), and panels B and C follow panels A and B of [Table 2](#). Standard error are spatially clustered with a distance cutoff of 100km. * $p < 0.1$, ** $p < 0.05$, *** $p < 0.01$

Table B-6: Robustness: Controlling for relative local resource rents r_l/r

	<i>Dependent variable:</i> <i>Log observed conflict exposure</i>			
	(1)	(2)	(3)	(4)
<i>Panel A: OLS cross-section</i>				
Log predicted conflict exposure	0.375** (0.168)	0.331** (0.139)	0.075** (0.030)	-0.006 (0.032)
Log relative resource rents	-0.619 (0.406)	-0.549* (0.332)	-0.048 (0.059)	0.143*** (0.053)
Population control	–	✓	✓	✓
Area control	–	–	✓	✓
Province-fixed effects	–	–	–	✓
Obs.	107	107	107	107
<i>Panel B: OLS panel</i>				
Log predicted conflict exposure	0.053** (0.027)	0.065*** (0.024)	0.076*** (0.024)	0.083*** (0.032)
Log relative resource rents	0.032 (0.079)	-0.056 (0.067)	-0.113* (0.068)	-0.142 (0.107)
Ward-fixed effects	✓	✓	✓	✓
Year-fixed effects	✓	✓	✓	✓
Province trends	–	✓	–	–
District trends	–	–	✓	–
Ward trends	–	–	–	✓
Obs.	2354	2354	2354	2354

Notes: This table replicates the main results reported in [Table 1](#) and [Table 2](#), controlling for the log of relative local resource rents r_l/r . Panel A follows panel A of [Table 1](#), and panels B and C follow panel A of [Table 2](#). We cannot conduct this robustness test for our 2SLS results, as the log of relative local resource rents absorbs the instrument power. Standard error are spatially clustered with a distance cutoff of 100km. * $p < 0.1$, ** $p < 0.05$, *** $p < 0.01$

Table B-7: Robustness: Controlling for the interaction term by [Berman et al. \(2017\)](#)

	<i>Dependent variable:</i>			
	<i>Log observed conflict exposure</i>			
	(1)	(2)	(3)	(4)
<i>Panel A: OLS panel</i>				
Log predicted conflict exposure	0.067*** (0.020)	0.049*** (0.018)	0.043** (0.018)	0.041** (0.019)
Mine ward × log mineral price	-1.463*** (0.441)	-0.819*** (0.308)	-0.738*** (0.213)	-1.100* (0.664)
<i>Panel B: 2SLS panel (second stage)</i>				
Log predicted conflict exposure	0.201*** (0.066)	0.186*** (0.070)	0.179*** (0.066)	0.158*** (0.058)
Mine ward × log mineral price	-1.857*** (0.431)	-1.236*** (0.337)	-1.190*** (0.335)	-0.838 (0.852)
First-stage F-stat	28.57	24.02	34.69	32.47
Ward-fixed effects	✓	✓	✓	✓
Year-fixed effects	✓	✓	✓	✓
Province trends	–	✓	–	–
District trends	–	–	✓	–
Ward trends	–	–	–	✓
Obs.	2354	2354	2354	2354

Notes: This table replicates the main results reported in panels A and B of [Table 2](#), controlling for the interaction term used in [Berman et al. \(2017\)](#), i.e., the interaction of an indicator variables for the presence of a mine in the given ward and the log of the global price of the main mineral extracted in this ward. Standard error are spatially clustered with a distance cutoff of 100km. * $p < 0.1$, ** $p < 0.05$, *** $p < 0.01$

Table B-8: Robustness: Controlling for the ward-level population share of the ethnic group of the country's political leader

	<i>Dependent variable:</i>			
	<i>Log observed conflict exposure</i>			
	(1)	(2)	(3)	(4)
<i>Panel A: OLS cross-section</i>				
Log predicted conflict exposure	0.188*** (0.064)	0.152*** (0.055)	0.070*** (0.021)	0.061** (0.025)
Share ethnic group of leader	14.717* (7.986)	9.219* (5.445)	3.968 (3.165)	5.960** (2.945)
Population control	–	✓	✓	✓
Area control	–	–	✓	✓
Province-fixed effects	–	–	–	✓
Obs.	107	107	107	107
<i>Panel B: OLS panel</i>				
Log predicted conflict exposure	0.056*** (0.019)	0.039** (0.018)	0.036* (0.018)	0.034* (0.020)
Share ethnic group of leader	0.178 (0.153)	0.285** (0.131)	0.311** (0.143)	0.362* (0.192)
<i>Panel (C): 2SLS panel (second stage)</i>				
Log predicted conflict exposure	0.217*** (0.075)	0.177** (0.071)	0.165** (0.069)	0.164*** (0.057)
Share ethnic group of leader	-0.138 (0.185)	0.103 (0.147)	0.198 (0.152)	0.197 (0.200)
First-stage F-stat	43.42	22.34	19.18	25.12
Ward-fixed effects	✓	✓	✓	✓
Year-fixed effects	✓	✓	✓	✓
Province trends	–	✓	–	–
District trends	–	–	✓	–
Ward trends	–	–	–	✓
Obs.	2354	2354	2354	2354

Notes: This table replicates the main results reported in [Table 1](#) and [Table 2](#), controlling for the ward-level population share of the ethnic group of the country's political leader. Panel A follows panel A of [Table 1](#), and panels B and C follow panels A and B of [Table 2](#). Standard error are spatially clustered with a distance cutoff of 100km. * $p < 0.1$, ** $p < 0.05$, *** $p < 0.01$

Table B-9: Roubstness: 2SLS results using all industrially mined minerals in the first stage

	(1)	(2)	(3)	(4)
<i>Panel A: Second stage of 2SLS – Dependent variables: Log observed conflict exposure</i>				
Log predicted conflict exposure	0.187*** (0.058)	0.172*** (0.063)	0.167** (0.069)	0.157*** (0.042)
<i>Panel B: First stage of 2SLS – Dependent variables: Log predicted conflict exposure</i>				
Bauxite proximity-price interaction	3.571*** (0.515)	3.512*** (0.512)	3.212*** (0.467)	3.070*** (0.501)
Diamond proximity-price interaction	-2.728*** (0.315)	-1.506*** (0.353)	-0.674* (0.361)	-0.615 (0.414)
Iron proximity-price interaction	0.339*** (0.111)	0.139 (0.113)	-0.013 (0.119)	-0.439*** (0.158)
Rutile proximity-price interaction	-0.735** (0.295)	-0.606* (0.324)	-0.113 (0.233)	0.246 (0.287)
First stage F-stats	39.00	19.37	15.70	32.16
Ward-fixed effects	✓	✓	✓	✓
Year-fixed effects	✓	✓	✓	✓
Province trends	–	✓	–	–
District trends	–	–	✓	–
Ward trends	–	–	–	✓
Obs.	2354	2354	2354	2354

Notes: This table replicates the 2SLS results reported in panels B and C of [Table 2](#), adding the proximity-price interaction for rutile to the first stage (see [eq. 10](#) for the functional form). We omit this interaction in our main specification because export revenues from rutile are much smaller than those from bauxite, diamonds, and iron; and because we only observe exports and prices for titanium metals (which include rutile), but not for rutile specifically. The reported first-stage F-stat is the Kleibergen-Paap rk Wald F statistic. Standard error are spatially clustered with a distance cutoff of 100km. * $p < 0.1$, ** $p < 0.05$, *** $p < 0.01$

C External validity: West Africa

In this appendix, we investigate the external validity of our main results in a sample of eight West African countries: Burkina Faso, Côte d’Ivoire, Ghana, Guinea, Liberia, Mali, Niger, and Sierra Leone.⁴³ The units of observation are gridcells of 0.5 degree \times 0.5 degree, which corresponds to around 50km \times 50km at the equator. These grid cells are provided by Tollefsen et al. (2012) and commonly used in the recent literature on conflict (e.g., Berman and Couttenier, 2015; Berman et al., 2017; Eberle et al., 2020; McGuirk and Nunn, 2020).

C-1 External validity: Data and measures

Local over-representation of ethnic groups: In the absence of available census data, we use the Spatially Interpolated Data on Ethnicity (SIDE) by Müller-Crepon and Hunziker (2018) and the Global Human Settlement Layer (GHSL) to derive a proxy for the population of each ethnic group in each gridcell of each country.⁴⁴ SIDE provides local population shares of ethnic groups at 30 arc-second resolution, which corresponds to around one square kilometer at the equator, based on the spatial interpolation of geo-coded Demographic and Health Surveys. GHSL provides local population estimates at the same 30 arc-second resolution. We multiply the local population shares of ethnic groups (by SIDE) with the local population estimates for 1990 (by GHSL) to obtain a proxy for the local population of each group in each of these small cells. We can then compute the over-representation s_l^g/s^g of each ethnic group g in each gridcell l of each country.

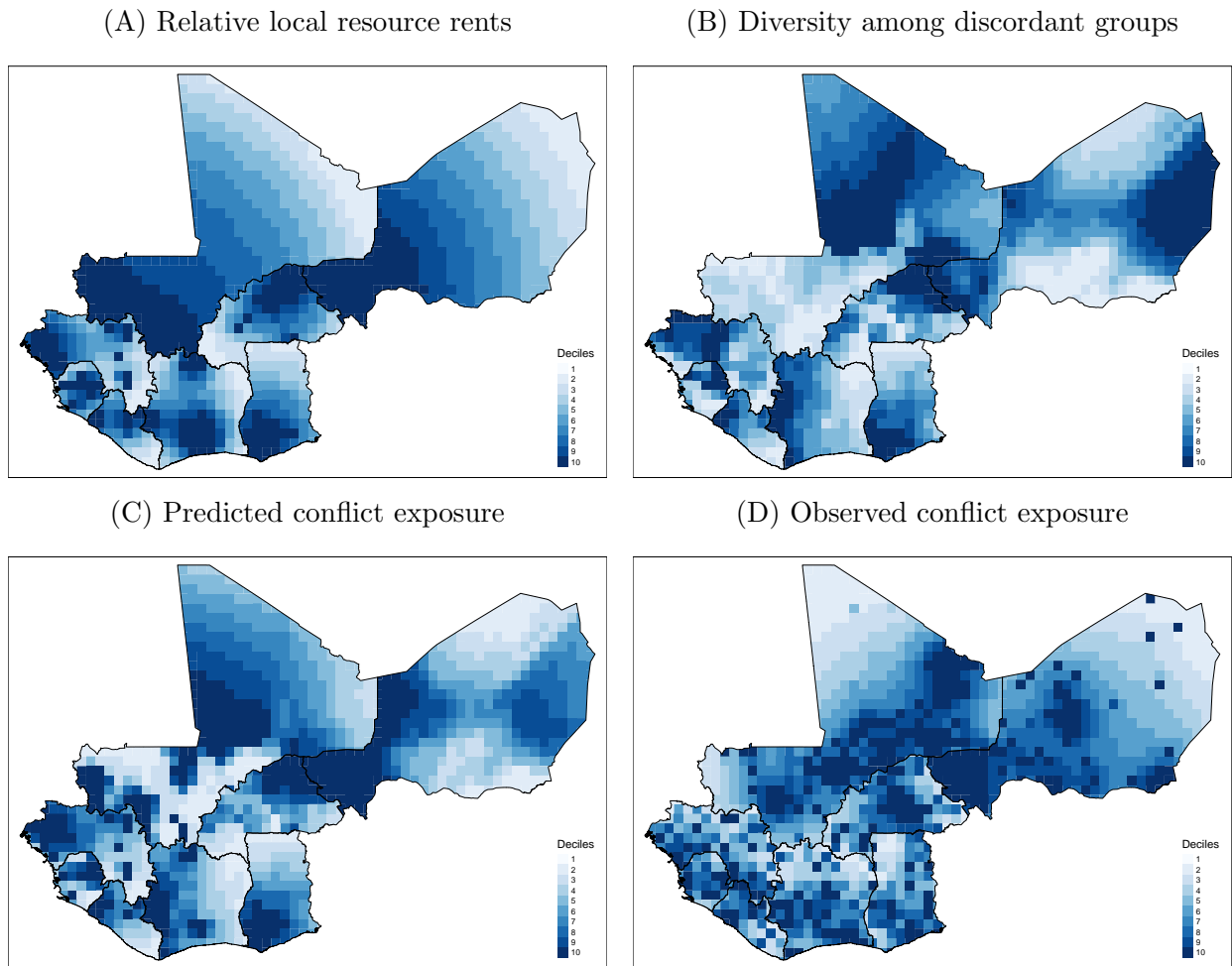
Relative local resource rents: We use the same data and the same methodology as described in Section 3.2.2 (with gridcells replacing wards) to compute the relative local resource rents r_l/r in each gridcell l , country, and year. Panel A of Figure C-1 shows the resulting spatial distribution of the time-averaged relative local resource rents within each country.

Predicted conflict exposure: We derive the predicted conflict exposure e_l , defined in eq. 6, in four steps: First, we determine the set of discordant groups in each country and year. Second, we determine the ethnic diversity among discordant groups D_{l,G^*} in each gridcell, country, and year. Panel B of Figure C-1 plots the time-averaged values of this diversity measure in space. Third, we use this diversity measure and the relative local resource rents

⁴³These are all West African countries for which the data on ethnicities introduced below are available *and* for which the Raw Material Data (RMD) report industrial mines that are active during our sample period from 1997–2018.

⁴⁴The GHSL is constructed by the Joint Research Centre and the Directorate General for Regional and Urban Policy of the European Commission. It is publicly available at <https://ghsl.jrc.ec.europa.eu>.

Figure C-1: External validity: Resources, diversity, and conflict exposure across gridcells



Notes: This figure plots time-averaged values of key variables across the gridcells of each of the eight West African countries in our sample, with darker colors representing values in higher deciles. Panel A plots the relative local resource rents r_l/r , panel B the ethnic diversity among discordant groups D_{l,G^*} , panel C the predicted conflict exposure e_l , and panel D the observed conflict exposure.

to compute the predicted conflict exposure e_l in each gridcell, country, and year. Finally, we average the predicted conflict exposure e_l in each gridcell and country over the entire sample period, leading to the spatial distribution of the predicted conflict exposure shown in Panel C of [Figure C-1](#).

Observed conflict exposure: We use the same data and the same methodology as described in [Section 3.2.3](#) (with gridcells replacing wards) to compute the observed conflict exposure in each gridcell, country, and year. Panel D of [Figure C-1](#) shows the spatial distribution of the time-averaged observed conflict exposure.

C-2 External validity: Results

We now test whether the positive and statistically significant elasticity between predicted and observed conflict exposure also holds in this new sample. First, we rerun our cross-sectional analysis for both Sierra Leone and the full set of these eight West African countries. Second, we test for effect heterogeneity across countries.

Panel A of [Table C-1](#) shows that our main results broadly hold for Sierra Leone and West Africa. In fact, the point estimates for Sierra Leone are similar to our main results reported in [Table 1](#) (panel A, columns (1) and (3)). The point estimates for West Africa are about half the size. Panel B shows results when limiting the analysis to politically relevant ethnic groups based on the ethnic power relation (EPR) data by [Wucherpfennig et al. \(2011\)](#). The point estimates converge somewhat between the two samples.

Table C-1: External validity

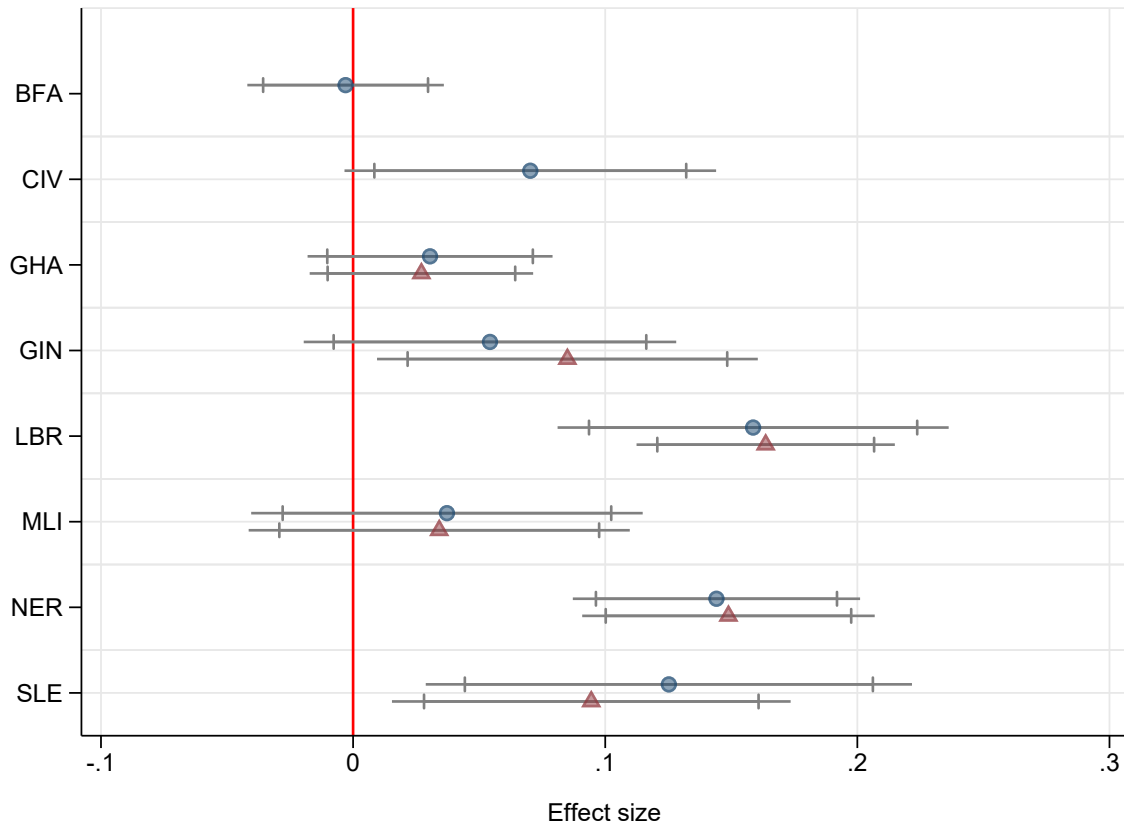
	<i>Dependent variable:</i>			
	<i>Log observed conflict exposure</i>			
	<i>Sierra Leone</i>		<i>West Africa</i>	
	(1)	(2)	(3)	(4)
<i>Panel A: All ethnic groups</i>				
Log predicted conflict exposure	0.121** (0.059)	0.150*** (0.053)	0.074*** (0.015)	0.061*** (0.013)
Obs.	39	39	1534	1534
<i>Panel B: Politically relevant ethnic groups</i>				
Log predicted conflict exposure	0.103** (0.040)	0.117*** (0.040)	0.090*** (0.015)	0.090*** (0.015)
Obs.	39	39	1275	1275
Population and area controls	–	✓	–	✓
Country-fixed effects	✓	✓	✓	✓

Notes: This table reports the results of regressing the log of observed conflict exposure on the log of predicted conflict exposure (e_t). Population and area controls are log of gridcell population in 1975 based on GHSL and the log of gridcell area. Columns (1)–(2) report results for Sierra Leone, and columns (3)–(4) results for our sample of eight West African countries. Panel A is based on all ethnic groups, and panel B only on ethnic groups listed as politically relevant by EPR. We cannot match EPR and SIDE groups for Burkina Faso and Côte d’Ivoire, resulting in a reduced sample in columns (3)–(4) of panel B. Standard errors are spatially clustered with a distance cutoff of 100km. * $p < 0.1$, ** $p < 0.05$, *** $p < 0.01$

[Figure C-2](#) reports the point estimates for each of the West African countries. We again compute the predicted conflict exposure first based on all ethnic groups within the country and then based on the politically relevant groups according to the EPR data if possible. We find

considerable effect heterogeneity, but no indication that Sierra Leone is a special case.

Figure C-2: External validity: Single-country estimates



Notes: This figure reports country-specific results of regressing the log of observed conflict exposure on the log of predicted conflict exposure in nested interaction models. The regressions include country-fixed effects and the same area and population controls as columns (2) and (4) in [Table C-1](#). Blue dots represent point estimates when using all ethnic groups, and red triangles represent point estimates when relying solely on ethnic groups listed as politically relevant by EPR. We cannot match EPR and SIDE groups for Burkina Faso and Côte d'Ivoire, resulting in missing triangles for these countries. The 95% confidence intervals are based on spatially clustered standard errors with a distance cutoff of 100km.